Investigation on the thermal stability of

technical and cosmetic emulsions

Von der Fakultät für Mathematik, Informatik und Naturwissenschaften der Rheinisch-Westfälischen Technischen Hochschule Aachen zur Erlangung des akademischen Grades eines Doktors der Naturwissenschaften genehmigte Dissertation

vorgelegt von

Diplom-Physikerin
Cristina-Alina Iliescu
aus
Bukarest, Rumänien

To my parents

Motto:

„Wir sehen jetzt durch einen Spiegel

in einem dunkeln Wort;

dann aber von Angesicht zu Angesicht.

Jetzt erkenne ich es stückweise;

Dann aber werde ich es erkennen,

gleichwie ich erkannt bin."

(I Korinther 13,12)

ACKNOWLEDGEMENTS

CONTENTS

Contents

ZUSAMMENFASSUNG

Ein grosses Problem der Lebensmittel-, Arzneimittel-, Waschmittel- und Kosmetik-Industrie ist das nach wie vor lückenhafte Wissen über die Mechanismen und Gesetzmäßigkeiten, welche das thermische Verhalten ihrer emulsionsartigen Produkte kontrollieren und die damit verbundenen Schwierigkeiten, Prognosen über die thermische Stabilität solcher Formulierungen abzugeben.

Die hier vorliegende Arbeit stellt eine Methode vor, die es durch Interpretation thermisch analytischer Daten erlaubt, Aussagen über die thermische Stabilität sowohl einfacher Emulsionsrezepturen als auch komplexer Mehrkomponentensysteme zu treffen. Die experimentelle Basis dieser Arbeit stellen Dynamische-Differenz-Kalorimetrie (DSC) Messungen ausgewählter Emulsionsrezepturen – Weichspüler als einfache Emulsionssysteme, sowie kommerzielle kosmetische Cremes und Lotionen als Vertreter komplexer Mehrkomponentensysteme - dar, deren Messdaten mit den Methoden der nicht-isothermen Reaktionskinetik interpretiert wurden. Zusätzliche strukturelle Informationen über die Emulsionsproben wurden sowohl durch optische Durchlichtmikroskopie, als auch durch Polarisationsmikroskopie erhalten, welche durch thermisch mikroskopischen Untersuchungen unter nicht-isothermen Bedingungen ergänzt wurden.

In der Literatur wird über physikalische Instabilitätsphänomene berichtet, die in Weich-spülerformulierungen als Folge von Lagerzeit, Temperaturänderung und Parfümölzugabe auftreten. Für die in der hier vorliegenden Stabilitätsstudie ausgewählte Gruppe von Weichspülerbasen wurde der Einfluss der Parfümölzugabe, der Lagerung sowohl bei hohen als auch bei niedrigen Temperaturen sowie der Einfluß der Lagerungszeit auf unparfümierte Proben untersucht. Die DSC Kurvenprofile, die Werte der kinetischen Parameter (in komprimierter Form als Reaktionsgeschwindigkeitskonstante) und die mikroskopischen Erscheinungsbilder wurden miteinander korreliert, um das thermische Verhalten der Proben zu interpretieren.

Um die strukturellen Veränderungen, die auf die in den Emulsionen stattfindenden Langzeitrelaxationsprozesse zurückzuführen sind, zu beseitigen und aus Reproduzierbarkeitsgründen wurden die DSC Kurvenprofile erst analysiert, nachdem ein sogenannter „Entalterungsvorgang" durchgeführt wurde. Zur Herleitung der kinetischen Parameter benötigt man Daten aus Experimenten mit unterschiedlichen Heizraten. Um die Allgemeingültigkeit und Genauigkeit des kinetischen Ansatzes zu gewährleisten, ist es

erforderlich, eine modellfreie kinetische Analysenmethode einzusetzen, wofür die differentiale Methode (für gleiche Umsätze) von Friedman[175] gewählt wurde. Aufgrund der Quasi-Umkehrbarkeit von DSC-Signalen während der Abkühlung, wurden zyklische Temperaturprogramme mit unterschiedlichen Aufheizraten und konstanten Abkühlraten durchgeführt; die kinetischen Parameter wurden aus den endothermen Prozessen, die während des Aufheizvorgangs auftreten, berechnet. Die komplexen Kurvenprofile erfordern die Extraktion der individuellen Prozesse vom gesamten endothermen Signal. Hierfür eignet sich besonders eine lineare Dekonvolution (Entfaltung) mittels Gauss-Kurven, da Gauss-Kurven sehr gut geeignet sind, kinetische Prozesse zu beschreiben. Die Einführung zusätzlichen Bedingungen, um zu besseren Übereinstimmungen mit der physikalischen Realität zu gelangen, führt zu verbesserten Anpassungen.

Eine weitere Methode zur Berechnung der kinetischen Parameter der vom gesamten Signal abgetrennten individuellen Prozesse mit Hilfe eines modellbezogenen kinetischen Ansatzes ist die Methode von Kissinger[172], die eine allgemeine Form der kinetischen Funktion voraussetzt. Die Übereinstimmung der Ergebnisse, die mit der Methode von Kissinger und der modellfreien Methode von Friedman erhalten werden, unterstützt die ausgewählte Form der kinetischen Funktion und erlaubt eine Vereinfachung der kinetischen Analyse.

Eine andere modellfreie Methode, die integrale Methode (für gleiche Umsätze) von Flynn-Wall-Ozawa[176], führt zu vergleichbaren Ergebnissen für die Aktivierungsenergie der individuellen Prozesse. Der Vergleich der kinetischen Parameter der individuellen Prozesse mit denen des gesamten endothermen Prozesses, deutet darauf hin, daß für einfache DSC Kurvenmuster auf es Dekonvolutionverfahren verzichtet werden kann.

Es konnte gezeigt werden, dass man mit Hilfe der in dieser Arbeit vorgestellten Methode gelingt unterschiedliche thermische Stabilitäten der untersuchten Weichspülerformulierungen zu identifizieren. Ein Lagerungsversuch über 2,5 Jahre bestätigt die Ergebnisse der kinetischen Auswertung und der Kurvenprofildekonvolution.

Ebenfalls wurde untersucht, welchen Einfluß die Anzahl der thermischen Entalterungszyklen (der zyklischen Hoch/Niedrigtemperaturprogramme) auf die kinetischen Parameter von parfümierten und unparfümierten Basen hat. Für zwei der unparfümierten Basen wurde ein vergleichbares Verhalten beobachtet: ein erster Zyklus verursacht eine leichte Destabilisierung, ein zusätzlicher Zyklus eliminiert diese Destabilisierung und die Probe ist nicht mehr vom Ausgangszustand unterscheidbar.

Für die eine der beiden ausgewählten unparfümierten Basen, ist es möglich eine Zunahme der Instabilität mit Parfümölzugabe bereits ab dem ersten Temperaturzyklus zu

erkennen; die Instabilität ist ausgeprägter nach einem zweiten Temperaturzyklus. Für die stabilste der unparfümierten Basen, ist eine Zunahme der Instabilität als Folge der Parfümölzugabe erst nach einem zweiten Temperaturzyklus festzustellen.

Die Lagerung der parfümölfreien Basen bei hohen und niedrigen Temperaturen führt zu einer neuen, kompakteren, definierten und stabileren Struktur.

Die Analyse der Abkühlkurven zeigt, daß die exothermen Prozesse schneller als die endothermen ablaufen und daher für die Stabilität der Proben entscheidend sein können.

Eine Erweiterung der Analysezielsetzung fand anschließend durch die Untersuchung ausgewählter kommerzieller kosmetischer Cremes und Lotionen mittels DSC statt. Die aus DSC Kurvenprofilen und deren kinetischer Analyse erhaltenen Informationen wurden mit optisch mikroskopischen Untersuchungen korreliert. Sowohl thermischer Stress, als auch Zeitlagerung führen zur Entstehung neuer, stabiler Strukturen. Die stabilste und die am wenigsten stabilste kosmetische Emulsion der untersuchten Gruppe konnten identifiziert werden.

ABSTRACT

One of the major problems which food, pharmaceutical, washing and cosmetic industry are confronted with, is the thermal stability of their products in emulsion form.

This work proposes an evaluation of the thermal stability of selected emulsion formulations – fabric softeners, as simple emulsion systems, and cosmetic creams and lotions, as complex multicomponent systems – by interpreting thermal analysis data, obtained from differential scanning calorimetry (DSC) experiments with the tool of nonisothermal reaction kinetics. This approach is supplemented with structural information about the emulsion samples from optical microscopy observations in bright and polarised light and thermo-microscopy examination under non-isothermal conditions.

Literature reports about phenomena of physical instabilities appearing in fabric softener formulations as consequence of time of storage, temperature and fragrance addition. For a selected group of fabric softener bases, chosen for the stability studies, the influence of fragrance addition, as well as of storage at high and low temperatures and of time of storage on unperfumed samples is investigated. DSC profiles, kinetic parameters values (in the compact form of the rate constant) and microscopic appearance are correlated in order to arrive for the samples at an interpretation for their thermal behaviour.

In order to eliminate the structural changes corresponding to long-time relaxation phenomena occurring in the softeners with time, and for the sake of reproducibility of the signal, the DSC profiles have been analysed after performing a de-ageing operation ("rejuvenation"). To derive the kinetic parameters the complexity of the DSC patterns requires multiple thermal scans. To maintain generality and precision of the kinetic approach it is necessary to use a model-free method of analysis, for which the isoconversional differential method of Friedman[175] is chosen. Because of the quasi-reversibility of the DSC curves during cooling, cyclic temperature programmes with different heating rates and constant cooling rate are performed; kinetic parameters are calculated from the endothermic processes occurring during heating. Complex curve profiles also demand the separation of the overall endothermic effect into individual processes. For signal separation into the underlying individual processes a linear deconvolution procedure using Gaussian curves is applied. The Gaussian curve form represents a good approximation for a kinetic process. Imposing additional restrictions to arrive at a better agreement with the physical reality, lead to improved fits.

Kinetic parameter calculation for the separated processes with a model-based approach – the Kissinger method[172] - which assumes a general form for the kinetic function, leads to values which are in good agreement with those obtained from the model-free method of Friedman. This supports the chosen form of the kinetic function and allows a simplification of the kinetic analysis.

Another model-free method, the integral isoconversional method of Flynn-Wall-Ozawa[176], gives comparable results for the activation energy of the individual processes. Comparing the kinetic parameters obtained for individual processes with those for entire endothermic processes suggests that for simple DSC patterns, the deconvolution procedure can be avoided.

Nonisothermal reaction kinetical methods applied to fabric softener samples proved to be able to differentiate the thermal stability of the different groups of bases. Practical experience confirms the results of the kinetic evaluation and of DSC profile deconvolution.

The extent to which the number of thermal cycles of de-ageing (high-low temperature cycling) affects the kinetic parameters of perfumed and unperfumed bases is also analysed. For two unperfumed bases a similar behaviour with respect to the number of thermal cycles could be shown: a first thermal cycle causes a slight destabilisation, an additional one, however, leads to almost a recovery of the initial state.

For one of the two chosen, unperfumed bases it is possible to discern an increase of instability with fragrance addition already from the first thermal cycle; the instability is more pronounced after a second thermal cycle. For the other unperfumed base (the most stable one) an increase of instability as a consequence of fragrance addition can be noticed only after a second thermal cycle.

High and low temperature storage of fragrance-free bases leads to new, more compact, defined and stable structures.

Cooling curve analysis shows that exothermic processes occur faster than the endothermic ones and may be crucial for samples' stability.

Extending the scope of the investigation, selected, commercial cosmetic creams and lotions are investigated by DSC and the information obtained from the DSC profiles and their kinetic analysis are correlated with thermo-microscopy examinations. Thermal stress as well as storage time lead to the formation of new, stable structures. The most stable and the least stable cosmetic emulsion in the chosen set are identified.

LIST OF SYMBOLS

α	conversion degree
β	scanning rate
γ	surface tension
δ	thickness of surfactant or polymer adsorbed layer
μ	centre of Gaussian peak, arithmetic mean
ν	number of mols (stoechiometric coefficient)
$1/\chi$	thickness of electrical double layer
σ	standard deviation
ΔQ	differential heat
A	pre-exponential factor
ac 1,2,3	industrial fragrances compositions (alcohols)
ad 1,2,3	industrial fragrances compositions (aldehydes)
B1, B2, B3	fabric softener bases
c	molar concentration
C_i	constants
CMC	critical micelle concentration
$d\alpha/dt$	conversion rate
$d(\Delta Q)/dt$	heat flow
DLVO theory	Dejaguin-Landau-Verwey-Overbeek theory
DMA	dynamic mechanical analysis
DSC	differential scanning calorimetry
DTA	differential thermal analysis
E_a	activation energy
ESR	electron spin resonance
$f(\alpha)$	kinetic function
F-value	value of F-statistic
FWO	Flynn-Wall Ozawa method
G	Gibbs potential
$g(\alpha)$	integral of the kinetic function
H	specific enthalpy (J/g)
h(T)	temperature integral
H_0	total enthalpy (total area under the DSC peak)

HBL	hydrophilic-lipophilic-balance
H_t	enthalpy for time t (area under the DSC peak up to time t)
k	rate constant
$k_{25°C}$	rate constant at 25°C (approx. room temperature)
k_B	Boltzmann's constant
kt 1,2,3	industrial fragrances compositions
L_β	gel lamellar phase
L_α	liquid crystalline lamellar phase
n	reaction order
NMR	nuclear magnetic resonance
O/W	oil-in-water emulsion
O/W/O	oil -in- water-in- oil emulsion
P	measured property of a system
PEO	poly(ethylene oxide)
PIT	phase inversion temperature
R	general gas constant
r	interparticle distance
r_0	particle radius
R^2	correlation coefficient
SANS	small-angle neutron scattering
SAXS	small-angle X-ray scattering
t	time
T	temperature
TGA	thermogravimetry
T_m	melting temperature
TMA	thermomechanical analysis
T_p	peak temperature
v	rate of chemical reaction
W	interaction energy
W/O	water-in-oil emulsion
W/O/W	water-in-oil-in-water emulsion
W_{el}	electrostatic interaction energy
W_{en}	entropic part of interaction free energy
W_{mix}	mixing interaction free energy

W_T total interaction free energy

W_{VDW} Van-der-Waals interaction energy

1. OBJECTIVE OF THE INVESTIGATION IN THE ACTUAL SCIENTIFIC PERSPECTIVE

In the pharmaceutical and food as well as in the cosmetic industry, one of the major challenges is to produce not only efficacious, safe, cost-effective and elegant, but also stable emulsion formulations. Emulsions are complex systems and because of the increasing requirements to fulfil, the problem to ensure their stability is becoming more and more difficult.

Often emulsions are exposed to environmental influences. Factors that can alter emulsions' stability can be physical (such as temperature, pressure, mechanical stress, sun irradiation, microwaves), chemical (such as essential oils, gases - especially oxygen -, metals, salts, pH-value) or microbiological (different micro-organisms such as yeast, bacteria, fungi, viruses). Usually, in order to test emulsion stability, accelerated stability procedures for physical stability (high or low temperatures, high humidities, freeze/thaw cycles, mechanical stress, exposure to irradiation) - are employed[1,2].

A large variety of methods were developed for characterising emulsion stability. The most important ones are:

- *rheological measurements* for determination of viscosity and viscoelastic properties[3,4,5,6,7]
- *near-infrared multiple light scattering measurements* for information about mean particle size[8]
- *photomicrography in normal and polarised light/ thermal optical analysis* for structural (also temperature-dependent) information [9,10]
- *electron microscopy (freeze fracture technique)* for ultrastructural information[11,12]
- *atomic force microscopy* for determination of droplet-droplet interactions[13]
- *conductivity* between different parts of an emulsion, e.g. between top and bottom[14,15]
- *small-angle X-ray scattering (SAXS)*[16,17,18] for particle size analysis and structure determination, also temperature-dependent
- *small-angle neutron scattering (SANS)*[19] for interface study of solid-stabilised emulsions
- *zeta-potential (electrokinetic potential) measurements* for determination of the surface charge and, in this way, of the aggregation degree[20]
- *electron spin resonance (ESR)* for measurement of viscosity[21]

- *acoustic* and *electro-acustic spectroscopy* for determination of particle size distribution and zeta-potential in real time, also for determination of elastic and viscous properties without dilution[22]

- *turbidity ratio measurements* for information about particle size distribution[23]

- *dielectric spectroscopy* for structural differences between emulsions due to interfacial polarisation in an external electric field[24]

- *3-D cross-correlation spectroscopy* for determination of particle size distribution[25]

- *interfacial tension measurements* for characterisation of emulsion thin films[26] and surfactant films in emulsions[27]- also temperature-dependent[28]

- *nuclear magnetic resonance (NMR)* for characterisation of surfactant mobility in emulsion formulations[29]

Temperature, as well as accelerated ageing can be well simulated by means of thermal analysis under non-isothermal conditions. Among thermal analysis techniques, differential scanning calorimetry (DSC) is widely used in the cosmetic industry, being applied successfully for the structural characterisation of hair and also for studying the effects of cosmetic hair products[30,31,**32**]. For membranes[33,34] and skin lipid models[35,36], DSC is able to describe structural transitions; these can provide useful information about the action of skin cosmetic products[37,38]. Moreover, cosmetic cream structures can display gel and liquid crystal lamellar phases similar to those found in stratum corneum lipids and in biological membranes[39,40,41] and therefore can undergo similar kinds of transitions. Literature reports about the characterisation of temperature-induced transitions in cosmetic emulsion formulations by means of DSC experiments, although little is known about their relationship to structural changes [42,43,44,45,46,47,48].

DSC has been proven to be a suitable technique for gaining information on the stability of emulsion formulations. However, assessments of the stability of pharmaceutical[49,50,51] or food emulsions[52,16,17,18] could be only derived when DSC experiments were combined with other experimental techniques such as thermo-microscopy or rheology.

Information about the stability of solid samples can be derived from non-isothermal data (DSC combined with thermogravimetric, TGA, measurements)[53,54]. TGA measurements are difficult to perform with emulsions, but DSC is a very suitable technique. Kinetic evaluation of DSC data for emulsion samples in order to obtain information about their stability is a pioneer work of our group[55]. It has been shown that for simple cosmetic creams, DSC provides useful information for kinetic studies, although no predictions about sample stability at room temperature can be inferred. The simple extrapolation procedure

for shelf-life time predictions seems to be a more general problem, regardless the experimental method in "accelerated" conditions utilised for gaining information about emulsions[56].

Because of the complexity of commercial emulsion compositions and structures, this work, firstly aims to investigate comparatively simple emulsion systems, namely fabric softeners.

Fabric softeners on the market are usually in the form of macro-[57] or micro-emulsions, stabilised with organic solvents[58], oily sugar derivatives[59], or polymeric structurants[60]. The chosen models are model fabric softeners kindly provided by International Flavours & Fragrances (IFF). These were manufactured from a limited number of components: cationic surfactants (esterquats) & non-ionic co-surfactants, polymer and water. To these different types of fragrances were added. Addition of fragrances tends to cause instability effects with time. This instability has two different facets: „breaking" (phase separation) and „hardening" of the emulsion[61]. This is, why fabric softeners are usually supplied to the consumer as perfume-free concentrates to which fragrance may be added before utilisation[62]. Temperature is also one of the most important factors which contributes to instability. This effect is usually accentuated when the composition is stored at low (e.g. at 5°C or below) or high temperatures (e.g. at 40°C or above). Temperature stress can be well reproduced by measuring characteristic parameters of the samples under accelerated conditions, such as through dynamic experiments in thermal analysis.

The aim of this work was to study the effects of temperature and fragrance addition to fabric softener samples and relate the emulsions' thermal behaviour to their observed instability. Thermal analysis measurements, in particular differential scanning calorimetry (DSC) investigations, were performed in order to provide experimental data for non-isothermal kinetic calculations. Through the application of kinetic models information about thermal stability could be inferred.

In order to gain a deeper insight into the processes occurring within the samples, DSC measurements were supplemented by optical microscopic examinations in transmitted and polarised light as well as through thermo-microscopic studies, i.e. dynamic optical microscopic investigations under non-isothermal conditions. The idea was to correlate changes in thermal behaviour with structural changes.

To carry the approach beyond the "simple" emulsions represented by the fabric softeners, furthermore, commercial cosmetic emulsions, choosing one example each of the oil-in-water, water-in-oil and water-in-oil-in water type, were investigated from the perspective of their thermal stability with time and their microstructural appearance.

3

2. <u>THEORETICAL BACKGROUND</u>

2.1. Emulsions

2.1.1. General considerations

Emulsions are dispersed systems of two or more immiscible or incompletely miscible liquids in form of small droplets - building the disperse medium or internal phase - distributed in a continuous dispersion medium or external phase, also called „closed" phase[63,64,65,66,67,68,69,70]. Recent expansion of the definition also includes liquid crystals in the disperse phase[71]. Emulsions are called in this case "structured emulsions". Multi-phase systems are formed in this way[72,73] with improved emulsion stability[74,75] and slow delivery of active substances or drugs, e.g. into the skin[76]. Emulsions are colloidal systems[77].

A classification of most important emulsion systems with respect to size, macroscopic appearance and thermodynamic stability is given in Table 1[78,79,80,81,82,83,84].

Table 1: Classification and characteristics of emulsion systems

Emulsion system	Characteristics		
	Optical appearance	*Particle size (nm)*	*Thermodynamic stability*
Macroemulsion	milky opaque	>1000	no
Micro/Nanoemulsion	transparent or translucent	100-200	approaching
Micro/Nanoemulsion	transparent or translucent	10-100	yes
Micellar solution	transparent	2-10	no

Disperse phase formation is not a spontaneous process ($\Delta G < 0$) and requires the supply of external energy, such as mechanical energy (i.e. stirring). However, the process of droplet dispersion is associated with an increase of the surface/volume ratio and therefore with the requirements of large surface energy in order to achieve long time stability. Therefore, emulsions are generally thermodynamically unstable unless emulsifying agents

are added. These are surfactants (tensides)[85] - amphiphilic molecules which reduce the surface tension between the two phases. Because of their structure - they have both a hydrophilic and a hydrophobic part - they are able to bind to both phases, building a monomolecular film at the interface (in the form of a sterical or electrical barrier) which hinders the emulsified droplets to come together and break the emulsion. The interface adsorption of the emulgator leads to a decrease of surface tension and is thermodynamically described by the Gibbs equation[86,87].

Depending on whether the phases are as dispersions of water in an organic solvent, such as oil, or vice versa, emulsions are classified as water-in-oil (W/O or H-L) or oil-in-water (O/W or L-H) emulsions. The principal mechanism of O/W and W/O emulsion stabilisation by addition of emulsifiers is shown in Figure 1.
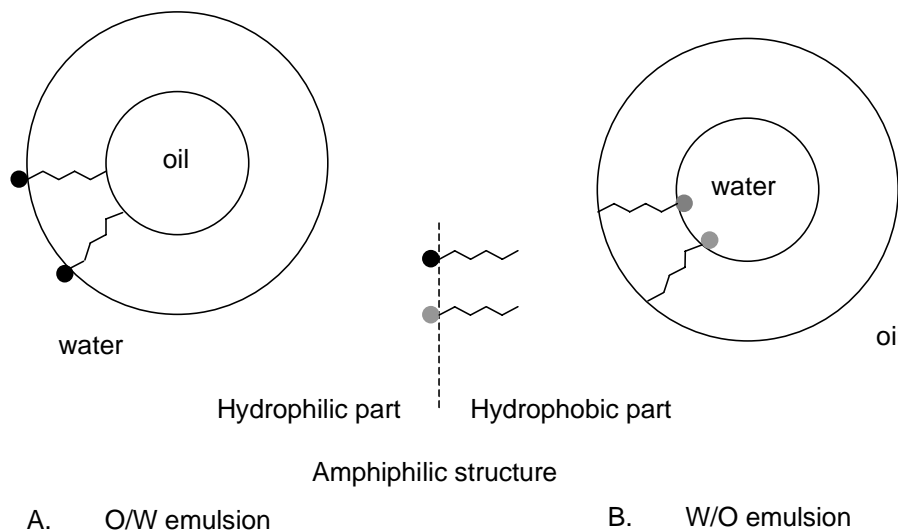
Fig. 1: The stabilising effect of an O/W emulsifier (A) and of an W/O emulsifier (B) at the interface oil/water; reproduced from[86]

Thus, emulsifier properties are of tremendous importance for emulsion formation and stability; a key role plays their hydrophilic-lipophilic-balance (HLB) value[64], a measure of their solubility in water or oil. This determines whether an O/W or rather an O/W system is formed. On a scale from 1 to 20, emulsifiers with an HLB-value < 9 are generally good W/O-stabilising agents; those with HLB-values > 10 are used as O/W-stabilising agents. The explanation of their action at the interface (oil/water) is the following: if the interfacial tension at the interface oil/agent γ_I is greater than the water/agent interface γ_{II} , the oil/agent interface will tend to have a smaller area than the water/agent interface and the formation of an oil in water type emulsion will be favoured (Figure 2 A). If the relative

values of the two interfacial tensions are reversed, as in Figure 2 B, a water in oil type will have preferred stability.

Oil   I   Oil

Stabilising agent   Stabilising agent

    II   I

Water   Water   II

A.   O/W   B.   W/O

$\gamma_I > \gamma_{II}$ $\gamma_I < \gamma_{II}$
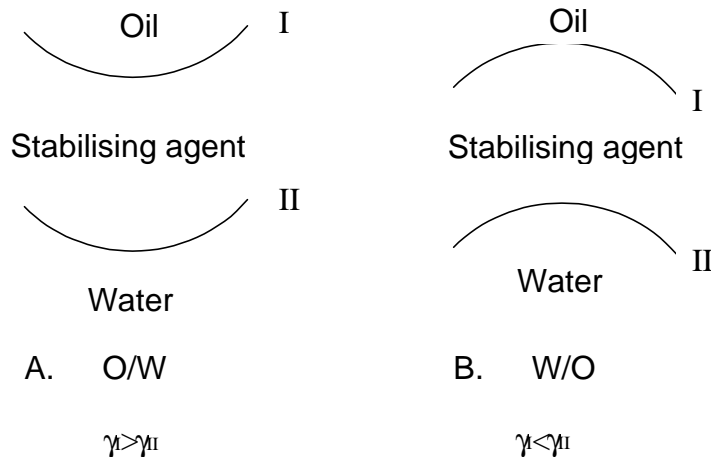
Fig. 2:   Emulsifier affinities at the interface oil/water I and II in emulsion stabilisation; reproduced from[86]

Within the concentration range of the emulsifying agents used in typical emulsions, some surfactants may form particular colloidal aggregates such as lyotropic mesophases or liquid crystal structures (lamellar, hexagonal or cubic type)[88,89]. Surfactant associations are thus the ones responsible for building liquid crystalline phases around the dispersed droplets, preventing in this way droplet coalescence. This protective action can be compared with the protective liquid crystalline structure of lipids and protein membranes in living cells; a quite flexible structure enabling the cells to exert their specific functions far from a rigidity that would be incompatible with life.

Another class of emulsions are multiple emulsions, complex systems of an emulsion within an emulsion such as O/W/O (i.e. oil droplets contained within aqueous droplets dispersed in a continuous oil phase) or W/O/W (i.e. water droplets contained within oil droplets dispersed in a continuous water phase) emulsions[90]. Producing multiple emulsions with good stability was a major challenge in cosmetics[91,92,93,94], which has successfully been met[95]. A new galenical approach in cosmetics is represented by solid lipid nanoparticles and nanostructured lipid carriers; they enable the stabilisation of sensitive ingredients and controlled release of drugs or active substances[96,97].

Macroemulsions are essential formulations for application in personal care and cosmetics. In case of microemulsions, their potential for skin irritation should be taken into account, which is due to the higher amount of incorporated surfactants.

2.1.2. Stability of emulsions

2.1.2.1.   Thermodynamical aspects of emulsion stabilisation

Emulsions are colloidal dispersions tending to aggregate and eventually to coagulate with time due to van der Waals inter-particle attractive forces.

Stability can be promoted by the creation of a repulsive energy barrier between the droplets. This can be achieved by two mechanisms, namely, either by charge-stabilisation or by steric stabilisation (or by a combination of the both)[98,99].

2.1.2.1.1.   Charge stabilisation

A charge is created on the emulsion droplet by adsorption of an ionic surfactant with the formation of an electric double layer on its surface; electrostatic repulsion results from the interaction between the electrical double layers of thickness $1/\chi$ surrounding each of the two droplets. This mechanism of charge-stabilisation is shown in Figure 3, for two spherical droplets of radius r_0. This mechanism is only possible for O/W emulsions, since charge separation can occur only in aqueous medium which has a high dielectric constant.
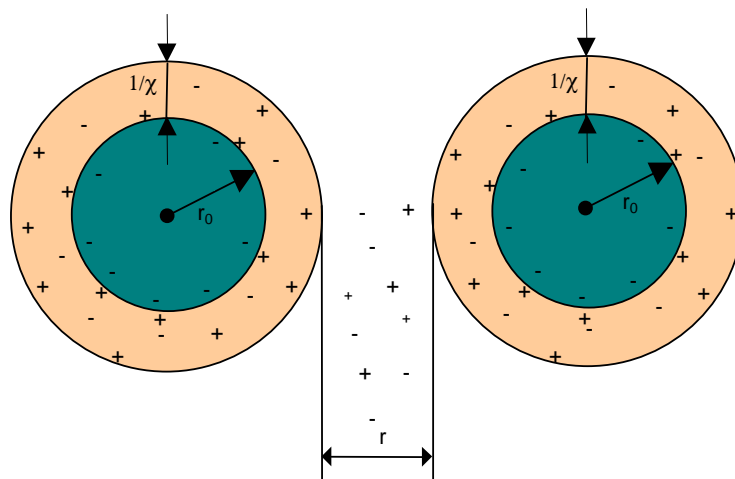
Fig. 3: Charge stabilisation of colloidal particles; reproduced and adapted from [101]

Derjaguin, Landau, Verwey, Overbeek[100,101] developed a theory (abbreviated DLVO) for describing colloid particle stability. The DLVO theory accounts for the interaction between particles approaching one another at distances r smaller than r_0. It states that the interaction energy between two charged colloidal particles results from the repulsion of the

electric double layers around the two particles and from the van der Waals attractive energy of the fluctuations in charge distribution within the two particles. In this way, the total interaction energy:

$$W_T = W_{el} + W_{VDW} \qquad\qquad\qquad \textbf{(2.1.)}$$

is the superposition of the two contributions, attractive and repulsive as illustrated in Figure 4:
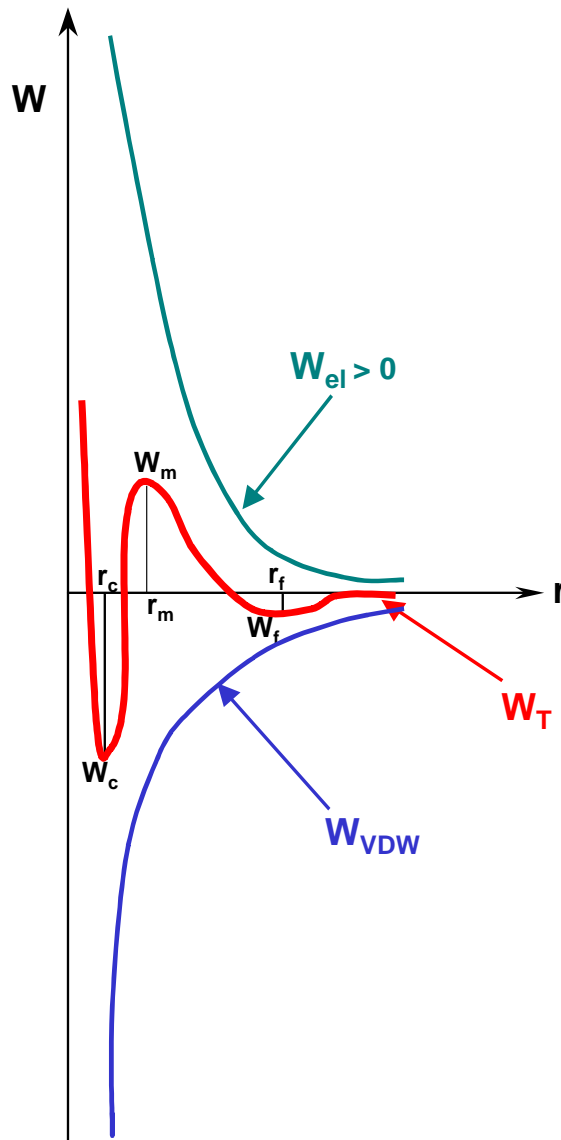
Fig. 4: Interaction energy between two colloidal particles (spheres) as a function of the separation distance r (DLVO theory); W_{VDW}=Van der Waals attractive energy; W_{el}=electrostatic repulsive energy; W_T=total energy (after superposition) reproduced and adapted from [100]

The total interaction energy has a relative minimum at long distances (r_f); this corresponds to particle flocculation, a phenomenon of reversible aggregation. Droplets are in a

metastable configuration (mechanical or thermal fluctuations can destabilise it) and separated by a solvent film. Secondary minimum flocculation plays an important role for the stability of certain emulsions, such as creams which are highly concentrated emulsions.

For very small interparticle distances, the interaction energy reaches the absolute energetic minimum which corresponds to coagulation (r_c), an irreversible aggregation. This situation may be prevented by enhancing the height of the repulsive maximum W_m in the energetic diagram.

Because of the complexity of real interparticles interactions, there is no final theory of emulsion stability[102]. Several approximations may be performed in each particular case to obtain analytical solutions for inter-particle interactions.

2.1.2.1.2. Steric stabilisation

Steric stabilisation of an emulsion is provided by adsorption of a nonionic surfactant or polymer on droplet interfaces[103], as shown in Figure 5. This is the most common way of stabilision, which unlike charge stabilisation, is applicable for both O/W and W/O emulsions.
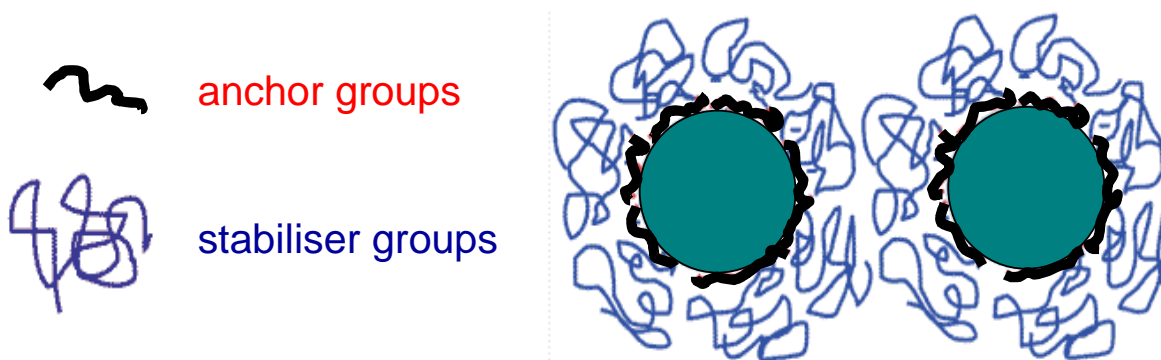
Fig. 5: Steric stabilisation of colloidal particles; adapted from[103]

Steric stabilisers consist of two components: a lipophilic part, with strong affinity and even solubility in oil (the „anchor" chain) and a hydrophobic part, with strong affinity to the aqueous phase and strongly solvated by water molecules (referred to as the stabilising chain). Nonionic surfactants like ethoxylated alcohols, such as $C_{12}H_{25}$-$O(CH_2$-CH_2-$O)_6$-H (abbreviated $C_{12}E_6$) are the simplest steric stabilisers for O/W emulsions. The alkyl chain

forms the „anchor" chain, whereas the poly(ethylene oxide) (PEO) chain is the stabilising chain. For stabilisation of W/O emulsions, polymeric surfactants (e.g. in the form of block copolymers) can be used.

The interaction energy between two droplets with an adsorbed surfactant or polymer layer of thickness δ that approach r<2δ is shown in Figure 6.

Steric repulsion is provided by two main effects. On the one hand, an unfavorable mixing of the stabilising chains with the continuous medium (for example PEO with water) accounts for a repulsive mixing interaction W_{mix}. On the other hand when particles collide at distance δ, their adsorbed layers may be compressed without penetrating each other; this is accompanied by a decrease in entropy of the chains and stands for the elastic, or entropic repulsive interaction W_{en}.
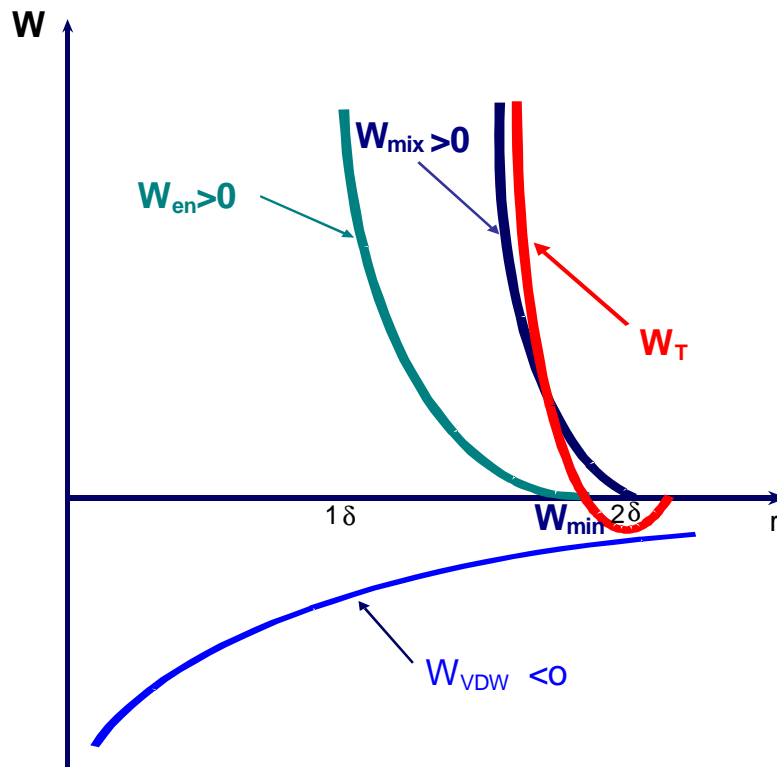
Fig. 6: Steric interaction energy between two colloidal particles with an adsorbed surfactant with thickness δ as a function of the separation distance r; W_{VDW}=Van der Waals energy (attractive); W_{en}=elastic or entropic free energy (repulsive); W_{mix}=mixing interaction free energy (repulsive); W_T=total interaction free energy (after superposition); reproduced and adapted from[98]

The total energy-distance curve W_T from Figure 6 is obtained from the interplay of these repulsive effects with van der Waals attraction:

$$W_T = W_{mix} + W_{en} + W_{VDW}$$ **(2.2.)**

This resultant interaction free energy has a single minimum at a distance of $r \sim 2\delta$; the size of the minimum depends on the ratio of layer thickness, δ, to droplet radius, r_0. For relatively thick adsorbed layers and very small droplets (as in the case of nanoemulsions), the ratio δ/r_0 will be so large that W_{min} may be neglected in comparison to the thermal energy $E_T = k_B T$ (where k_B is Boltzmann's constant and T the absolute temperature). In this case, no flocculation occurs and the system approaches thermodynamic stability. For $r < 2\delta$ steric repulsion is increasing so rapidly with decreasing separation distance that stability is readily realised.

A combined charge and steric stabilisation presumes an intricate interaction between surfactant and polymers (water-soluble or nonionic type)[104,105,106]. In order to understand this stabilisation phenomenon, surfactant-oil[107,108], surfactant-water[109], oil-water[110], polymer-water [111] systems have to be analysed in detail.

2.1.2.2.   *Main breakdown processes and methods of enhancing stability*

Creaming, sedimentation, flocculation, coalescence, Ostwald ripening and phase inversion are the most important processes associated with emulsion instability[63,98,112,113]. They are illustrated in Figure 7. In practice, all of these breakdown processes occur more or less simultaneously.
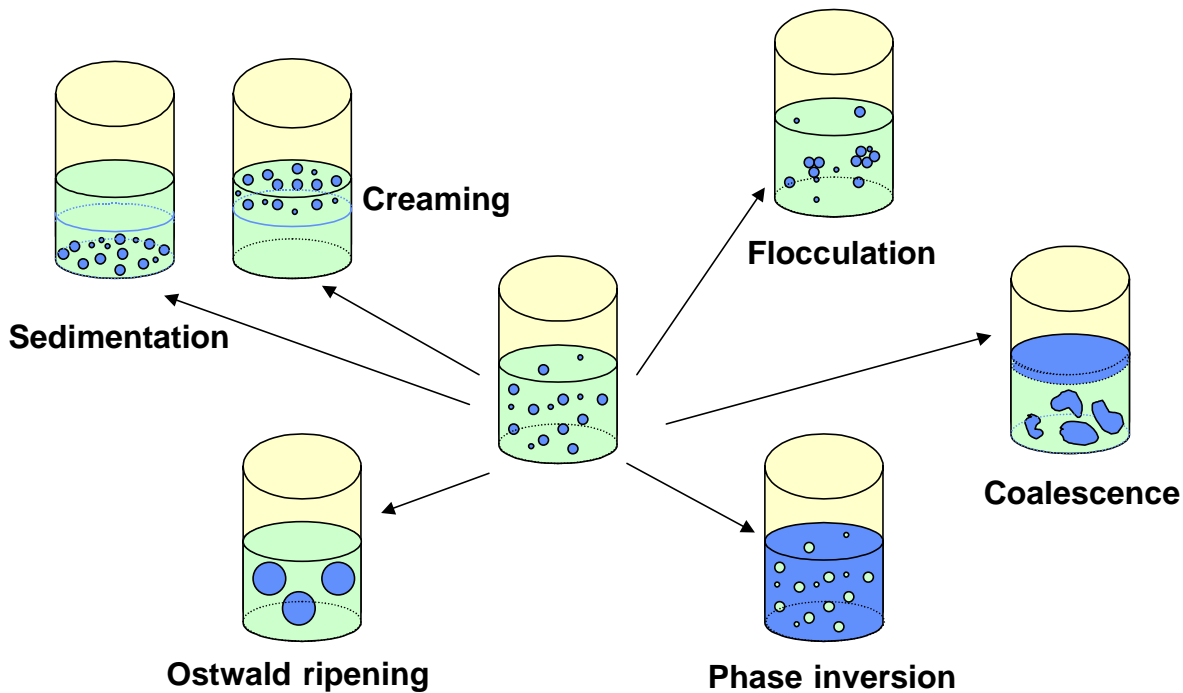
Fig. 7: Main breakdown processes of emulsions; adapted from[80]

Creaming and sedimentation are the result of gravitation. When the conformational energy of the dispersed droplets in the gravitational field becomes larger than the thermal motion (Brownian diffusion), creaming (with O/W emulsions) or sedimentation (with W/O emulsions) occurs. The result is a build-up of a concentration gradient. This case occurs for macroemulsions. It is reversible and shaking can restore the initial state.

This phenomenon does not occur in the case of very small particles ($r_0 < 0,7 \mu m$). The thermal kinetic energy is large enough to overcome the gravitation and no separation occurs. This explains the absence of creaming/ sedimentation for nanoemulsions.

The rate of sedimentation and creaming is the result of the balance between gravitational and frictional forces. In order to reduce the velocity of the process one can i) decrease the droplet radius (nanoemulsions); ii) increase the frictional force by adding thickeners or gelating agents; iii) decrease the difference in density between particles and medium as much as possible by choosing appropriate ingredients.

Flocculation (aggregation) is a reversible process and corresponds to the relative minimum in the interaction energy-separation distance diagram for two colloidal particles (Fig.4). Flocculation can be therefore prevented by creating high energy between the droplets. This can be achieved by using polymeric surfactants of block or graft copolymer types, which provide good steric stabilisation .

Coalescence (coagulation) is the result of thinning and disruption of the liquid film between the droplets. The removal of the thin liquid film is an irreversible process and it is described by the absolute minimum position in the interaction energy-separation distance diagram for two colloidal particles (Fig.4).

One way to reduce coalescence is to use mixed surfactant films which enhance the Gibbs-Marangoni effect[112], i.e. the diffusion of surfactant molecules from the bulk to the interfacial layers. Another way is to use surfactants that produce lamellar liquid crystalline structures which surround the oil droplets in several bilayers. One other possibility is the application of macromolecular surfactants because of their rheological properties; these polymeric surfactants build with their loops and tails viscoelastic interfacial film layers between flocculated particles that increase viscosity.

Solid particles can also provide stabilisation against coalescence[114,115]. Depending of the type of emulsion (O/W or W/O) it is necessary to choose a different kind of particles to be preferentially wetted by one phase or the other, respectively.

Ostwald ripening results from the difference in solubility between small and large droplets and occurs mainly in nanoemulsions. It is characterised by the increase of droplets' size with time.

The reduction of the interfacial energy by incorporating surfactants into the dispersed phase which strongly adsorb at the interface and have low solubility in the continuous phase may reduce Ostwald ripening significantly. Another method is to add a second disperse phase component, concentrated in smaller droplets and being insoluble or less soluble than the first one in the continuous phase.

Ostwald ripening may also be reduced by increasing surfactant concentration beyond the critical micellar concentration (CMC) so that micelles are formed; these can solubilise large amounts of oil as "swollen micelles", decreasing the ripening rate.

Finally the less polydisperse the nanoemulsion is, the lower is the Ostwald ripening rate.

Phase inversion is a process whereby the internal and external phases of the emulsion suddenly invert (O/W changing to W/O or vice versa). This phenomenon can be induced either by changing the volume fraction of one of the phases (catastrophic inversion) or by changing the affinity of the surfactants towards the two phases (transition inversion).

In the first case, the increase of one fraction above a critical value induces a phase inversion; the latter accounts for certain nonionic surfactants, which in an O/W system can alter the phase affinity with temperature. The critical temperature at which a phase inversion may take place is referred to as the phase inversion temperature (PIT) and is an important parameter to be taken into account when preparing nanoemulsions.

Among factors that affect the phase inversion of an O/W emulsion are the nature of the oil phase, the surfactant type and its concentration, the temperature of the system, the oil-to-water ratio, the presence of additives in the oil or water phase, the mixing conditions and the rate and order of addition of the different components.

2.1.3. Fabric softeners: a special kind of emulsions

Fabric softeners play a key role in the textile and detergent industry. They are predominantly used for textiles to assure pleasant smoothness, suppleness and elasticity, to improve technical properties such as antistaticity, hydrophilicity, sewability and rubfastness. They give synthetic fibres a certain "natural touch" and enhance the wear comfort by promoting secondary effects such as moisture regulation. Last but not least, they extend textile product life[116]. For saleability „soft handle" is one of the most important criteria.

As for any surfactant, the chemical nature of softeners can be either cationic, anionic, amphoteric or non-ionic[117,118,119]. A special class of softeners with outstanding specific properties such as highly reduced fibre friction and stain repellence are silicone-based textile-finishing agents[120]. For permanent effects softeners with reactive groups were developed.

The four chemical classes of agents regarded as „softeners" are the fatty acid esters and their derivatives, polyethylenes, paraffins and polydimethylsiloxanes and their derivatives. Softeners for consumer use are predominantly liquid dispersions with common ranges of 15-25% active matter. Beside the active agents they contain emulsifiers to produce stable dispersions, dispersants and defoamers. Further additives such as viscosity adjusters, perfumes, preservatives and pH adjusters may also be added.

The most well-known and mainly-used among the different types of softeners are the cationic agents. They contain long alkyl chains and a water-soluble cationic group. Representative for this class are salts of primary or tertiary amines, salts of quaternary ammonium compounds from tertiary amines, amino amides, imidazolines or amino-esters (called also esterquats)[121].

The driving force for the deposition process of cationic softener on textile surfaces of charge-free synthethics is the hydrophobic effect. In case of natural and some synthethic fabrics the electrostatic attraction between the positive centre of the cationic softener molecules and the negative charges on the fibres in water plays an important role.

In some commercial products, a combination of cationic softeners (15-35%) with 5-30% nonionic softeners (for instance non-ionic ethoxylated products) is chosen to improve formulation stability toward high temperatures, pH and hard water. Fabric conditioners of such concentrated mixtures have a complex phase behaviour with liposomes, lamellar fragments and micelles. Polymers may also be added to these softener formulations to improve mesophases stability by steric insertion between alkyl chains.

Addition of fragrances to washing products was introduced for better consumer acceptance. For fabric conditioners as well as for cosmetic formulations, this step may play a decisive role for emulsion consistency and shelf-life.

Aroma chemical molecules are usually of the ester-, ether-, aldehyde-, ketone-, alcohol- or carbohydrate-type [122,123]. Most fragrances are strongly hydrophobic in nature and, hence, poorly water-soluble, causing a problem in product formulation. The solution is either to solubilise them in organic solvents or to emulsify them to microemulsion, micelles or liposomes[124,125,126,127,128,129]. Fragrance molecules are trapped in the bilayers of liposomes and in the core of the micelles as illustrated in Figure 8. Fragrance-containing emulsions provide complex stability problems[130, 131,132,133,134,135].
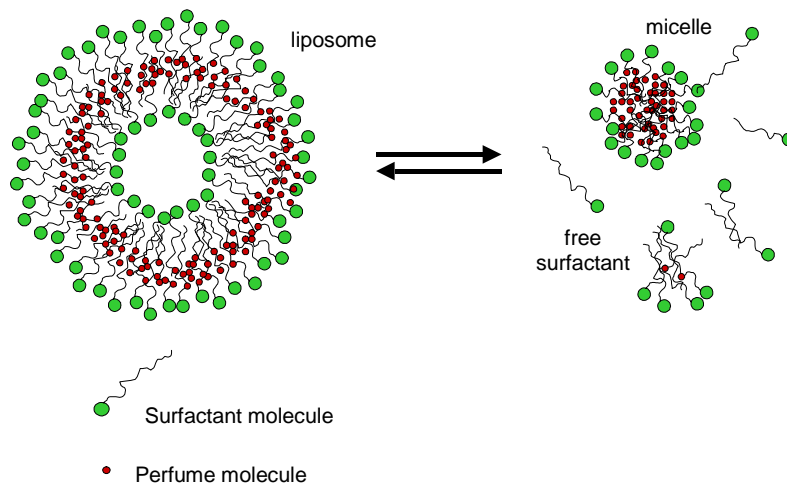
Fig. 8: Emulsification of perfume molecules by a surfactant. Equilibrium state between different structures: liposomes, micelles and free surfactant molecules; adapted from[124]

2.2. Principles of thermal analysis

Thermal analysis is a term applied to a group of methods and techniques in which a physical property of a substance is measured as a function of temperature, while the substance is subjected to a controlled temperature programme[136,137,138,139,140]. A controlled temperature programme implies that the sample is measured at predetermined constant temperature (isothermal conditions) or that the temperature varies linearly with time (dynamic or nonisothermal conditions). This means that in nonisothermal experiments the heating or cooling rate β is given by a constant parameter:

$$\beta = \frac{dT}{dt}$$ **(2.3.)**

Depending on the physical property which is measured as a function of temperature and time, a classification of the main methods of thermal analysis includes Thermogravimetry (TG) for the determination of weight, Differential Thermal Analysis (DTA) for temperature differences, Differential Scanning Calorimetry (DSC) for the absorbed or evolved heat of reaction (enthalpy), Thermomechanical Analysis (TMA) and Thermodilatometry for dimensional changes, Dynamic Mechanical Analysis (DMA), Thermomicroscopy, Thermomagnetometry, Thermoelectrometry, to mention just the more important ones[141,142,143,144,145,146].

The techniques of DTA and DSC are both concerned with the measurement of energy changes in a substance. While DTA measures temperature differences between sample and reference, DSC measures the thermal power required by the sample for keeping it at the same temperature as the reference. Therefore, DSC is usually regarded as a more quantitative technique. The word "differential" emphasises that measurements involve both the substance itself and a reference material. There are two types of DSC techniques: heat flow DSC and power compensation DSC. Whereas in heat flow DSC the instrument signal is derived from the temperature difference between the sample and reference, in power compensation DSC the signal is obtained from the differential heat supplied to the sample and reference for maintaining equal temperatures, as shown in Figure 9[147].
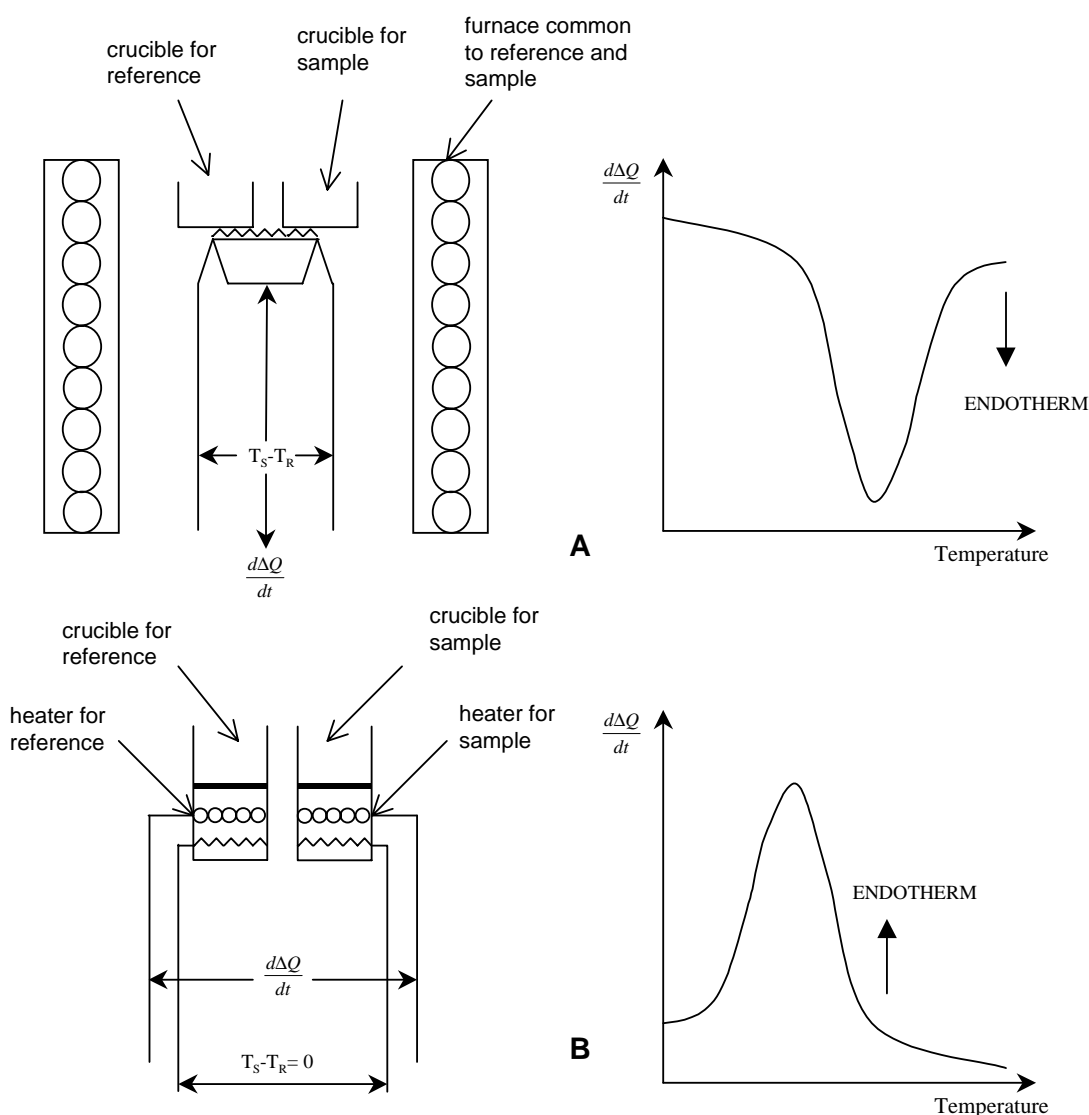
Fig. 9: The principle of (A) heat flow DSC and (B) power compensation DSC; reproduced from[144]

DSC allows following physical transitions (such as melting, crystallisation, glass transition) and chemical reactions (such as thermal decompositions, polymerisation and polycondensation) and determining heat capacity and purity.

In this work experiments were done with DSC equipments of both the power compensation (Perkin-Elmer) as well as the heat flow (Netzsch) type.

The first group of emulsions which was analysed – the fabric softener bases – show a noisy DSC pattern when first heated. This pattern simplifies after a heating-cooling procedure. Figures 10 A and B illustrate by way of example the DSC signals of a fabric softener base containing fragrance (B1_ad1) during the first heating and after a first heating-cooling procedure. It makes sense therefore in the case of fabric softener bases to perform temperature cycles which cancel the physical history of the sample in order to

obtain noise-free, reproductible signals for further analysis. This procedure is called de-ageing.

Fig. 10 A: DSC signal of a perfumed fabric softener base (B1_ad1) recorded at a heating rate of 10°C/min

Fig. 10 B: DSC signal of a perfumed fabric softener base (B1_ad1) recorded at a second heating rate of 10°C/min, after a heating-cooling programme with 10°C/min
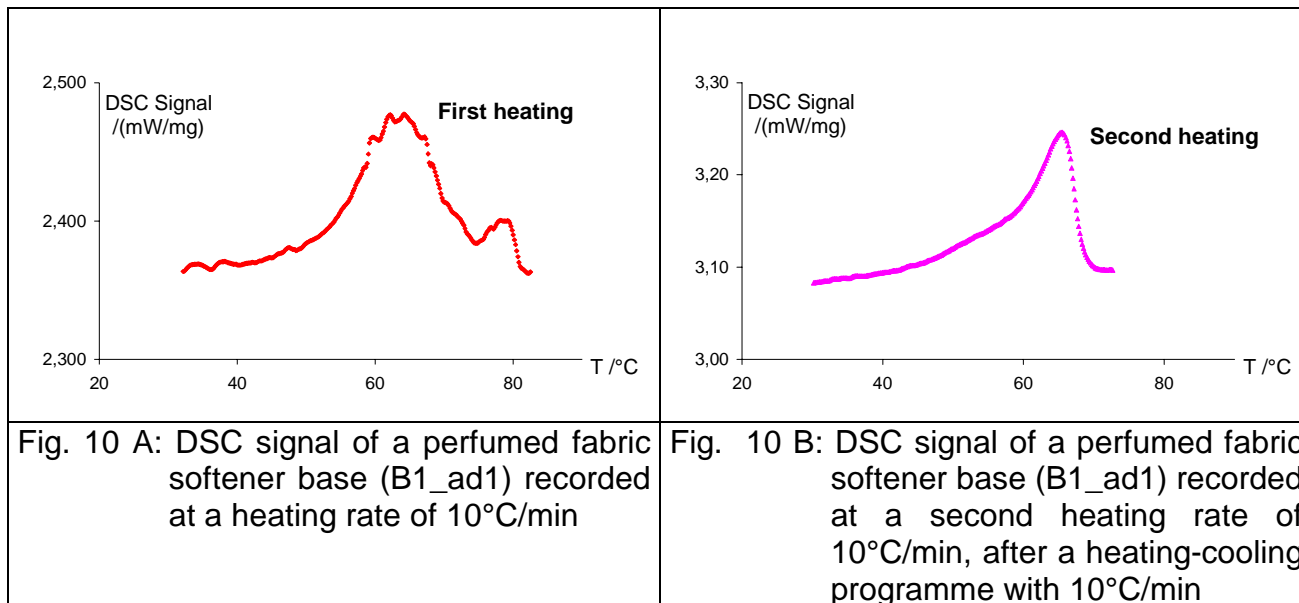
2.3. Kinetics of chemical reactions

2.3.1. Background of chemical reaction kinetics for thermal analysis

The thermodynamic condition for a reaction to take place is that the difference in chemical potential (or Gibbs free energy, G) between product(s) and educt(s) should be negative, i.e. $\Delta G \leq 0$ (thermodynamic condition) and the kinetic condition is that the energetic barrier called activation energy of the reaction, E_a is overcome, as illustrated in Figure 11.
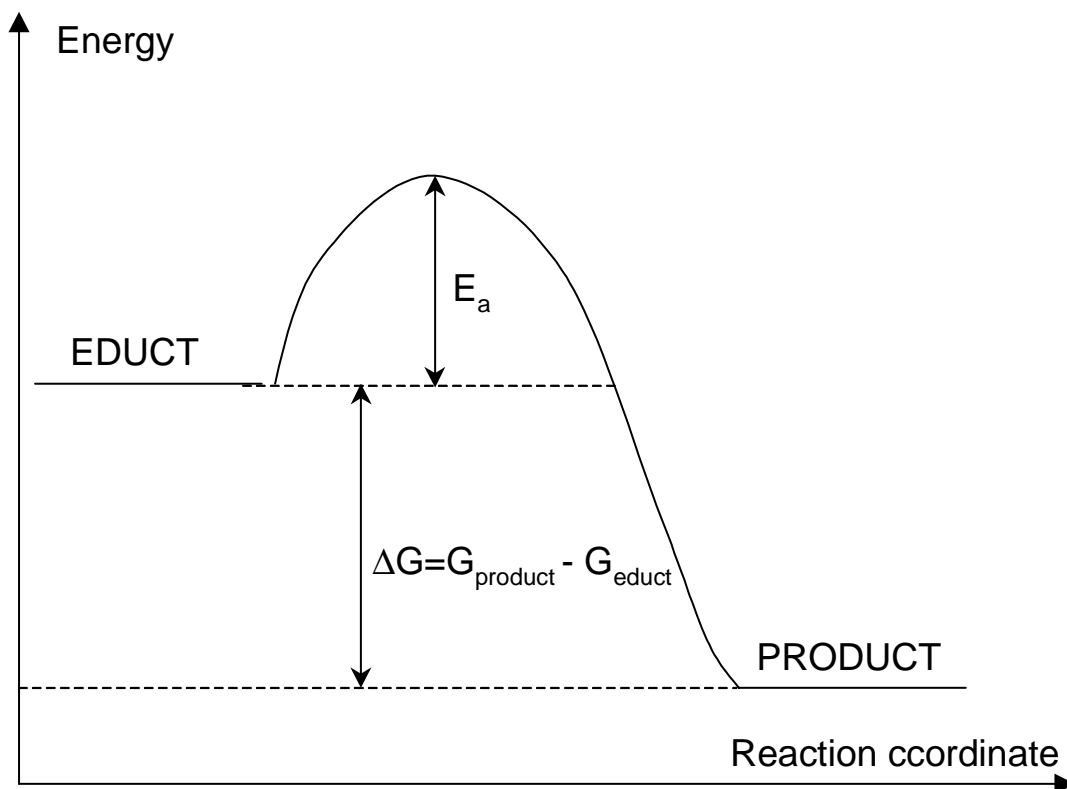
Fig. 11: Energetic diagramm for a chemical reaction; adapted from[100]

For the chemical reaction in the general form of

$$\sum_i \nu_i Educt_i \xrightarrow{k} \sum_j \nu_j Product_j \qquad \textbf{(2.4.)}$$

where ν are the stoichiometric coefficients, the rate of the reaction is described as the variation of concentration as intensive parameter (or of mass as extensive parameter) of the reactants (educts) with time depends on the activation energy required to overcome the energetic barrier[87,148,86,149,150]:

$$v = -\frac{dc_{educt_i}}{dt} = \frac{dc_{product_j}}{dt} \qquad \textbf{(2.5.)}$$

where c is the molar concentration and t is the time.

In a more general case, the reactant conversion concept replaces that of concentration/mass. The conversion degree is the fraction of molecules that have reacted up to a defined moment in time and is related to the degree of reaction advancement. It is defined in the most general case as[151,152] :

$$\alpha = \frac{P_t - P_0}{P_\infty - P_0}, \qquad \textbf{(2.6.)}$$

where P_t, P_0 and P_∞ is the measured property of the investigated system at moment t, at the beginning (t=0) and at the end of the reaction (t=∞), respectively. It is used to describe the chemical modifications within the investigated system. This change from the concentration/mass towards conversion of a reactant allows not only homogenous reactions but also heterogeneous reactions to be characterised and reactions with different reaction mechanisms to be compared. Taking this concept into account the rate of a chemical reaction, v, can be expressed as[151,152]:

$$v = \frac{d\alpha}{dt} = k(T) \cdot f(\alpha) \qquad \textbf{(2.7.)}$$

where $f(\alpha)$ is the kinetic function and $k(T)$ the rate constant as a function of the absolute temperature, T.

The reaction rate, v, depends on temperature and conversion as functions of separable variables, i.e. in the form of a product of the two functions $k(T)$ and $f(\alpha)$. This assumption is axiomatic. Another axiomatic assumption is that equation **2.7.** describes elementary steps only and not complex reactions. Non-axiomatic assumptions are made about the form of the functions $k(T)$ and $f(\alpha)$[153].

It was found empirically that $k(T)$ reflects the increase of the reaction rate with temperature in an exponential way. In this case the dependence on temperature is of the Arrhenius-type[154,87] :

$$k(T) = A \cdot exp\left(-\frac{E_a}{RT}\right) \qquad \textbf{(2.8.)}$$

where R is the gas constant, E_a the activation energy and A the pre exponential factor. E_a and A are called the activation parameters. E_a is the energy necessary to initiate the

reaction and A the initial fraction of molecules from which only $\exp\left(-\dfrac{E_a}{RT}\right)$ have an energy greater than E_a. Thus, the product $A \cdot \exp\left(-\dfrac{E_a}{RT}\right)$ represents the fraction of molecules which have sufficient energy to enter into the reaction.

The temperature dependence of reactions may be non-Arrhenius. However, also in these special cases it is possible to define an activation energy as [100]:

$$E_a = R \cdot T^2 \cdot \frac{d\ln k}{dT} = -R \cdot \frac{d\ln k}{d\left(\dfrac{1}{T}\right)} \qquad \textbf{(2.9.)}$$

which leads to equation **2.8.** when E_a is temperature-independent.

As for the kinetic function $f(\alpha)$, which gives the dependence of the reaction rate on the extent of the reaction α, it is presumed to obey the general equation in the case of homogenous reactions:

$$f(\alpha) = (1-\alpha)^n \qquad \textbf{(2.10.)}$$

This form describes a reaction of nth order, n being the sum of exponents in the reaction rate equation.

For the case of heterogeneous reactions, the most general form proposed for the function $f(\alpha)$ has the following expression[155]:

$$v = \frac{d\alpha}{dt} = \alpha^n \cdot (1-\alpha)^m \cdot \left[-\ln(1-\alpha)\right]^p \qquad \textbf{(2.11.)}$$

where the values of n, m, p allows retrieving the particular form of kinetic models of heterogeneous reactions.

The task of kinetic analysis is to find the analytical expressions of the functions k(T) and $f(\alpha)$. This is equivalent to finding the values of the three kinetic parameters, Ea, A and n, providing $f(\alpha)$ has the simple analytical form given in equation **2.10.**. The group (Ea, A, $f(\alpha)$) or (Ea, A, n) is called the kinetic triplet which is considered to fully characterise the processes taking place.

2.3.2. Nonisothermal reaction kinetics. Deconvolution procedure

During a thermal analysis experiment, the physical property of the investigated system is measured as a function of time, while a temperature programme is run with a constant scanning rate β. This physical property could be the weight of a substance (in TG), the heat flow (in DSC) or the lengh of a fibre (in TMA).

Whenever an effect is observed on a DSC trace while the sample is subjected to a controlled temperature ramp, it is reasonable to assume that there has been a transformation, which can be represented for the simplest case as:

$$A \xrightarrow{k} B$$
(2.12.)

where A is the material before transformation and B the material after transformation. Any conversion is accompanied by an absorption or release of heat. This heat is that of a physical transition or of a chemical reaction. In a quantitative way it is expressed by means of the apparent enthalpy of the process.

Therefore, for DSC, the measured property P from equation **2.6.** is the heat (enthalpy), H. Because the enthalpy H is refered to the mass of the sample, H is defined further as a specific enthalpy, in J/g. In this case, equation **2.6.** leads to:

$$\alpha = \frac{H_t}{H_0}$$
(2.13.)

where H_t is the enthalpy value at time t (the area under the recorded DSC signal up to time t) and H_0 is the total enthalpy of the reaction (the total area under the recorded signal curve).

While running a DSC temperature programm, the recorded signal – the heat variation in time or the heat flow $\dfrac{dQ}{dt}$ - reflects at any moment the enthalpy variation in the sample, $\dfrac{dH_t}{dt}$. When a thermal effect is observed, the conversion rate will be:

$$\frac{d\alpha}{dt} = \frac{d\left(\dfrac{H_t}{H_0}\right)}{dt}$$
(2.14.)

This equation links the data obtained from thermal analysis measurements to the non-isothermal kinetic parameters[141,142,143,144,145,146].

Since the evolution of enthalpy during the process reflects the reaction, parameters measured from DSC temperature programms can be inserted in the general kinetic equation for chemical reaction **2.7.**, leading to the following expression:

$$\frac{d\left(\frac{H_t}{H_0}\right)}{dt} = A \cdot f\left(\frac{H_t}{H_0}\right) \cdot \exp\left(-\frac{E_a}{RT}\right)$$

(2.15.)

This equation allows to obtain the analytical expressions of the functions k(T) and f(α) or the values of the kinetic triplet (E_a, A and n) from DSC experiments.

For nonisothernal experiments a convenient change of variable from time t into temperature T turns equation **2.15.** with the definition of β from equation **2.3.** into:

$$\frac{d\alpha}{dT} = \frac{1}{\beta} \cdot k(T) \cdot f(\alpha)$$

(2.16.)

The approach of solving this equation to obtain the kinetic parameters for thermally initiated chemical or physical processes has to take into account the particular form of the signal, for instance whether it displays single or multiple peaks. In the case of a multiple peak pattern, equation **2.16.** will be true only for separate independent processes.

For complex, for instance competitive or reversible reactions or those complicated by diffusion, E_a varies with α. For these cases, α and T are not any more independent. Under such circumstances equation **2.1.** remains valid only locally and the kinetic parameters have to be calculated for each experimental point or rather, on small intervals for which they are considered as constants[156].

Therefore, a complicated pattern needs to be separated into elementary processes to enable further analysis[157,158]. This procedure is called deconvolution ("defolding").

There are several linear and non-linear algorithms of deconvolution, depending on the specific physical process under investigation (as time-dependent phenomena in seismology[159], geology[160], etc). If the system, whose thermal properties are analysed, is made of components that are not reacting chemically with each other - as we can suppose for emulsion components - and the thermally-induced physical transitions of each components are independent of each other, we can assume a linear deconvolution model as the best choice for extracting the individual processes from the overall signal.

The reaction rate equation **2.16.** shows the dependence on two parameters, α and T, through the product of two independent functions, f(α) and k(T). Assuming the validity of

the superposition principle[161] which states that a recorded signal is equivalent to the signal of each component in proportion of its participation percentage yields

$$\frac{d\alpha}{dt} = \sum_{i=1}^{p} C_i \cdot \frac{d\alpha_i}{dt}$$

(2.17.)

C_1, C_2,.......,C_p are constants (the weight values) and p being the number of processes. The overall DSC signal $\frac{d\alpha}{dt}$, describing the superposition of independent processes and applying equations **2.8.** and **2.10.**, is given by:

$$\frac{d\alpha}{dt} = \sum_{i=1}^{p} C_i \cdot A_i \cdot (1-\alpha_i)^{n_i} \cdot e^{-\frac{E_{a_i}}{R \cdot T}}$$

(2.18.)

where E_{a_i} is the activation energy of each process „i". We assume that the overall reaction rate is a linearly weighted superposition of such products of two independent functions, characterising each individual process. From a mathematical point of view, this superposition presumes the dependence of the conversion rate on two variables, α and T, and many parameters C_i. The number of parameters obviously complicates the straightfoward separation attempt of the initial conversion rate. The calculation of α under the most favourable circumstances, that is when but one constants are equal to zero, means solving the integral of a transcendental function, which gives only a recurrent solution[162]. This means the way of solving the deconvolution procedure needs to be simplified.

As the expression of the conversion rate suggests, an elementary processes „i" may be approximated graphically with a Gaussian curve:

$$\frac{d\alpha_i}{dt} = \frac{1}{\sqrt{2 \cdot \pi} \cdot \sigma_i} \cdot e^{-\frac{1}{2}\left(\frac{T-T_p}{\sigma_i}\right)^2}$$

(2.19.)

where the temperature T is the independent variable, T_p the location of the peak (the peak temperature) and σ_i the standard deviation.

Consequently, we assume that a linear sum of Gaussian curves suitably approximates the overall conversion of a DSC endothermic effect:

$$\frac{d\alpha}{dt} = \sum_{i=1}^{p} C_i \cdot \frac{1}{\sqrt{2 \cdot \pi} \cdot \sigma_i} \cdot e^{-\frac{1}{2}\left(\frac{T-T_p}{\sigma_i}\right)^2}$$

(2.20.)

where $C_i \cdot \dfrac{1}{\sqrt{2 \cdot \pi \cdot \sigma_i}}$ is the area of each fitted peak.

The suitable number of peaks, p, is determined by visual assessment of the overall shape of the signal.

The fabric softener bases display complex DSC patterns, even after erasure of their previous thermal history (de-ageing). Figure 12 illustrates, as an example, the DSC pattern of a de-aged unperfumed softener base, sample B1_u, during a heating run (β=5°C/min). The DSC signal was normalised by the area under the curve, H_0, the conversion rate obtained $\dfrac{d\left(\dfrac{H_t}{H_0}\right)}{dt}$ plotted as a function of temperature.
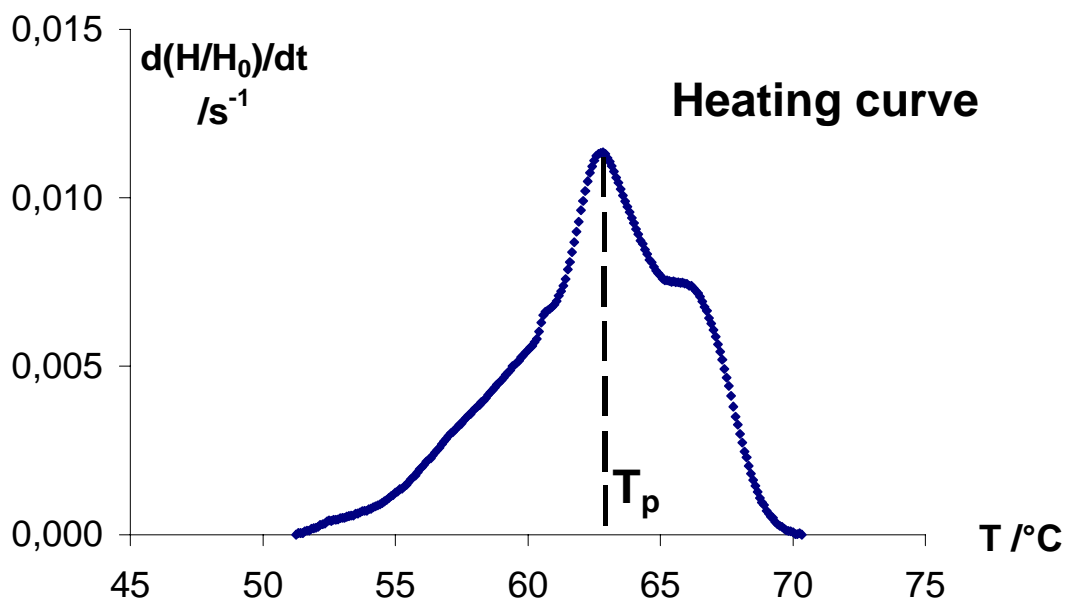
Fig. 12: Conversion rate (calculated from the DSC curve) of an unperfumed softener base (sample B1_u) recorded during heating with 5°C/min

Such complex patterns require a deconvolution procedure. In the case of the sample B1_u, the shape of the DSC signal strongly suggests the number of processes and consequently, the number of peaks, p, to be three.

The condition of performing the linear deconvolution algorithm requires that the linear combination of Gaussian functions is at each point as close as possible to the experimental data represented by the reaction rate of the whole endothermic process.

This is realised by applying the so-called least-square regression technique, which minimises the squared residuals. The fitting procedure is performed for a number of iterations until the coefficient of determination r^2, which characterises the quality of the fit, reaches its maximum.

For the sample taken as an example, namely the unperfumed softener base B1_u, the deconvolution procedure performed on the heating curve (Figure 12) and the three processes obtained in this way are shown in Figure 13. The heating curve obtained from the fitting procedure is also given; it approximates very well the experimental heating curve.
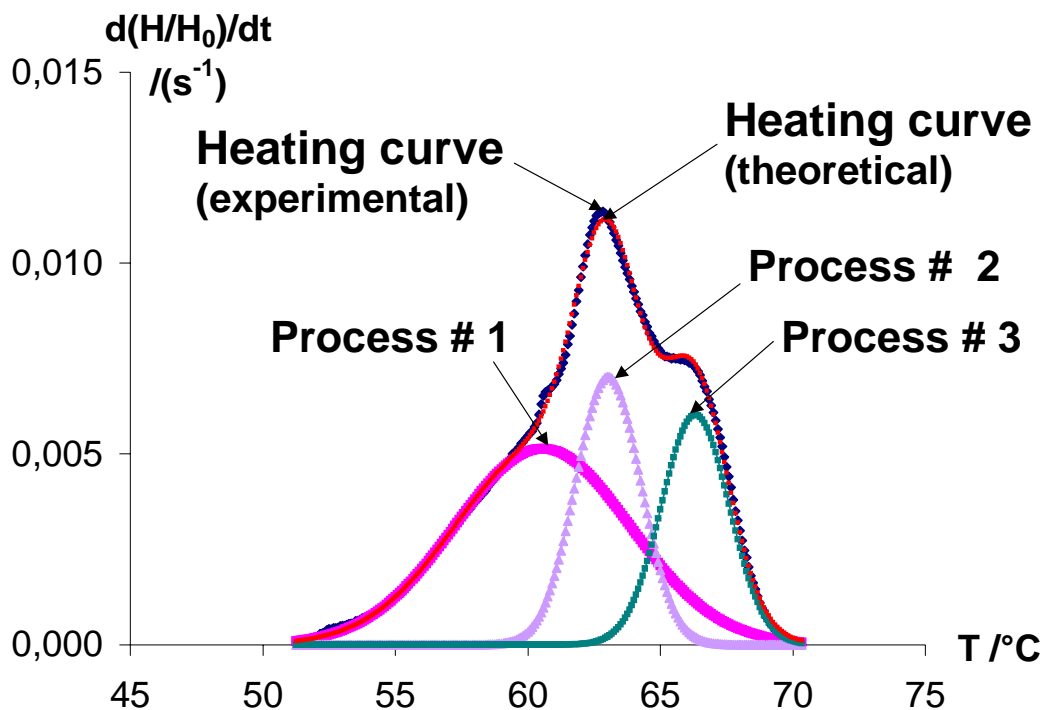
Fig. 13: The procedure of deconvolution for the DSC-heating curve of the sample B1_u (heating rate 5°C/min) with three Gauss curves corresponding to the underlying processes. The heating curve calculated from the fitting procedure is also shown.

After finding the best-fit parameters for the Gauss curves, the methods of non-isothermal kinetics are applied to each of these curves thus modelling the individual processes. This approach provides the values for their activation energies and pre-exponential factors, using the methods described below.

There are several methods for calculating the kinetic triplet, E_a, A and $f(\alpha)$, from thermal analysis data. The specific experimental conditions determine which approximation can be applied[163,164,165,166,167,168,169,170,171]. In some cases, a certain reaction model is assumed, implying a specific analytical form of the kinetic function, $f(\alpha)$.

There are also the so-called model-free methods which allow calculating the value of the activation energy, E_a, without any knowledge of the reaction pathway.
A simple approach is due to Kissinger[172]. The method is derived from the condition that the maximum of the signal is formed for the same degree of conversion for any heating rate, β. Imposing the condition for the signal to reach the maximum ($\frac{d^2\alpha}{dT^2}=0$ for T=T_p) and using equation **2.16.**, one obtains the equation that is the basis of Kissinger's method:

$$\ln\frac{\beta}{T_p^2} = -\frac{E_a}{R \cdot T_p} + \ln\frac{A \cdot R}{E_a} \cdot \left[-f_\alpha^{'}(\alpha)\right] \qquad \textbf{(2.21.)}$$

where T_p is the peak temperature and $f_\alpha^{'}(\alpha)=\frac{df(\alpha)}{d\alpha}$ the first derivative of the kinetic function refered to α.

The method allows to calculate the value of the activation energy, E_a, from the slope of the plot of $\ln\frac{\beta}{T_p^2}$ versus $\frac{1}{T_p}$. The pre-exponential factor, A, can be further inferred from the intercept, when $f(\alpha)$ is supposed to obey the relationship **2.10.**; in this case, $f'_\alpha(\alpha)$ = -1 in equation **2.21.**, if the assumption of first-order kinetics is made. Kissinger's method is a very powerful instrument for investigating the overall properties of a thermal effect.

However, the forced fitting of experimental data to simple reaction-order kinetic models can produce significant errors when predicting rates outside the experimental range of temperatures. For this reason, model-free methods are a suitable approach. These are iso-conversional methods[151], meaning that there are processing data acquired for the same degree of conversion from a series of experiments conducted at different heating rates. Literature considers them as the best approach for taking into account reaction mechanisms outside the experimental range of temperatures[173, 174].

There are two groups of such methods for calculating the parameters. First, there are:

- *differential methods* , which are based on the equation of the rate (in t) of the process **2.15.** in the logarithmic form:

$$\ln\left[\frac{d(\alpha)}{dt}\right] = -\frac{E_a}{R \cdot T} + \ln[A \cdot f(\alpha)] \qquad \textbf{(2.22.)}$$

The differential iso-conversional method is known in literature as Friedman's method[175]. It is based on a plot of $\left(\ln\dfrac{d\alpha}{dt}\right)$ versus $\left(\dfrac{1}{T}\right)$ for data acquired at several heating rates, β, for the same value of the conversion degree, $\alpha = \dfrac{H_t}{H_0}$, as given by equation **2.22.**. The slope of the plot is equal to $\left(-\dfrac{E_a}{R}\right)$, while the intercept is $\ln[A \cdot f(\alpha)]$. Assuming a certain form of f(α), the pre-exponential factor, A, can be further calculated. Several values of the degree of conversion, α, are selected, ranging from 0.2 to 0.9. The beginning and the end of the process are omitted (values below 0.2 and beyond 0.9) as the initiation and completion of a heterogeneous reaction are always complex processes.

There are also:

- *integral methods* , which consider the integral form of the reaction rate (in T) from equation **2.16.**:

$$\int_0^\alpha \frac{dx}{f(x)} = \frac{A}{\beta} \cdot \int_{T_0}^T e^{-\frac{E_a}{R \cdot y}} dy \qquad \textbf{(2.23.)}$$

where T_0 is the onset temperature (the highest temperature for which the reaction has not started). By writing:

$$g(\alpha) = \int \frac{d\alpha}{f(\alpha)} \qquad \textbf{(2.24.)}$$

for the integral of the kinetic function and

$$h(T) = \int \exp\left(-\frac{E_a}{RT}\right) dT \qquad \textbf{(2.25.)}$$

for the temperature integral, one may write

$$g(\alpha) = \frac{A}{\beta} \cdot h(T) \qquad \textbf{(2.26.)}$$

The temperature integral cannot be solved analytically and there are many approximations proposed for easy calculation. As a consequence, there are also many integral methods. All of them can be generally written as:

$$g(\alpha) = \frac{A}{\beta} \cdot e^{-\frac{E_a}{R \cdot T}} \cdot L(T)$$

(2.27.)

where L(T) is a constant depending on the approximation used.

For the same α (iso-conversional condition) on curves recorded at the same β, equation **2.27.** can be rewritten, after rearranging and taken the logarithms:

$$\ln\beta = -\frac{E_a}{R \cdot T} + \ln\left[\text{constant} \cdot A\right]$$

(2.28.)

where the "constant" term includes the integral of conversion and the approximation constants from the temperature integral.

The integral iso-conversional approach used in this work is Flynn-Wall-Ozawa's method[176]. It is based on a plot of $\ln(\beta)$ versus $\frac{1}{T}$ for data acquired at several heating rates, β, for the same value of the conversion degree, $\alpha = \frac{H_t}{H_0}$, as given by equation **2.28.**.

The slope of the plot equals $\left(-\frac{E_a}{R}\right)$. The plots are also considered within the 0.2-0.9 limits for α, for the reasons given above.

While the differential methods refer to local data and offer the values of the kinetic parameters at a given point, the integral ones refer to interval data and offer the values of the kinetic parameters averaged for the considered interval.

3.   **EXPERIMENTAL PART**

3.1. **Materials**

Initially, three softener bases have been used for evaluating the potential of thermal analysis methods to describe their stability. These bases were either unperfumed (reference) or supplemented with three different types of fragrances: alcohol, aldehyde and ketone (three of each type). Codes and description for all samples are given in Table 2.

Tab. 2: Fabric softener bases, unperfumed and perfumed with industrial fragrances and their codes

Code	Unperfumed	Perfumed with alcohol	Perfumed with aldehyde	Perfumed with ketone
Base 1	B1_u	B1_ac1	B1_ad1	B1_kt1
		B1_ac2	B1_ad2	B1_kt2
		B1_ac3	B1_ad3	B1_kt3
Base 2	B2_u	B2_ac1	B2_ad1	B2_kt1
		B2_ac2	B2_ad2	B2_kt2
		B2_ac3	B2_ad3	B2_kt3
Base 3	B3_u	B3_ac1	B3_ad1	B3_kt1
		B3_ac2	B3_ad2	B3_kt2
		B3_ac3	B3_ad3	B3_kt3

Fabric softeners bases were kindly provided by IFF B.V. (Hilversum, Nederland).

Different cosmetic creams have been also analysed, selecting three representative classes:

∗**o/w emulsion**

∗**w/o emulsion**

∗**w/o/w emulsion**

Cosmetic emulsions were kindly provided by Beiersdorf AG (Hamburg, Germany).

3.2. Methods and instruments

Thermal analysis

The non-isothermal experiments were first performed with a Power compensated DSC 7 (Perkin Elmer). Measurements were run in closed aluminium pans. An empty closed pan acted as reference. DSC calibration was done with indium (melting point T_m= 156.60°C, enthalpy ΔH=28.45J/g) and palmitic acid (melting point T_m= 63°C) for the temperature range 0 -150°C.

The usual temperature programme ranged from 0 to 100°C/min, with 1 min isothermal step before each heating or cooling. The temperature programme was run for the fabric softener with the same sample and comprised the folowing steps:

∗a de-ageing thermal cycle of two heating and cooling runs with 10°C/min for elimination of undesired relaxation processes

∗a second thermal cycle of two heatings and coolings with 10°C/min for reproducibility examination

∗a thermal cycle of four heatings with 5,10,15 and 20°C/min,

whereas the cooling rate remained always the same:10°C/min.

Temperature programme for cosmetic creams comprised:

∗a cycle of two heatings and coolings with the same heating rate: 1; 2.5, 5; 7.5; 10; 15 and 20°C/min, respectively,

whereas each step was run with different samples.

Non-isothermal measurements were also performed with the Heat flow DSC 204 (Netzsch) in closed aluminium pans.

The usual temperature programme ranged between 0 and 85°C/min, with isothermal steps of 5 min before each heating or cooling.

For cosmetic creams a temperature programme comprised:

∗a thermal cycle of two heating and cooling runs with the same heating rate: 5; 7.5; 10 and 12.5°C/min respectively,

whereas each step was run with different samples.

Optical microscopy

Optical microscopy examinations were performed with a Leitz-Aristoplan optical microscope equipped with a digital Quantimet 570 camera (Cambridge Instruments):

-**A steady-state examination** (magnification 400 x) in:

∗bright field

and

∗polarised light

or

- **A dynamic examination** (magnification 320 x) on a heating stage (Mettler), with a temperature programme comprising heating and cooling with 5°C/min between 0 and 85°C/min

Software for kinetical analysis: The DSC data were analysed with programmes written in Excel (Microsoft), with Origin (Microcal^{TM}) and Peak Fit (Jandel Scientific).

4. __RESULTS AND DISCUSSION__

4.1. DSC investigation of fabric softeners

Fabric softeners are simple technical emulsion systems and therefore suitable model formulations for studying their thermal behaviour and, as a consequence, their kinetic performance.

4.1.1. Investigations of three base formulations

Three different type of fabric softeners formulations, i.e. the unperfumed bases B1_u, B2_u and B3_u, with three different types of industrial fragrances, i.e. alcohol (ac_1, _2 and _3), aldehyde (ad_1, _2 and _3) and ketone (kt_1, _2 and _3), were first analysed. The unperfumed bases are emulsion systems of water, surfactant (cationic surfactant of the quaternary ammonium compound type) and polymer (as non-ionic co-surfactant). They are suitable emulsion models for investigating the influence of fragrance addition and of storage time as well as extreme temperatures on thermal stability.

4.1.1.1.   Qualitative observations

4.1.1.1.1.   Unperfumed samples. The concept of "rejuvenation"

A specific feature of the emulsions is, that in some cases their DSC plots show a complex, noisy pattern of superposed relaxation processes when they are heated and cooled from 0 to 100°C and back for the first time. These patterns may even differ for samples of the same product. After one heating/cooling cycle the DSC pattern obtained in a subsequent test appears to be free of the additional „noise" and generally simplified. The possible explanation of this phenomenon is that the first heating/cooling programme removes the thermal history of the sample. The sample can be seen as de-aged or "rejuvenated". This initial procedure of de-aging brings all samples to a comparable starting state. At the same time, this procedure enables to eliminate those thermal processes which play no relevant role in the long-term behaviour of the samples.

DSC heating curves show the occurrence of endothermic processes in the temperature range of 40-70°C. The reversibility of these processes is shown by the corresponding exothermic effects on the cooling plot.

In order to observe the effects of de-ageing on signal reproducibility, heating-cooling cycle was applied repeatedly.

The DSC profiles, that is the conversion rates $\dfrac{d\left(\dfrac{H_t}{H_0}\right)}{dt}$ are plotted in Figure 14 for the three unperfumed samples B1_u, B2_u, B3_u. The curves show that the second thermal cycle assures reproducible heating and cooling curves for all samples, with the exception of B1_u unperfumed sample, where the DSC during heating shows some differences. This sample will be considered separately.
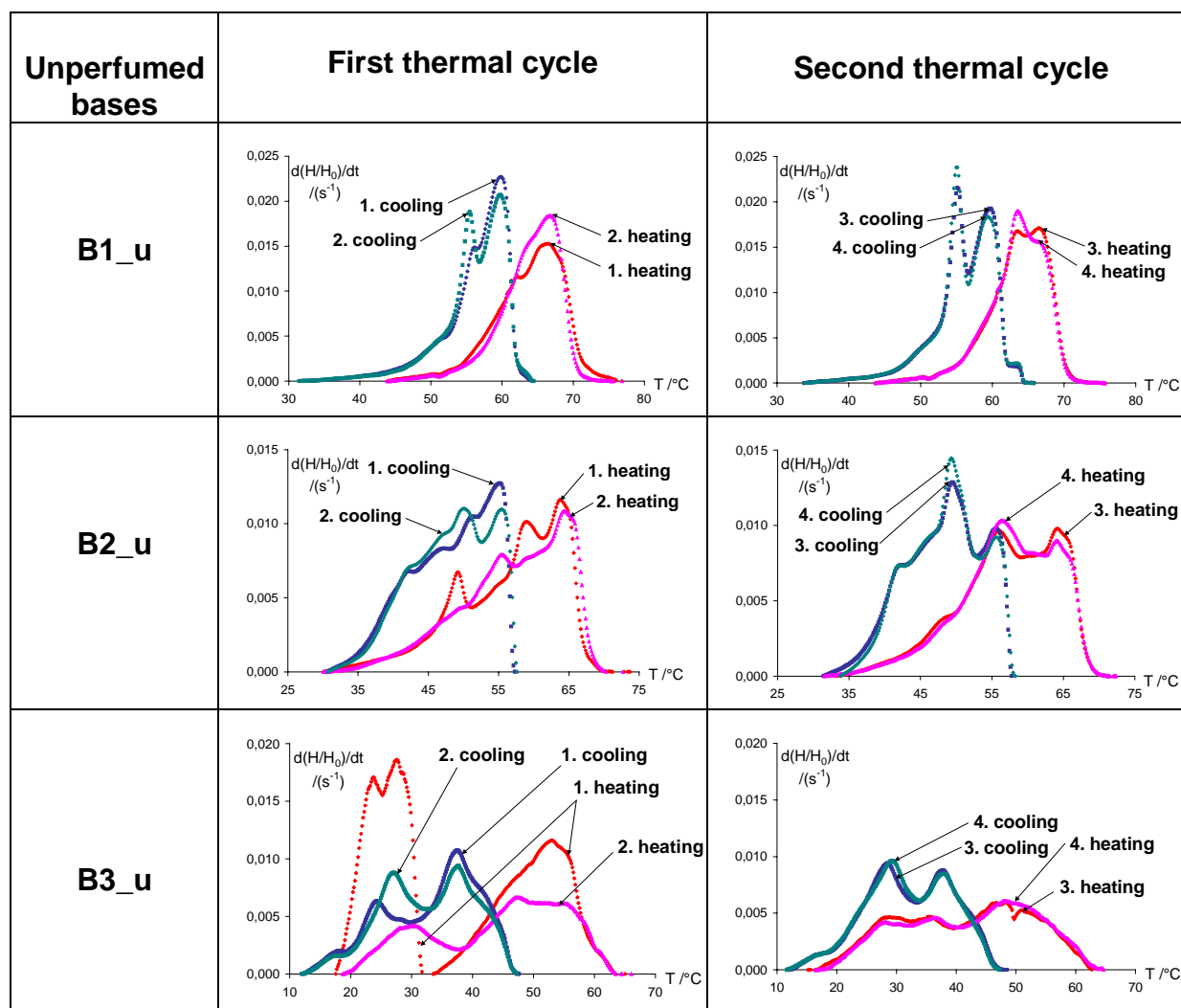
Fig. 14: Conversion rates (calculated from DSC plots) of the three *unperfumed bases B1_u, B2_u* and *B3_u* from two consecutive thermal cycles (β=10°C/min)

The low reproducibility shown by B1_u is probably due to continuously temperature-induced rearrangements of the sample during the two rejuvenation cycles. As a consequence of the consecutive tests, one observes the phenomenon of „interchange of importance" of the peaks. As a result, the initial main peak and the shoulder reverse their sizes. This curve appearance then corresponds to a stable state on 3rd and 4th heating, that can be further analysed.

Following these observations, the further analysis deals primarily with two-times thermally cycled samples.

The stability of the DSC patterns for B1_u is also reached with time, namely after 1.5 years of storage, as shown in Figure 15.
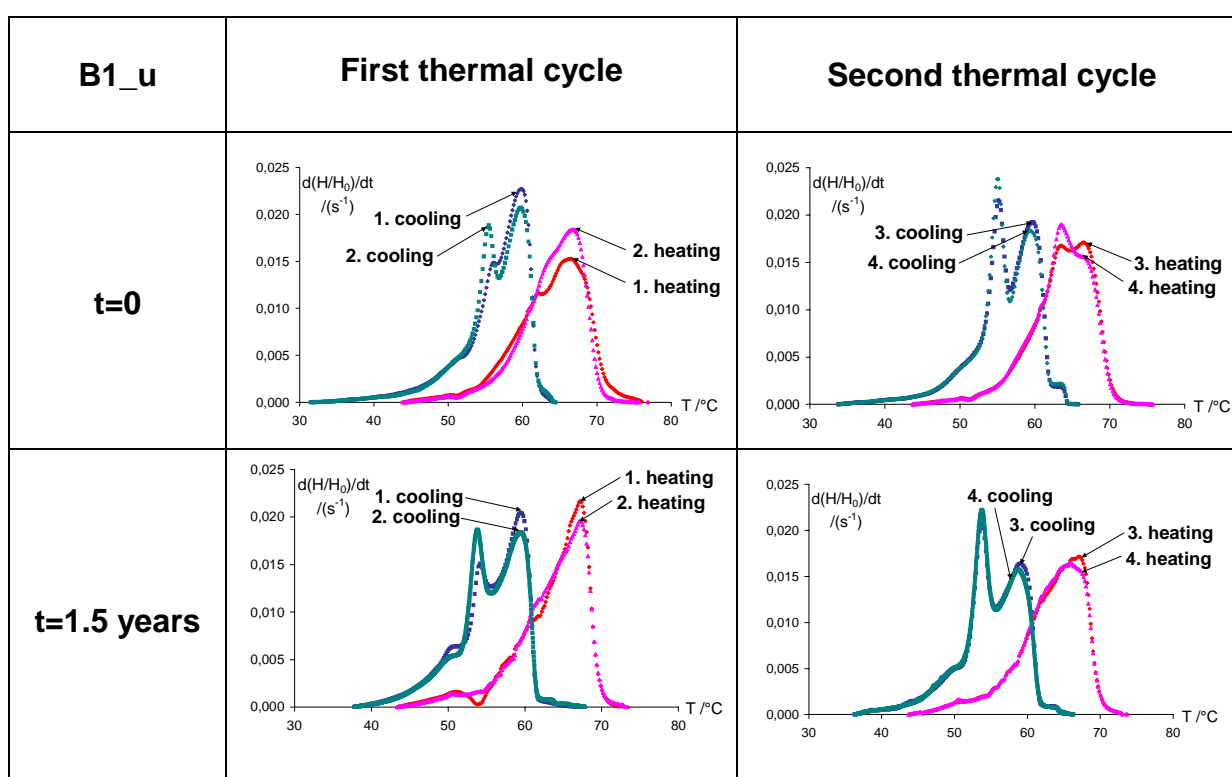
Fig. 15: Conversion rates (calculated from DSC plots) of *unperfumed base B1_u* for two different times and from two consecutive thermal (β=10°C/min)

4.1.1.1.2.   Influence of fragrance addition

The shape of the DSC signal changes, if fragrance is present in the formulation.

As may be seen in Figure 16 for samples containing one of each type of the industrial fragrances, namely the bases B1 _ac1, B1_ad1 and B1_kt1, the addition of fragrance to B1 base „simplifies" the DSC plot, in that the peak structure shows a less complicated

pattern. It is possible that the pattern "simplification" is due to a rearrangement of the surfactant when interacting with fragrance molecules, towards a simpler phase structure.
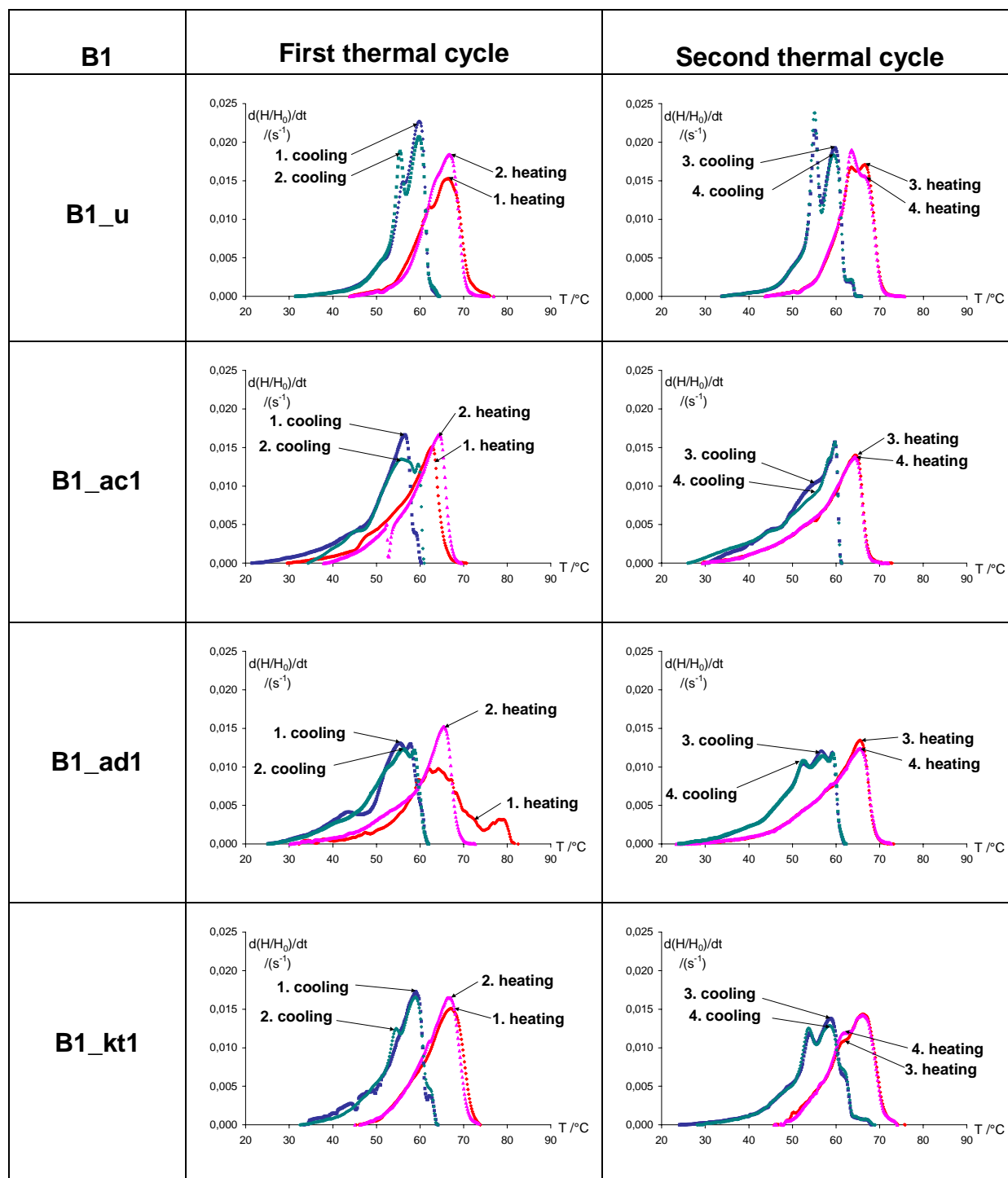
Fig. 16: Conversion rates of base *B1* with *ac_1, ad_1* and *kt_1* fragrances compared with the unperfumed base after two consecutive thermal cycles (two heating-cooling runs, β=10°C/min)

This feature is readily observed in the case of the perfumed samples group B1 _ac1, B1 _ac2, B1 _ac3, where the „simplification" leads to a single, but asymmetrical peak structure. In the case of bases with the other two different types of fragrances, namely the

group B1 _ad1, B1 _ad2, B1 _ad3 and the group B1 _kt1, B1 _ kt 2, B1 _ kt 3, it is noticed that the number of processes taking place upon cooling are more than the number of those which are observed upon heating. This may be explained by the different rates of structures reformation on cooling, due to a more complex kind of interaction between components when the two types of fragrances are present. The most complex type of interaction is surely present in the group of perfumed bases B1 _kt1 (see Figure 16), B1 _ kt 2, B1 _ kt 3, by which the heating as well as the cooling pattern show the occurrence of more thermal processes as in the case of the other two groups of perfumed samples.

As a general feature and compared to the unperfumed samples, the perfumed ones have not only reproducible cooling, but also heating curves while running the second thermal cycle. This fact suggests the formation of a defined structure after the performance of thermal cycles.

Selected samples of B2 and B3 perfumed bases are plotted in Figures 17 and Figure 18 and are compared with the unperfumed references. A similar „simplified" peak structure as well as reproducible conversion rates while running the second thermal cycle are observed for both perfumed B2 and B3 bases as well as in the case of bases B1 containing fragrances. One also observes more thermal processes in the cooling than in the heating curve, as for the perfumed samples of base B1.

As an overall observation, one may notice some other peculiarities. Regarding the shape of the DSC signal, one observes that B2 base perfumed with ac1, ad1 and kt1 forms a distinct group, similarly as ac2, ad2, kt 2, and ac3, ad3, kt3. Figure 17 shows as typical examples the conversion rates obtained for three of the B2 bases, each with a different type of fragrance.
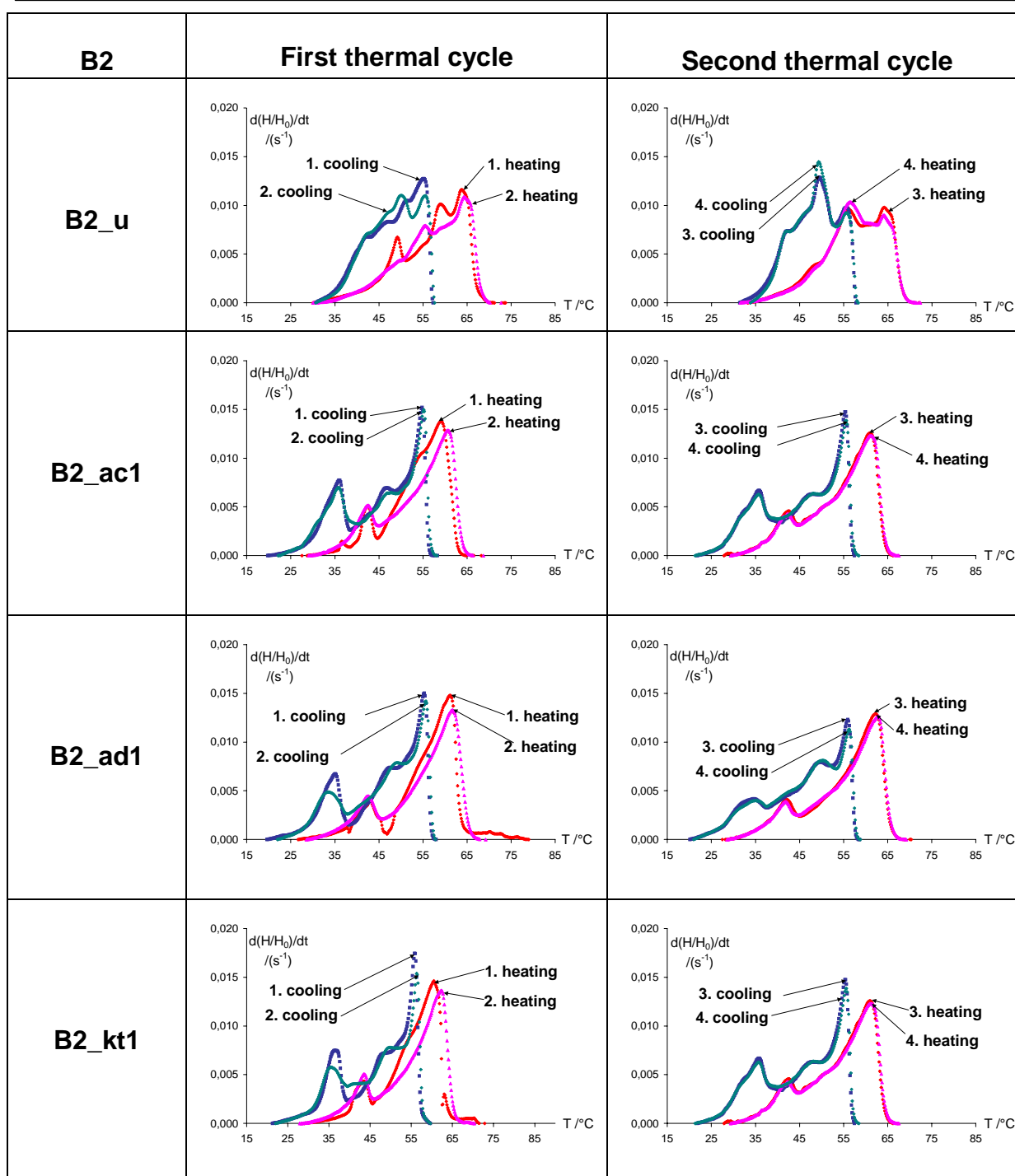
Fig. 17: Conversion rates of base *B2* with *ac_1, ad_1* and *kt_1* fragrances compared with the unperfumed base after two consecutive thermal cycles (two heating-cooling runs, β=10°C/min)

One also observes that base B3 seems to exhibit the same pattern irrespective of the fragrance added. Figure 18 illustrates the conversion rates for base B3 with three different types of fragrance.
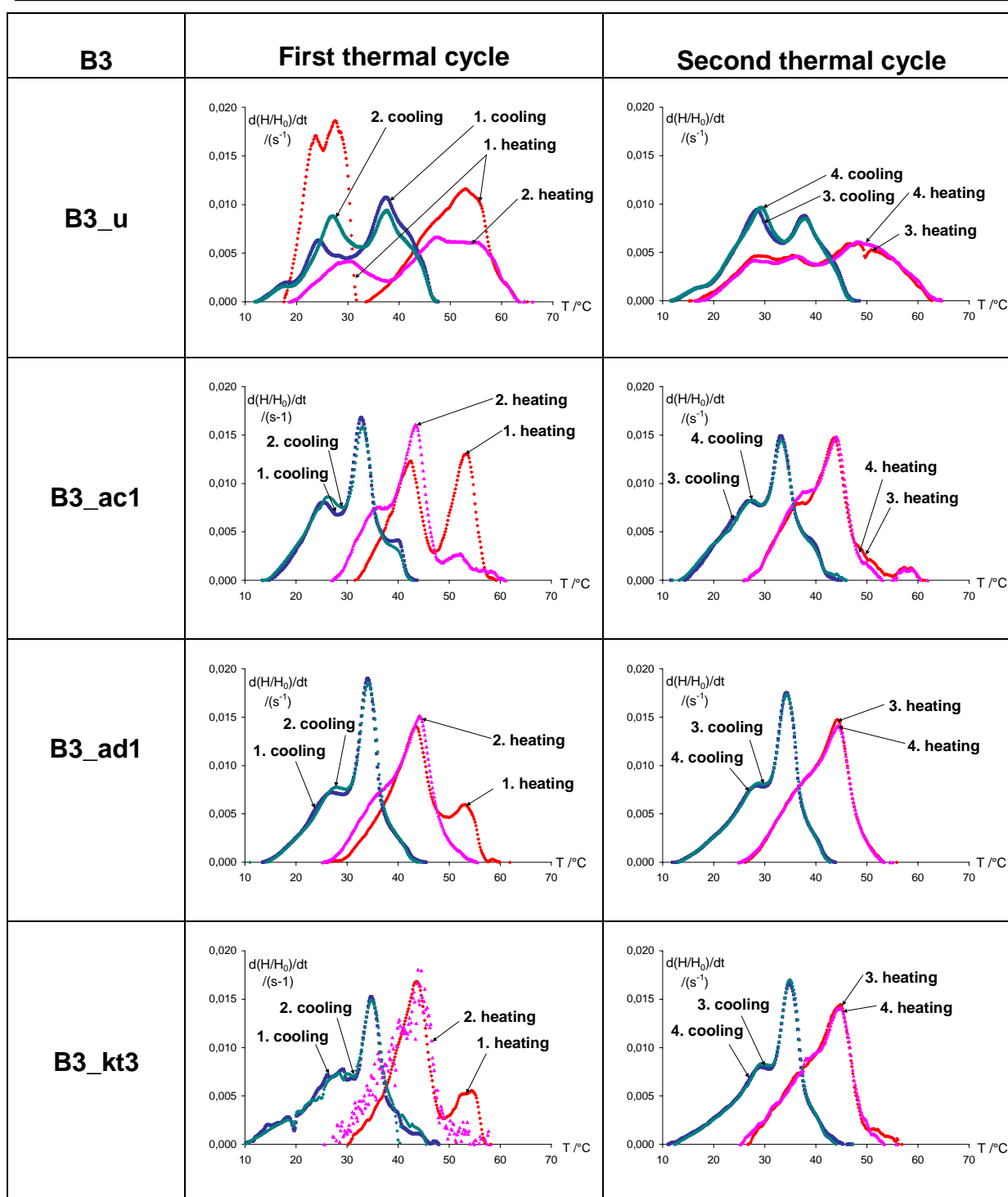
Fig. 18: Conversion rates of base *B3* with *ac_1, ad_1* and *kt_1* fragrances compared with the unperfumed base after two consecutive thermal cycles (two heating-cooling runs, β=10°C/min)

In order to examine the influence of fragrance addition in terms of structural changes, steady-state optical microcopy examinations were performed. The microscopic appearances of perfumed bases as compared to the unperfumed ones are illustrated in Figures 19, 20 and 21 for B1, B2 and B3 samples, respectively. As a general feature, the samples display a population of vesicles and lamellar structures with different vesicles/lamellae ratios. Most of the structures are of multilamellar type.

For B1 base, although the liposome density is rather low, there are multilamellar liposomes and associations of different geometrical structures to be seen. The samples are not hardened, except B1_ac3 base, where rod-like structures are present. Figure 19 shows photomicrographs of the unperfumed base B1_u and of three perfumed bases, each with a different type of fragrance, whose thermal behaviour has already been shown in Figure16 .
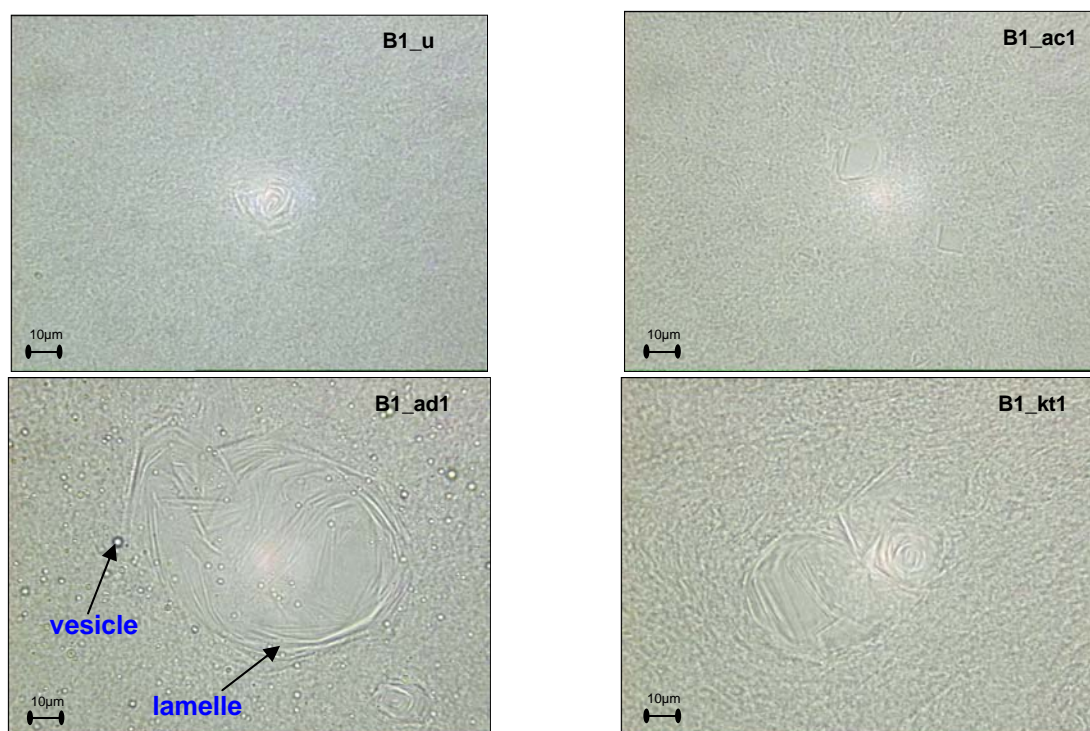
Fig. 19:   Optical micrographs of *B1 perfumed bases* compared with the unperfumed one (magnification 400 ×)

An interesting observation is that in case of base B2 all perfumed samples are hardened. The lamellar structures of various dimensions and number of lamellae as well as of different geometrical structures are of high density; the unperfumed sample shows even impressive big multilamellar structures. The microscopic aspect of the unperfumed base B2_u and of three different bases with fragrances whose DSC pattern was shown in Figure 17, is illustrated in Figure 20.
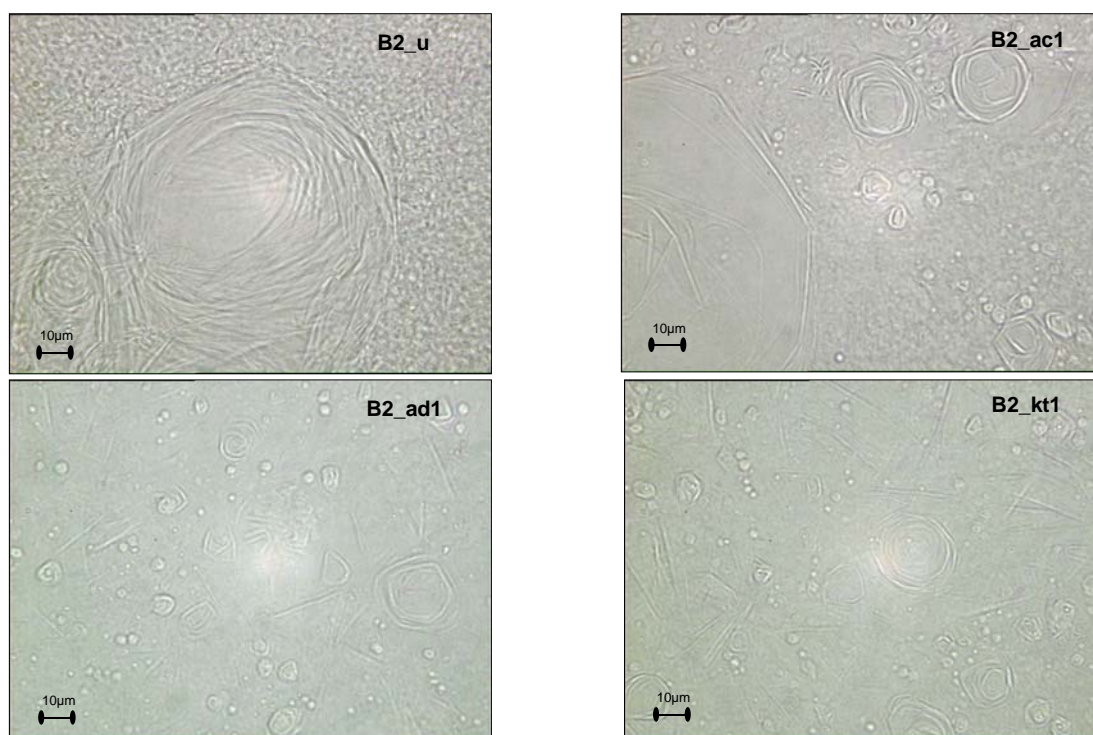
Fig. 20: Optical micrographs of *B2 perfumed bases* compared with the unperfumed one (magnification 400 ×)

The B3 base has a small lamellae population, which differentiate from each other by their density; the samples are of blue colour (they contain additionally a dye) and are not hardened. Figure 21 illustrates the microspopic appearance of the same samples chosen in Figure 18 to show their DSC profile: the unperfumed base B3_u and three other perfumed bases, each with a different type of fragrance.
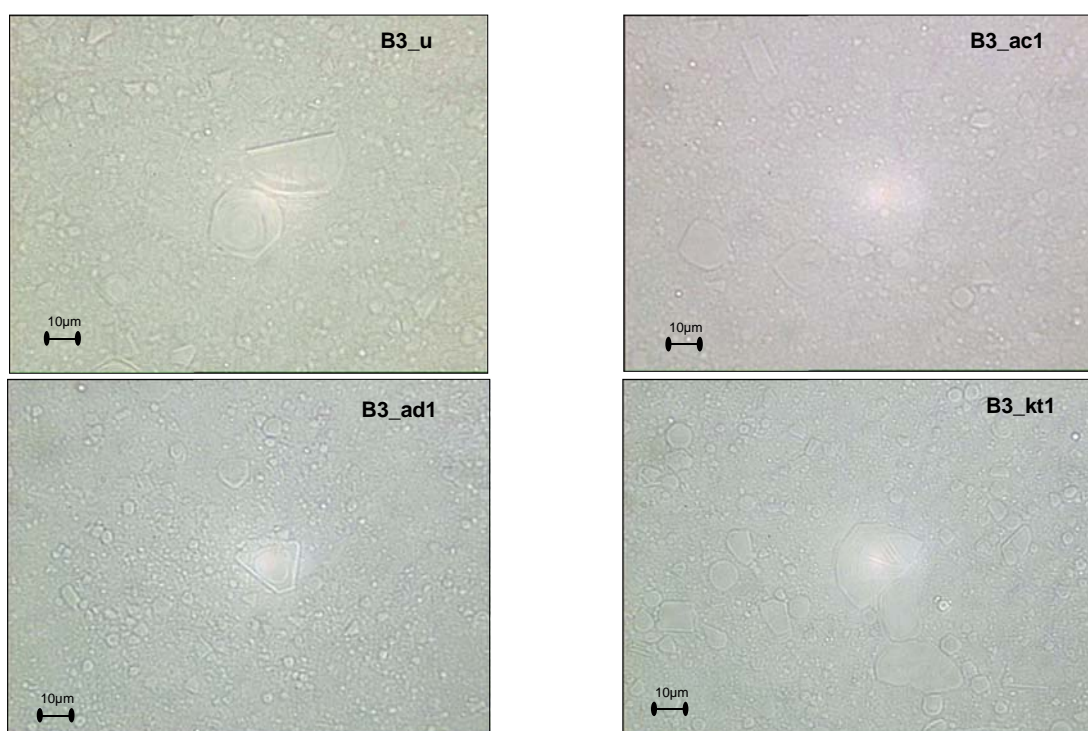
Fig. 21: Optical micrographs of *B3 perfumed bases* compared with the unperfumed one (magnification 400 ×)

4.1.1.1.3.   Influence of storage time on unperfumed base 1 (B1_u)

As already pointed out, the unperfumed sample B1_u shows some peculiarities which will be looked at more closely. In the following the influence of storage time on the stability of the sample is investigated. Figure 22 shows the conversion rate curves for five different storage times. A characteristic seems to be the disappearance of the shoulder at approximately 63°C from the heating curve and the gain of importance of the main shoulder at approximately 55°C on the cooling curve with time. There is a continuous change of the DSC curves with time toward a final structure, which becomes more and more evident after about 1.5 years. After 2.5 years, one observes that not only the heating and cooling curves are perfectly coinciding even from the first thermal cycle (this phenomenon starts already after two years), but also the shape of the cooling runs returns almost to an „initial" state, with the „reforming" of the shoulder at 55°C. It can be therefore observed, that a continuous change of DSC curves with time toward final structure after about 1.5 years takes place. The kinetic implication of this change will be discussed below.

The same samples were observed microscopically in bright and polarised light (400 x) with the optical microscope to obtain structural information about the extent to which the thermal cycle affects the emulsion appearance after long storage times, namely for 2 and 2.5 years. Figures 23 and 24 give the optical micrographs of sample B1_u for the long storage times before and after performing a thermal de-ageing cycle of two heatings and two coolings.

After running the temperature cycle, the 2 years old B1_u shows an increase in viscosity and restructuration of the vesicles and lamellae in a more compact structure with an increased concentration of multilamellar small vesicles and with additional other fine organised structures in the medium. In polarised light these fine structures are also visible and the lamellae appear both before and after the temperature cycle as anisotropic (birefringent). The stable structure formed after the thermal cycle, as seen in Figure 23, is similar to that already obtained after one heating-cooling run (here not shown). This fact corresponds clearly to that of the DSC patterns (Figure 22).

Storage time	First thermal cycle
0	
1 month	
1.5 years	
2 years	
2.5 years	
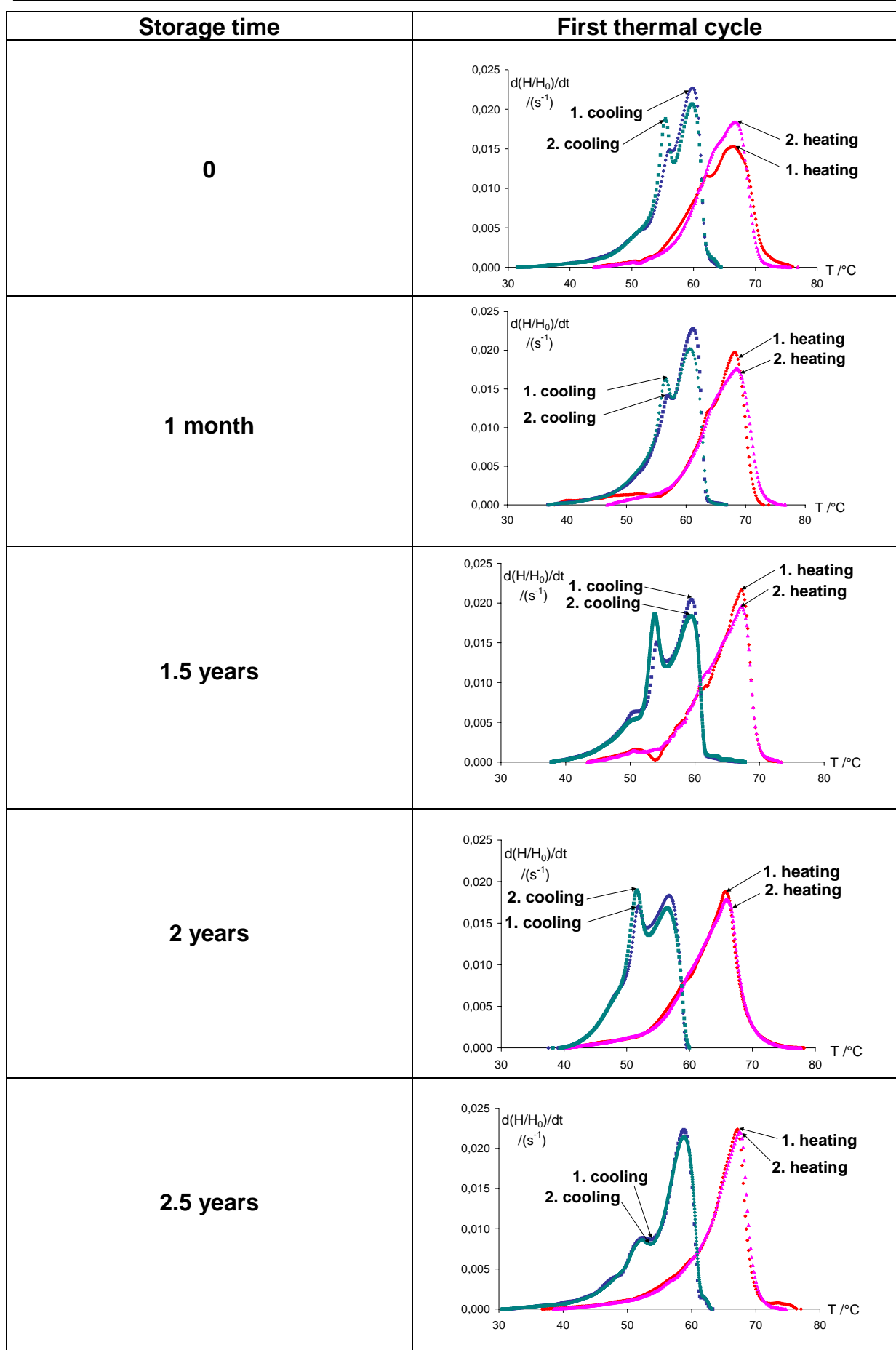
Fig. 22: B1_u *unperfumed base* at five different moments in time. Conversion rates from DSC plots recorded with 10°C/min during a de-ageing thermal cycle
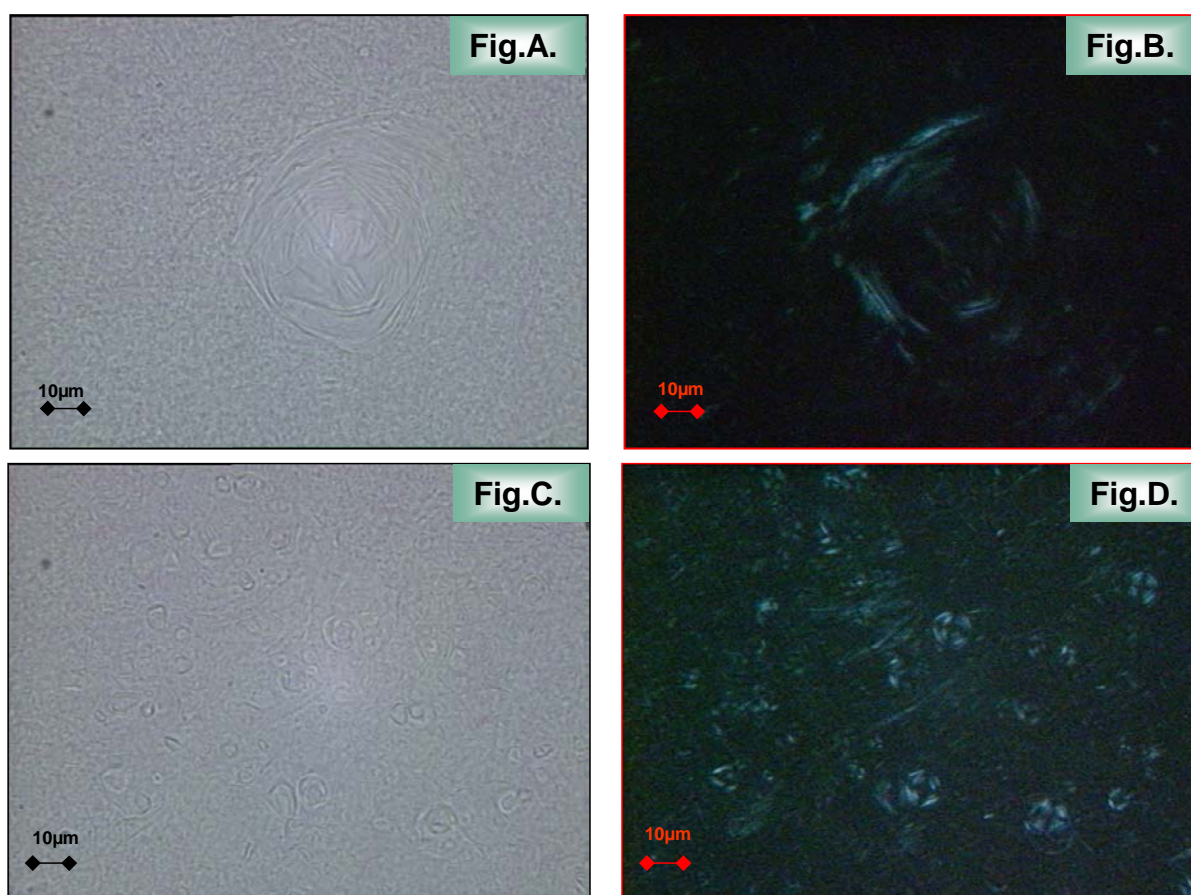
Fig. 23: Optical micrographs in bright light and polarised light of the 2 years old *unperfumed base B1_u* before (Fig.A and Fig.B) and after (Fig.C and Fig.D) a double thermal DSC heating-cooling programme with 10°C/min (magnification 400 ×)

The 2.5 years old unperfumed sample B1_u has a new, stable pattern after performing the temperature cycle with respect to the initial state, supporting also the results obtained in the DSC experiment. The vesicle population looses its importance beside the formation of lamellar structures of various dimensions, most of them with a multilamellar appearance, as shown in Figure 24.
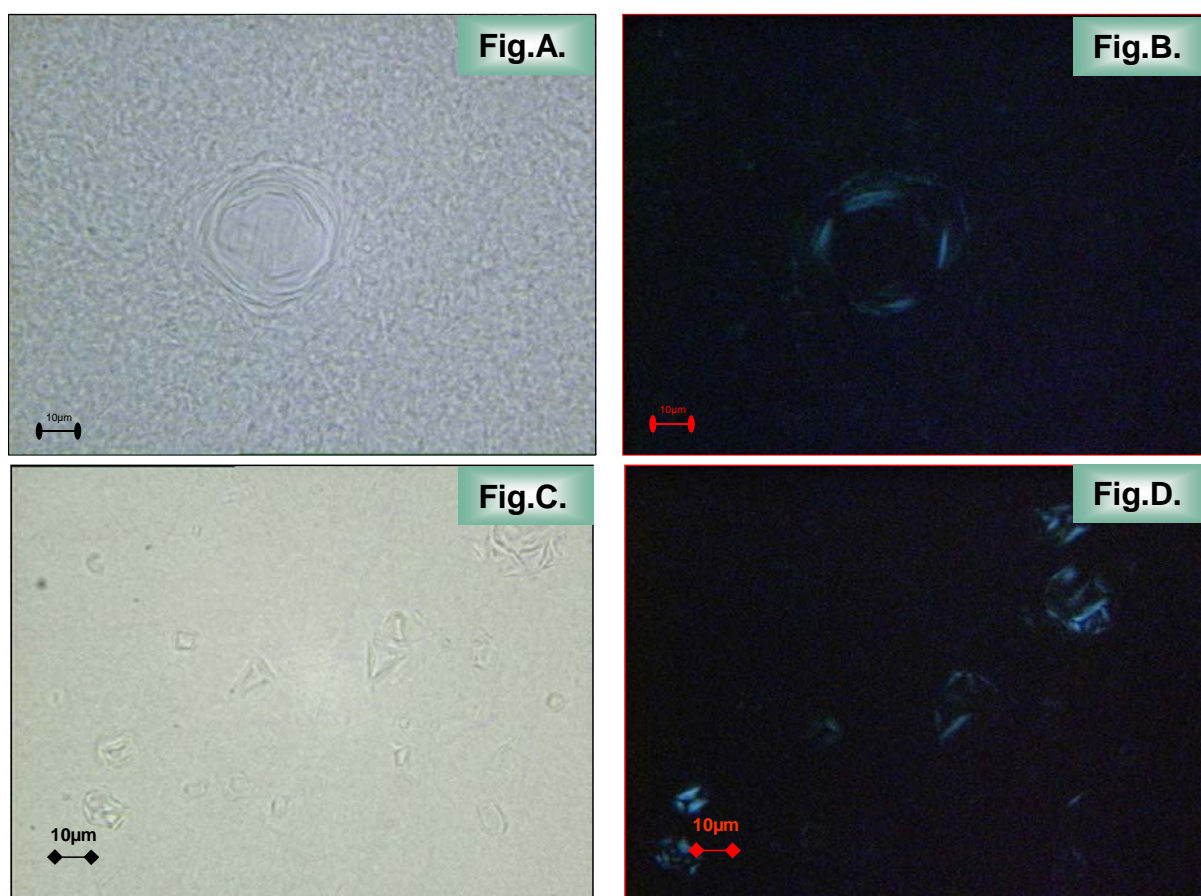
Fig. 24:   Optical micrographs in bright light and polarised light of an 2.5 years old *unperfumed base B1_u* before (Fig.A and Fig.B) and after (Fig.C and Fig.D) a double thermal DSC heating-cooling programme with 10°C/min (magnification 320 ×)

More refined information about the structural changes taking place in the sample, while running a heating followed by cooling, could be inferred from thermomicroscopy investigations. The 2 years old unperfumed sample B1, where both the heating and cooling curves are reproducible for the first time, is a very good choice for this analysis. The appropriate scanning rate is of 5°C/min.

Figure 25 shows the structural modifications which take place in the unperfumed sample B1_u while subjecting it to a heating-cooling programme with 5°C/min on a heating stage under the optical microscope. While heating, the vesicles undergo rearrangements.
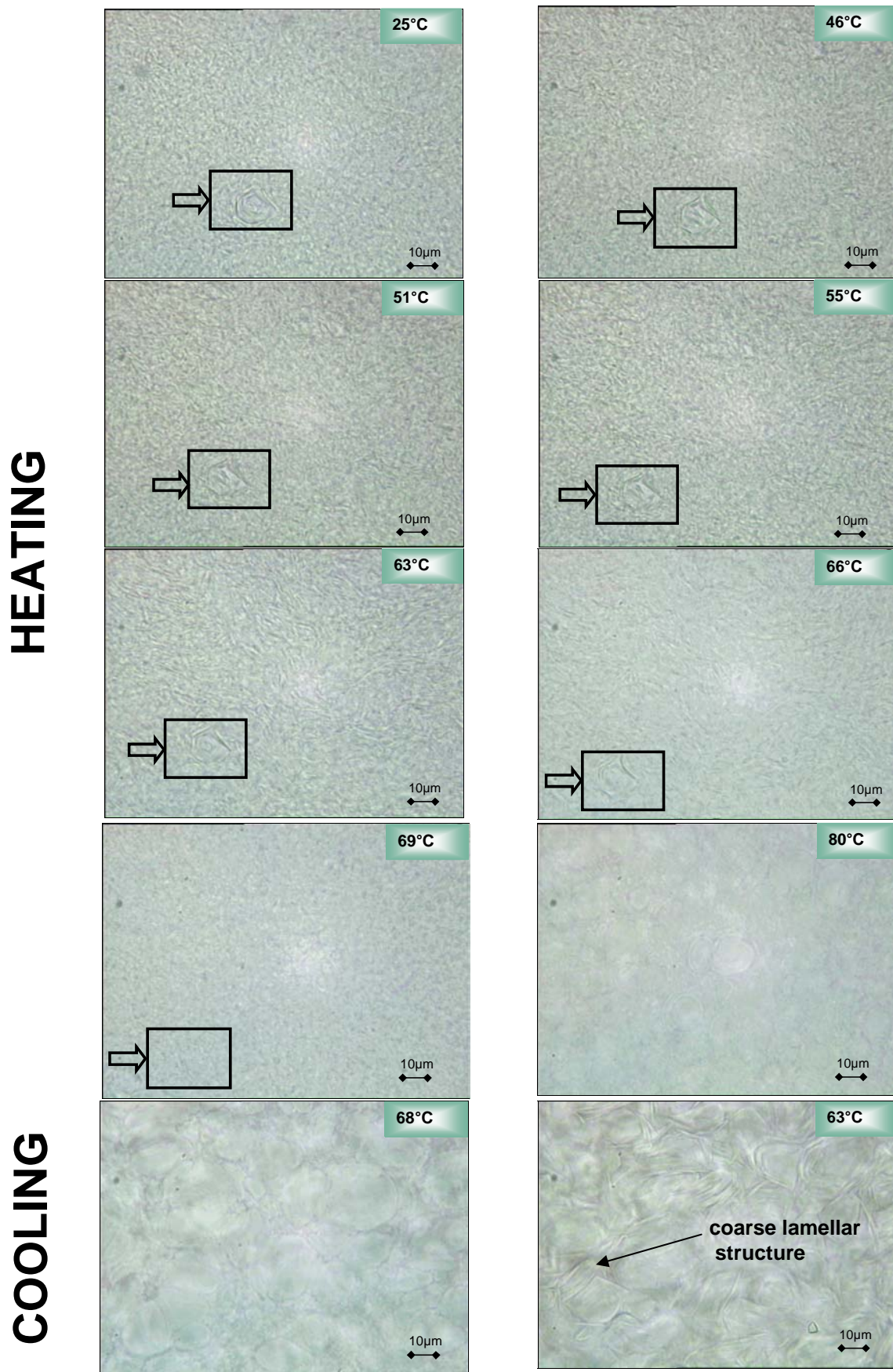
Fig. 25: Optical micrographs of *unperfumed base B1_u* during a heating/cooling programm with 5°C/min between 25°C and 80°C; in the frame: a multilamellar structure (magnification 320 ×)

The melting of vesicle structures begins at 66°C, corresponding to the main peak in the DSC heating curve, as shown in Figure 26. Further heating is accompanied by the gradual disappearance of the whole vesicular structure. While cooling progresses, structures are forming, at 60°C, corresponding to the main peak in the exothermic DSC pattern.
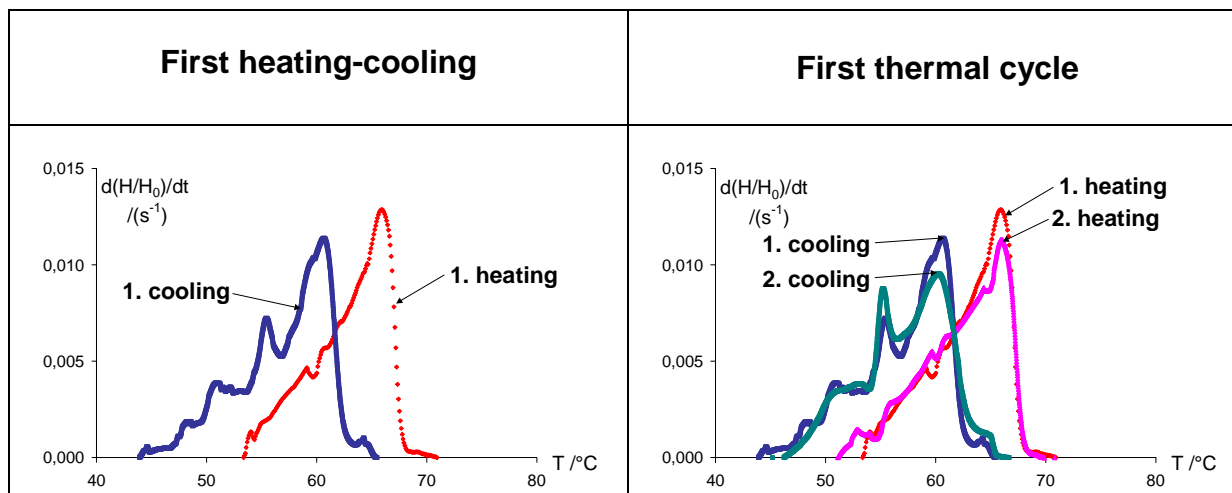
Fig. 26: Conversion rates of unperfumed base *B1_u* for the first heating/cooling run and for a thermal cycle of two heating/cooling runs (β=5°C/min)

It is worth noting that the modifications observed at different temperatures while cooling, differ from those shown on photos of samples from closed DSC pans after a temperature programme. This is due to the imperfect thermal insulation of the sample on the hot stage from the environment. Although this experiment is not able to reproduce entirely the processes taking place while performing the DSC temperature programme, it gives a deeper insight into the evolution of thermal processes while heating and cooling and gives also evidence on structural reformation of the emulsion after the temperature-induced disorder.

Because of the lack of other evidences it can only be speculated what happens with the bases when subjected to the DSC cycle only from optical microscopy appearance and its correlation with the DSC pattern. The fabric softeners display under the microscope a mixed vesicles/lamellae structure. Thermomicroscopical examination of the unperfumed sample shows that upon heating, the lamellae undergo a transition to vesicles in a defined temperature range; this corresponds to the endothermic peak observed in the DSC plots. The disorganisation of the vesicles into individual surfactant molecules follows later. Such vesicle-lamellae transition (in form of micelle-liposome transition) has already been observed when heating cationic lipid-based liposomes[177] used in biology for genetic transformation.

It is likely that before undergoing the transition, the lamellae must pass through a preliminary, gel-to-liquid crystalline phase (lamellar)-transition, that was observed for liposomal phospholipids[178]. Cationic stabilising agents and quaternary ammonium fabric softeners[179] also show such characteristic transition temperatures. The gel-to-lamelar liquid crystall (Lβ to Lα) transition of lamellae in the unperfumed base B1_u relates to the shoulder that accompanies the main peak of the endothermic effect. During the cooling run, the intermediate gel-to-liquid crystalline phase transition should also occur, because of the DSC plots showing identical patterns. We can, actually, observe thermomicroscopically the formation of lamellae structures upon cooling. Optical microscopy examination of the B1_u sample after a DSC heating-cooling run confirms the existence of a mixed vesicles/lamellae structure. Fusing of vesicles to lamellae has been observed to occur in some phospholipid dispersions upon cooling, although this has been proved to be an irreversible process[180]. Consequently, lamellae-to-vesicles transition in both directions seems to be, according to the literature, a composition-dependent process. The thermal behaviour of B1_u supports the hypothesis of a reversible process or at least of a quasi-reversible one, i.e. the formation, after a temperature cycle, of a new stable structure with a similar appearance as before the heating-cooling runs. The hypothesis of the formation of a stable, but new, emulsion structure after running temperature cycles can be extrapolated for the perfumed sample.

Although the thermal processes of fabric softeners (perfumed or unperfumed bases) are not perfectly reversible, as we expect in the case of simple surfactant associations in water, where the Krafft point of a surfactant decides about dissociation and reassociation phenomena of molecules as function of temperature, the shape of the DSC plots indicates a certain degree of reversibility, with reversible contributions being superposed with irreversible ones.

4.1.1.4.   Influence of low temperature storage on unperfumed base 1 (B1_u)

Extreme temperatures lead to instability efects, presumably in the form of hardening effects.

In order to investigate the effect of low temperatures on unperfumed base B1_u, three samples from a 1.5 years old base were stored in closed pans at 4°C for 7days, 14 days and for a month respectively. Before storage, they were de-aged, by running a double heating-cooling thermal run. After storage, before analysis, the samples were once de-aged, according to the same procedure. In this way, the samples were two-times de-aged before further analysis, enabling comparison. Conversion rates from DSC plots obtained before and after storage are illustrated in Figure 27.

One can observe that the storage at low temperature produces modifications both on the heating and on the cooling runs. These modifications are similar when stored at 4°C for one and for two weeks. The cooling runs are superposable, the main peak at 60°C becomes a shoulder and the secondary peak at 55°C transforms into the main peak. The heating curve has a double peak structure, which transforms into a single peak structure with a contribution at 60°C (corresponding to the initial shoulder in the heating curve) after the first heating-cooling procedure.

The storage of samples for 1 month at 4°C induces differences in both heating and cooling plots.

One also observes, that while the de-ageing progresses for B1_u, the peak at 55°C on cooling increases and becomes the main contribution in the DSC curve. This peak increases also with storage time and remains the only significant contribution after storage at low temperatures (4°C). Macroscopical observations show that the viscosity of the sample increased (hardening effect). This suggests that this peak may be related to the viscosity properties of the emulsion.
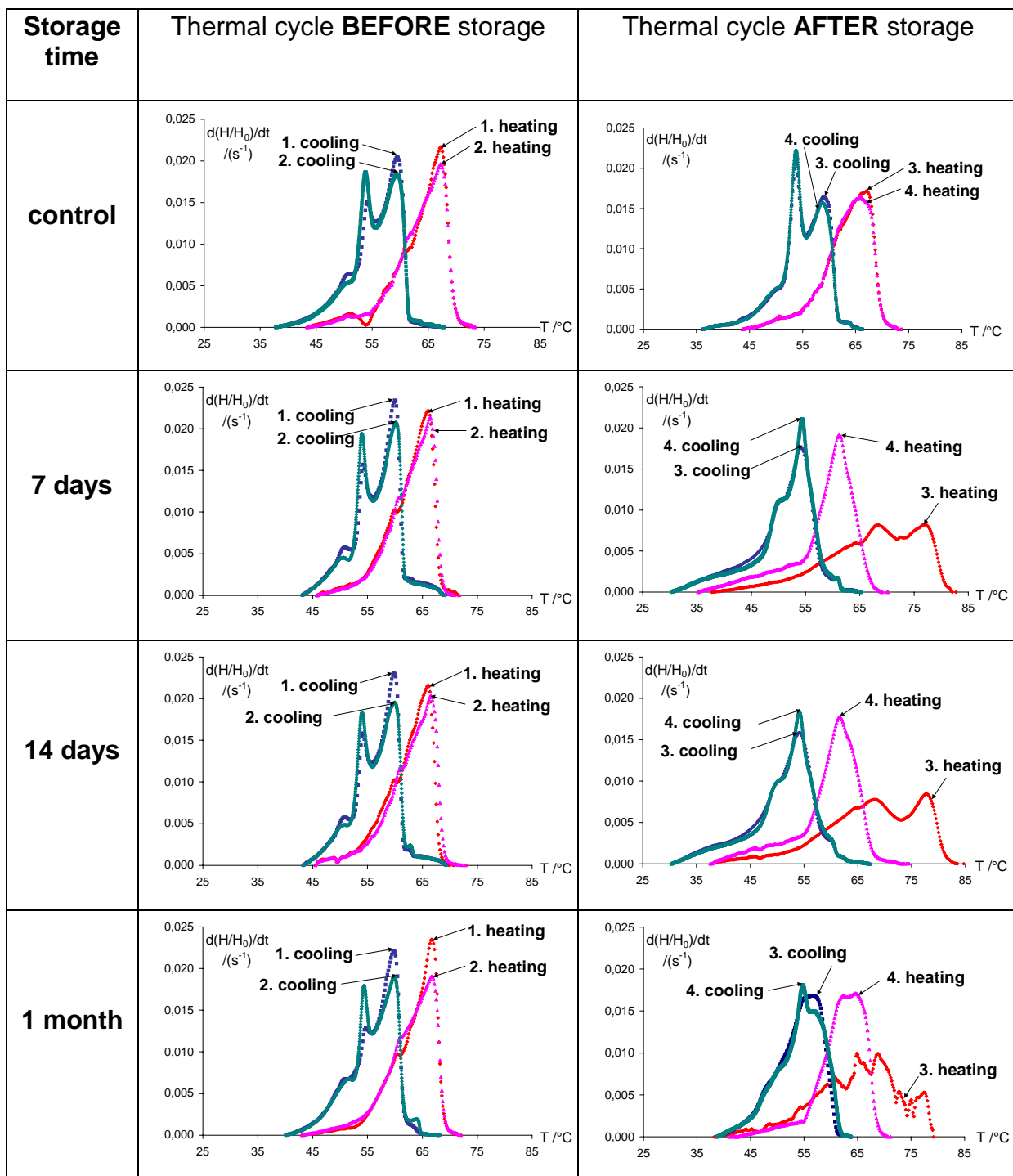
Fig. 27: *Unperfumed base B1_u* before and after storage at 4°C for three different time periods compared to the control (1.5 years old). Conversion rates from DSC plots recorded with 10°C/min during the de-ageing cycles performed before storage and analysis, respectively

4.1.1.2. Kinetic analysis of DSC-curves

Because of pattern complexity, it is not possible to derive the kinetic parameters from a single DSC scan. For this reason, the kinetic analysis was performed on DSC plots obtained for the de-aged samples subjected to a cyclic temperature programme with four different heating rates of 5, 10, 15 and 20°C. The cooling rate was kept constant (10°C/min). For each sample, the cooling curves coincided, indicating complete reversibility of the processes and justifying the use of cyclic tests. Figures 28 A and B illustrate the conversion rates calculated from DSC plots of unperfumed base B1_u. The peak shifts to higher temperature with increasing heating rate.

Fig. 28 A: Conversion rates for unperfumed base B1_u at four heating rates, (5, 10, 15 and 20°C/min)

Fig. 28 B: Superposition of the conversion rates recorded at cooling with 10°C/min for B1_u
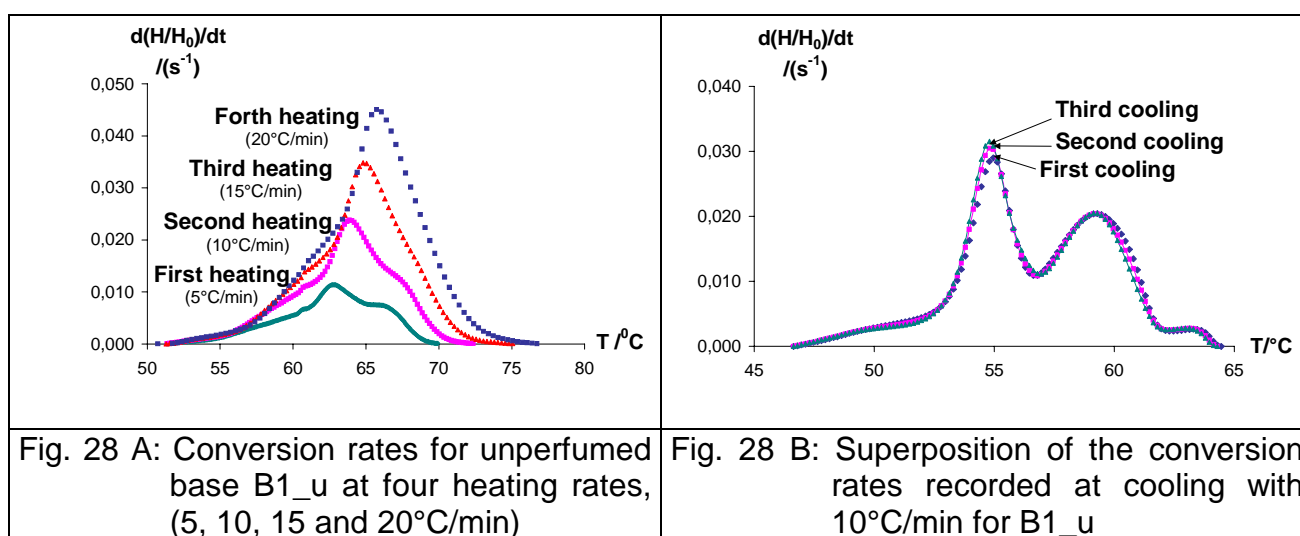
The shapes of the DSC curves suggest that heating induces disorganisation of the initial structure of vesicles and lamellar structures. During cooling, the "melt" reforms into stable structures which, as previously mentioned, are not necessarily the same as the original ones. These new structures remain stable at subsequent heatings, leading to stable shapes of the DSC curves. The fact that heating runs performed with the same rate are not in the same way superposable as cooling runs, indicates that each cooling is followed by specific relaxation phenomena of emulsion components; these relaxation phenomena are, however, too small to be discernible in the DSC cooling curve.

The kinetic analysis was done on the data corresponding to endothermic processes in the heating curves.

4.1.1.2.1. General kinetic description

The first step of the kinetic description was to analyse the endothermic processes as a whole and then to focus on the main contributions. Solid state non-isothermal kinetics offer different possibilities for kinetic parameters calculation[153]. In the case of emulsions, however, they should be used carefully in order to decide upon the limits of their applicability. Because of the complex pattern of the DSC curves, one cannot assume a simple kinetic model for the thermal process. In order not to force the data fitting on the basis of an *a priori* assumption which could introduce errors, the evaluation is first carried out by applying a model-free approach.

4.1.1.2.1.1. Model-free approach

A powerful kinetic characterisation using a model-free approach is possible by means of iso-conversional methods (analysis at constant conversion degree α)[151]. In case of multiple peaks, i.e. several overlapping processes, analysis should be done locally. The differential method of Friedman is known to be the most suitable approach in such a case[175]. It allows the calculation of the activation energy, E_a, without any assumption about the form of the kinetic function, $f(\alpha)$. It is applied for different values of the conversion degree, usually between $\alpha = 0.2$ and $\alpha = 0.9$. This choice assures the generality of the obtained E_a values.

By local integration of the conversion rates, the evolution of the degree of conversion with temperature can be followed for different heating rates. Figures 29 A and B illustrate this transformation for unperfumed base B1_u.

| Fig. 29 A: Conversion rates for B1_u vs. temperature at four heating rates (5, 10, 15, 20°C/min) | Fig. 29 B: Degree of conversion calculated for B1_u at four heating rates (5, 10, 15, 20°C/min) and plotted vs. reciprocal temperature |
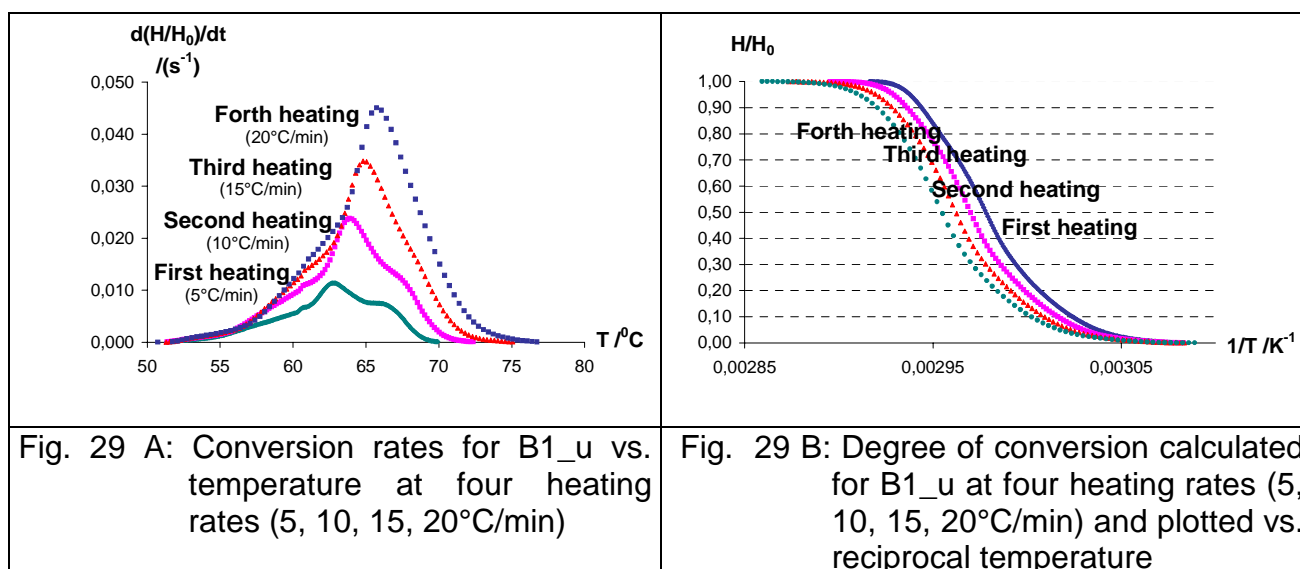
Having the values of the conversion rates, $\dfrac{d\left(\dfrac{H_t}{H_0}\right)}{dt}$ or $\dfrac{d\alpha}{dt}$, from the DSC curves and the

values of the degree of conversion, $\dfrac{H_t}{H_0}$ or α, obtained by integration, it is now possible to

plot $\ln\dfrac{d\left(\dfrac{H_t}{H_0}\right)}{dt}$ versus $\dfrac{1}{T}$ for every α from 0.2 to 0.9, which is the differential method of

Friedman. The application of the Friedman method - as described in chapter 2.3.2 by equation **2.18.** - to B1_u unperfumed base is shown in Figure 30.
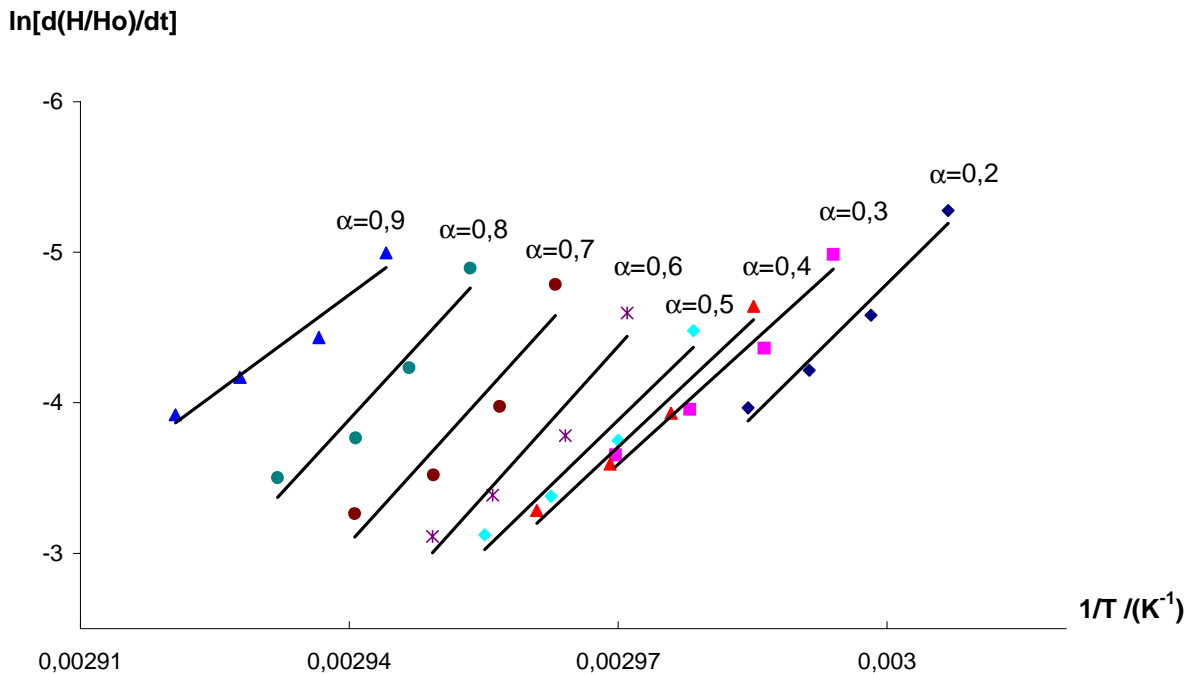
Fig. 30: Friedman plots for *unperfumed base B1_u*. The regression lines for every conversion degree, α, are shown

The slope of the regression lines in the Friedman plots enables the calculation of the activation energy, E_a, corresponding to each conversion degree α.

The evolution of the activation energy E_a with the conversion degree α is shown in Figure 31.
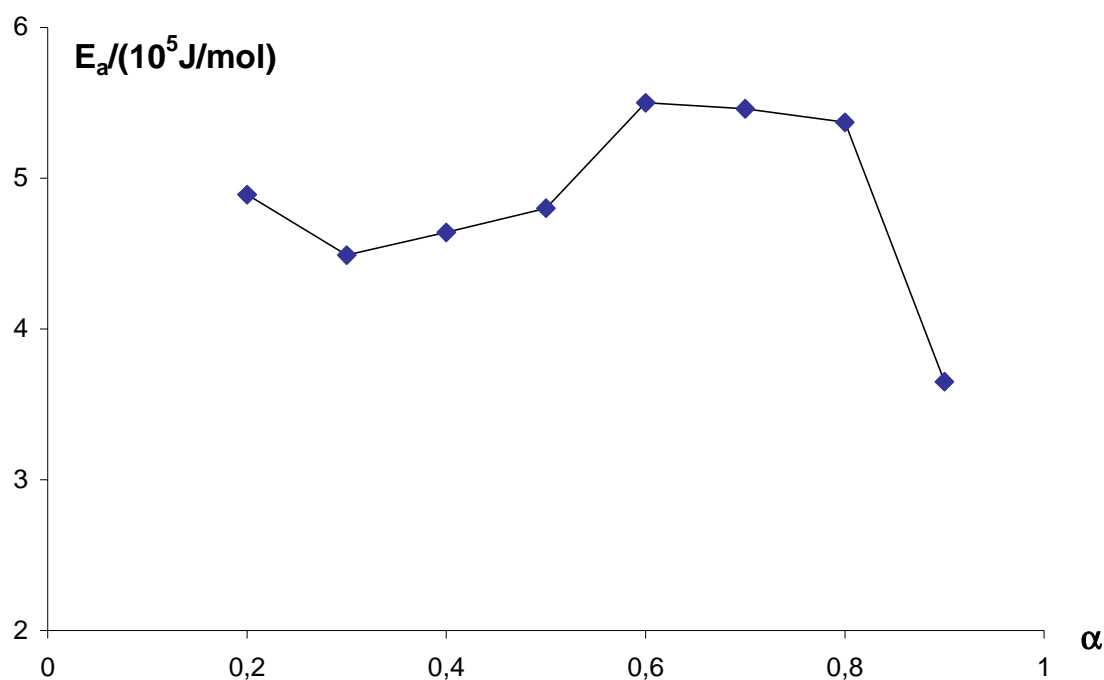
Fig. 31: The dependency of the activation energy E_a on the conversion degree α for the *unperfumed base B1_u*

The significant variation of the activation energy E_a with the conversion degree α (> 10%[151]) suggests the existence of more than one processes in the thermal evolution of the sample. This observation is confirmed by the DSC pattern which displays three different peaks. Furthermore, this result excludes the application of integral methods for data analysis [153].

The other two unperfumed bases show a similar behaviour. Figures 32 A and B illustrate for B2_u unperfumed base the conversion rates and the degrees of conversion with temperature for different heating rates.

Fig. 32 A: Conversion rates for B2_u vs. temperature at four heating rates (5, 10, 15, 20°C/min)	Fig. 32 B: Degree of conversion calculated for B2_u at four heating rates (5,10, 15, 20°C/min)
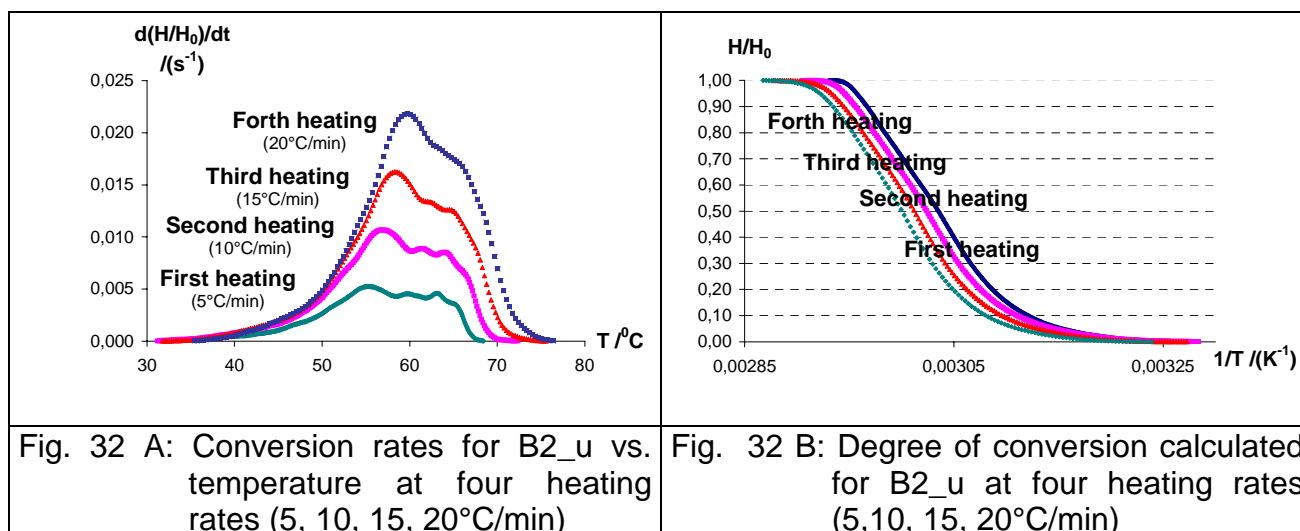
In a similar way as for B1_u, the Friedman method was applied and the values of the activation energy for every degree of conversion determined. Figure 33 shows the variation of the activation energy E_a with α for B2_u unperfumed base.
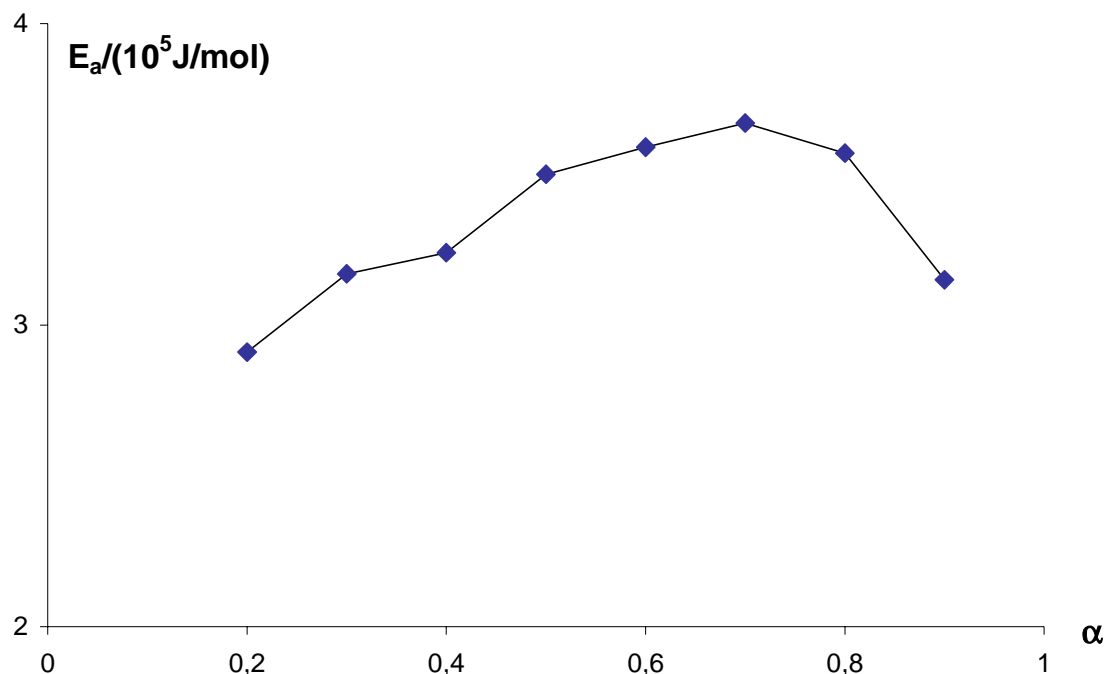
Fig. 33: The dependency of the activation energy E_a on the conversion degree α for *unperfumed base B2_u*

The DSC pattern of B2_u, as illustrated in Figure 32, exhibits four peaks, which show the existence of multiple processes. This is the reason, why the activation energy does not remain constant with the conversion degree α (see Figure 33). This is why Friedman's method cannot be applied for the whole endothermic effect.

Some perfumed samples show simpler DSC patterns. However, as it is illustrated for B1_u with various fragrances in Figure 34, the dependency of E_a on α suggests that no sample can be analysed by Friedman's method applied to the entire endothermic process and that the approach thus needs to be further refined.

Before going into a more detailed analysis, a general evaluation with a model-based approach of the kinetic parameters is done, in order to investigate their applicability for the overall endothermic process.
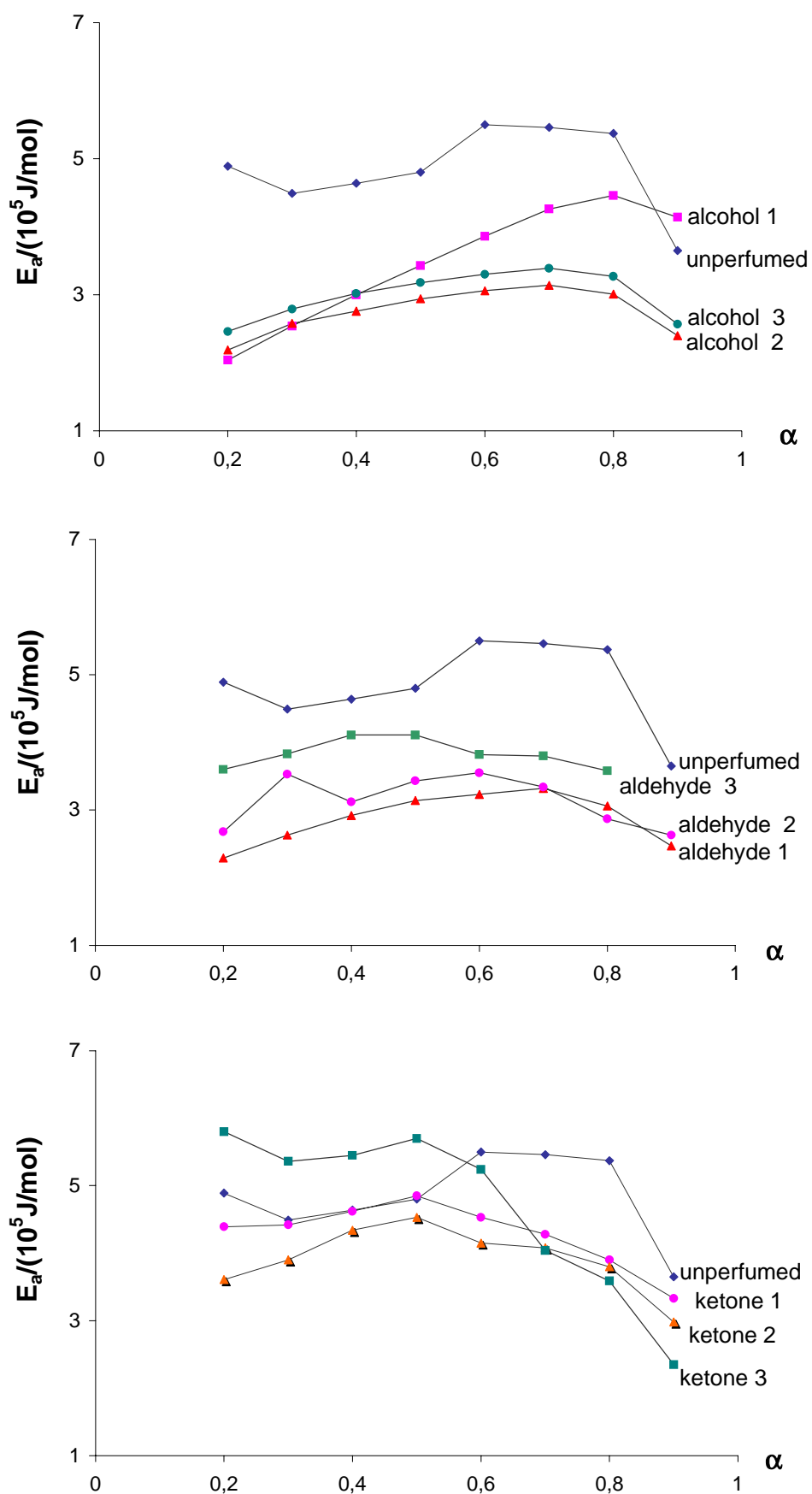
Fig. 34: The dependence of the activation energy E_a on the conversion degree α as determined by the Friedman method for *perfumed base B1* (with frangrances *ac_1,_2,_3*; *ad_1,_2,_3*; *kt_1,_2,_3*)

4.1.1.2.1.2.   Model based approach

Furtheron we assume a reaction order kinetic model for the thermal processes. Keeping in mind the pattern complexity, there is no reason to choose another model as long as no valid criterion against it can be identified. The use of $f(\alpha) = (1-\alpha)^n$ allows, by means of the Kissinger method[172] (see chapter 2.3.2, equation **2.22.**) the calculation of the activation energy, E_a. For the particular case of assuming first order kinetics, n=1, the preexponential factor, A, can be determined. The choice of n=1 makes also sense if individual main peaks are characterised.

For each case, the rate constant at room temperature (25°C) is inferred from the Arrhenius equation [87]:

$$\ln k_{25°c} = \ln A - \frac{E_a}{R \cdot T} \qquad \textbf{(4.1.)}$$

where T=(25+273) K. The rate constant, k, supplements the information contained in the activation energy, E_a, and preexponential factor, A, and is therefore an important kinetic parameter.

Kissinger's method enables the analysis of the main peak of the endothermic processes only. Figure 35 depicts the application of the Kissinger method to the main peak of unperfumed base B1_u, as they appear in the DSC curves in Figure 29 A for every heating rate. T_p is the peak temperature.
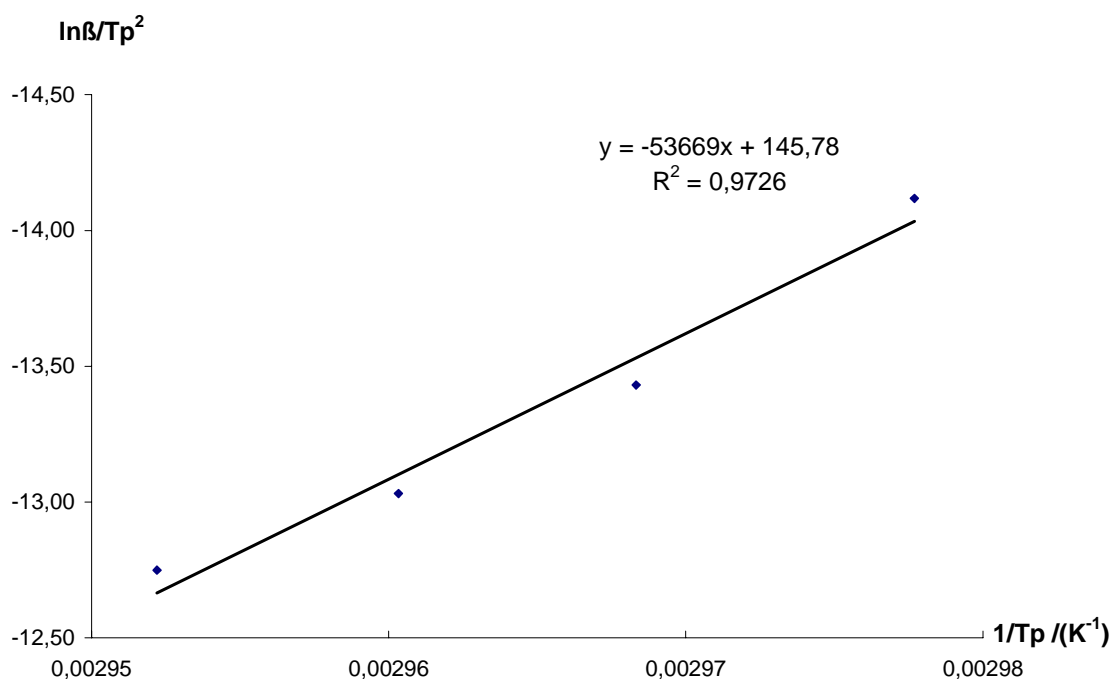
Fig.   35: Kissinger method for *unperfumed   base B1_u.* Regression line and equation are shown, together with the correlation coefficient, R^2

The results of the calculation of parameters E_a, A and $k_{25°C}$ for the whole process in the case of base B1_u are summarised in Table 3.

Tab. 3: Kinetic parameters of the main thermal process for *B1 perfumed and unperfumed bases*, calculated with the Kissinger method; the whole enthalpy of the process, H_0, and the peak temperature corresponding to β=10°C/min, $T_p^{β=10°C/min}$, are also given

Sample	$\dfrac{H_0}{J/g}$	$\dfrac{T_p^{β=10°C/min}}{°C}$	$\dfrac{E_a}{10^5 \, J/mol}$	$\ln(A/s^{-1})$	$\ln(k_{25°C}/s^{-1})$
B1_u	9.18 ± 0.10	63.9	4.46 ± 0.52	156 ± 26.9	- 23.3
B1_ac1	7.72 ± 2.75	63.9	4.76 ± 0.79	167 ± 37.3	- 24.7
B1_ac2	12.2 ± 0.52	64.5	3.66 ± 0.41	128 ± 23.1	-20.0
B1_ac3	9.89 ± 0.47	64.5	4.06 ± 0.73	142 ± 34.7	- 22.1
B1_ad1	10.5 ± 0.47	65.4	4.47 ± 0.75	156 ± 36.4	- 24.0
B1_ad2	10.3 ± 0.45	64.5	3.89 ± 0.59	135 ± 29.2	- 21.2
B1_ad3	9.80 ± 0.20	63.2	4.89 ± 0.96	172 ± 43.6	- 25.0
B1_kt1	*8.62 ± 0.35*	*65.0*	*7.29 ± 0.63*	*246 ± 31.2*	*- 48.2*
B1-kt2	9.78 ± 0.18	63.0	4.07 ± 0.51	143 ± 26.9	- 21.3
B1-kt3	9.52 ± 0.28	64.4	4.25 ± 0.18	149 ± 20.3	- 22.7

The values of $k_{25°C}$ for the B1 perfumed samples do not differ much from those for the unperfumed base; the only exception is the base with ketone1 fragrance (B1_u). Because of the complex pattern of overlapping processes, the $k_{25°C}$ value obtained should be considered carefully and interpreted in the light of a more refined analysis, after separating the underlying peaks. The peak temperatures are not changed by the addition of fragrance.

For the B2 samples, the parameters obtained from applying the Kissinger method to the main peaks of the DSC curves (see Figure 32 A) are given in Table 4. As a consequence of the de-ageing procedure, the main peak of the unperfumed base turns into a secondary one when adding perfume. The temperature value of this secondary peak corresponds to the main peak of the perfumed samples and should be taken into account on comparison. The $k_{25°C}$ values obtained for the main peak of the perfumed bases are close to each other. The comparison of the $k_{25°C}$ values corresponding to this peak from the unperfumed base (the secondary one), indicates that these values are higher, demonstrating a tendency toward instability as a consequence of fragrance addition.

Tab. 4: Kinetic parameters of the main thermal processes for *B2 perfumed and unperfumed base*, calculated with the Kissinger method; the whole enthalpy of the process, H_0, the peak temperature corresponding to the $\beta=10°C/min$, $T_p^{\beta=10°C/min}$, and the type of the process are also given

Sample	$\dfrac{H_0}{J/g}$	$\dfrac{T_p^{\beta=10°C/min}}{°C}$	Type of process	$\dfrac{E_a}{10^5\,J/mol}$	$\ln(A/s^{-1})$	$\ln(k_{25°C}/s^{-1})$
B2_u	9.36 ± 0.15	57.0	main	2.89 ± 0.34	102 ± 20.9	- 14.4
		64.0	secondary	5.84 ± 0.77	206 ± 36.6	-29.6
B2_ac1	9.79 ± 0.43	61.7	main	3.11 ± 0.34	109 ± 20.5	- 16.6
		42.0	secondary	3.40 ± 0.69	127 ± 34.8	-10.4
B2_ac2	7.40 ± 0.23	61.6	main	3.98 ± 0.54	140 ± 28.1	- 20.3
B2_ac3	7.42 ± 0.33	61.9	main	3.95 ± 0.63	139 ± 31.4	- 19.8
B2_ad1	9.18 ± 0.34	63.0	main	3.98 ± 0.44	140 ± 24.3	- 20.9
		41.5	secondary	3.81 ± 0.41	143 ± 24.0	-10.7
B2_ad2	10.7 ± 0.74	63.0	main	4.17 ± 0.59	147 ± 29.7	- 21.7
B2_ad3	6.75 ± 0.16	63.2	main	3.90 ± 0.57	137 ± 29.0	- 20.9
B2_kt1	9.28 ± 0.36	63.5	main	4.32 ± 0.44	152 ± 24.3	- 22.8
		43.9	secondary	3.81 ± 0.67	142 ± 35.1	-11.6
B2_kt2	8.30 ± 0.50	62.9	main	4.08 ± 0.50	144 ± 26.4	- 20.8
B2_kt3	9.11 ± 0.34	64.3	main	3.80 ± 0.38	133 ± 21.9	- 20.4

As for the B3 bases, the unperfumed sample displays three prominent peaks, but of very small characteristic enthalpy. This fact indicates a very low concentration of the sample. As expected already from the shape of the DSC curves, the perfumed samples show no significant difference of the $k_{25°C}$ values obtained for different fragrances as shown in Table 5. The comparison of these values with those obtained for the main peak of the unperfumed sample shows that the addition of fragrance seems to play a less important role in this case.

Tab. 5: Kinetic parameters of the main thermal processes in *B3 perfumed and unperfumed base*, calculated with the Kissinger method; the whole enthalpy of the process, H_0, the peak temperature corresponding to the $\beta=10°C/min$, $T_p^{\beta=10°C/min}$, and the type of the process are also given

Sample	$\dfrac{H_0}{J/g}$	$\dfrac{T_p^{\beta=10°C/min}}{°C}$	Type of process	$\dfrac{E_a}{10^5\,J/mol}$	$\ln(A/s^{-1})$	$\ln(k_{25°C}/s^{-1})$
B3_u	< 0.10	27.7	secondary II	1.27 ± 0.68	47.2 ± 35.9	- 4.02
	< 0.10	38.4	secondary I	1.51 ± 0.05	54.8 ± 8.22	-6.17
	< 0.10	48.7	main	3.11 ± 0.36	114 ± 21.7	-12.0
B3_ac1	0.67 ± 0.18	42.8	main	3.49 ± 0.10	130 ± 8.91	- 11.2
B3_ac2	1.33 ± 0.45	43.5	main	3.57 ± 0.01	132 ± 9.70	-11.8
B3_ac3	2.17 ± 0.22	43.4	main	4.13 ± 0.24	154 ± 16.5	- 12.7
B3_ad1	1.80 ± 0.16	43.4	main	3.71 ± 0.75	138 ± 27.0	- 12.1
B3_ad2	2.26 ± 0.25	44.3	main	4.12 ± 0.35	153 ± 21.4	- 13.3
B3_ad3	1.97 ± 0.25	43.8	main	3.19 ± 0.29	118 ± 19.3	- 11.1
B3_kt1	1.03 ± 0.29	42.9	main	3.62 ± 0.25	134 ± 17.6	- 11.7
B3_kt2	1.85 ± 0.09	43.0	main	2.73 ± 0.26	100 ± 18.0	- 9.96
B3_kt3	1.68 ± 0.19	43.1	main	3.20 ± 0.12	119 ± 11.4	- 10.7

One can observe that the values of the rate constant are lower for B1_u than for the other two. This suggests that B1_u is the most stable among all unperfumed samples.

The fact is confirmed by 2.5 years storage, after which B1_u is the only one which remains stable. B2_u exhibits a hardening effect, whereas for B3_u one observes the separation effect. B2_u, after 2.5 years of storage, displays, beside liposomes, rod-like structures possibly resulting from micelle associations and potentially responsible for the hardening effect. The microscopical appearance of B2_u base after 2.5 years storage is illustrated in Figure 36.

B3 base containing various fragrance substances gives the samples with the largest values of the kinetic constant, meaning the highest tendency toward instability. This is well supported by the practical test of 2.5 years storage, after which all of these samples show phase separation. In Figure 37 the appearance of one of the B3 perfumed base - the sample B3_ad1 - is shown in bright and polarised light; anisotropic structures associated with interference phenomena are clearly visible.
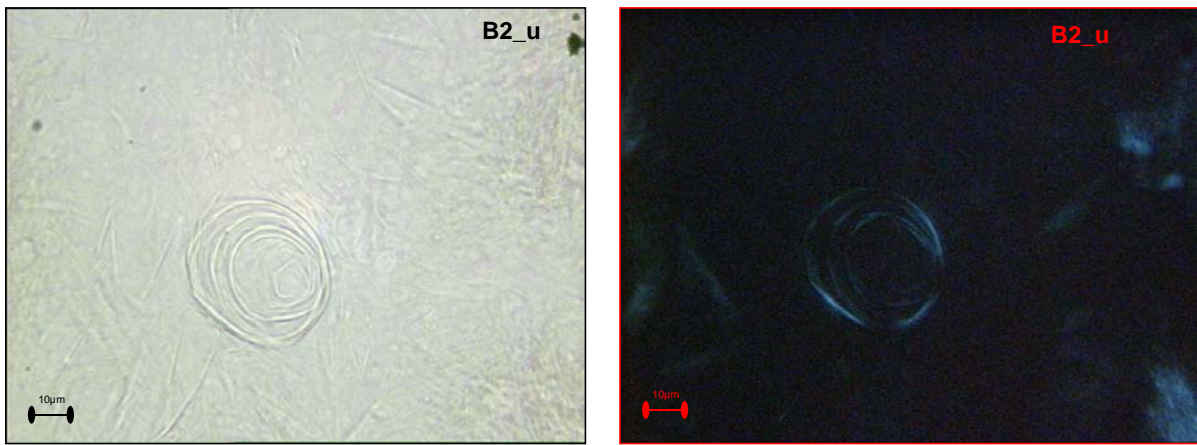
Fig. 36: Optical micrographs of 2.5 years old, hardened *B2_u unperfumed base* in bright and polarised light (magnification 400 ×)
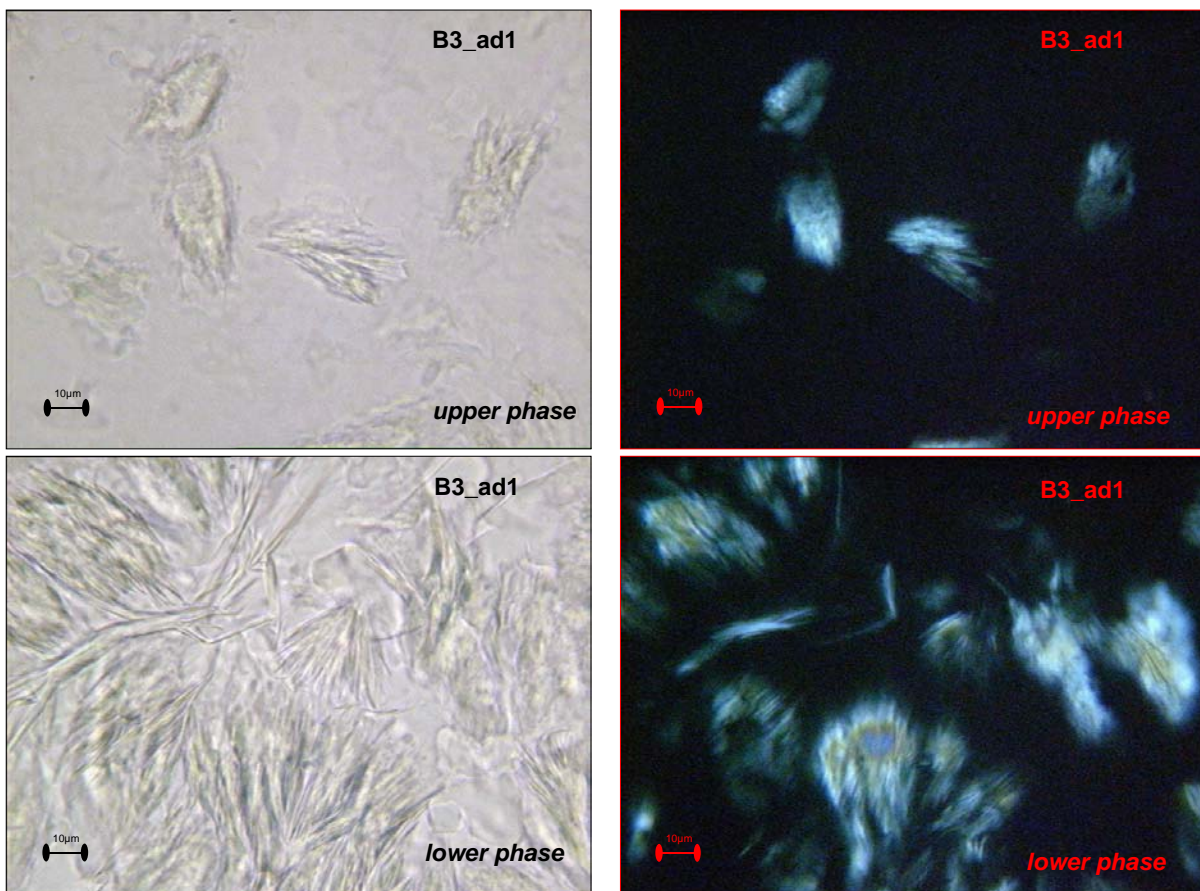
Fig. 37: Optical micrographs of an 2.5 years old *B3_ad1* base in bright and polarised light from the upper and lower phase of the separated emulsion (magnification 400 ×)

As a concluding remark, the Kissinger method, which is based on the simplifying hypothesis of a reaction of first order (n=1) for the calculation of the kinetic parameters, gives promising results. It indicates a good stability for one of the samples and allows grading the samples according to their stability.

4.1.1.2.2. Detailed kinetic description

As pointed out in chapter 2, the equation of the reaction rate **(2.7.)** describing thermally initiated reactions applies only to elementary processes. A complicated DSC pattern with multiple peaks, such as for the fabric softeners, together with the significant variation of E_a with α for the whole endothermic process, suggests that several elementary processes occur. It is, therefore, important to develop a deconvolution procedure to separate the overlapping processes.

4.1.1.2.2.1. *Deconvolution with best fit conditions*

In the case of fabric softeners, we assume that the emulsion components are not reacting with each other and that the samples are undergoing only physical transitions, which we assume to be independent of each other. Therefore, a linear model of deconvolution appears to be the most appropriate one.

As pointed out in chapter 2.3.2, an overall complex DSC signal $\dfrac{d\alpha}{dt}$, with $\alpha = \dfrac{H}{H_0}$, can be expressed as a linearly weighted superposition of individual processes, each of them obeying the general equation of non-isothermal kinetics for the conversion rate:

$$\frac{d\alpha}{dt} = \sum_{i=1}^{p} C_i \cdot A_i \cdot (1-\alpha_i)^{n_i} \cdot e^{-\frac{E_{a_i}}{R \cdot T}} \qquad \textbf{(2.18.)}$$

where p is the total number of independent processes and E_{a_i} the corresponding activation energy.

Analysing the mathematical expression of the conversion rate, it appears that each of the elementary processes can be graphically well approximated by a Gaussian curve.

Consequently, the overall reaction rate of a complex DSC signal turns into:

$$\frac{d\alpha}{dt} = \sum_{i=1}^{p} C_i \cdot \frac{1}{\sqrt{2 \cdot \pi} \cdot \sigma_i} \cdot e^{-\frac{1}{2}\left(\frac{T-T_p}{\sigma_i}\right)^2} \qquad \textbf{(2.20.)}$$

Imposing best fit conditions through a least square regression technique, the experimental curve is as optimally as possible approximated by the linear combination of Gaussian functions according to equation **4.3.**. Through this the coefficient of determination r^2 and the F-value reach their optimum. The kinetic parameters which characterise each elementary process (see equation **4.2.**), can be inferred by means of non-isothermal kinetics methods. These methods are applied to the individual curves obtained for different heating rates.

The separation of a more complex endothermic process is shown in Figure 38 for each heating rate of the temperature programme in the case of the unperfumed base B1_u. Each individual process obtained from the linear deconvolution is followed as a function of heating rate and can on this basis be further analysed.
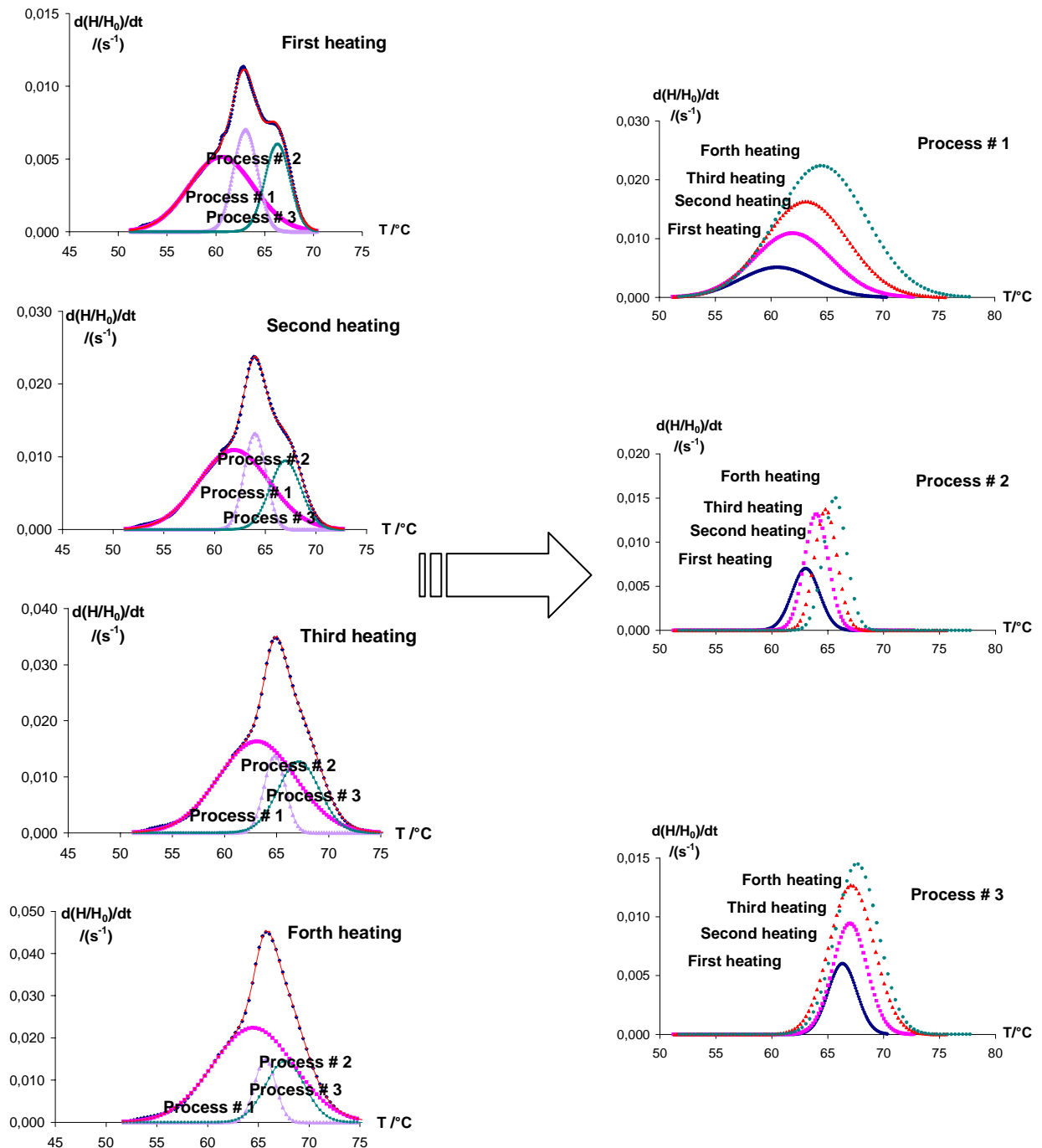
Fig. 38: Separation of individual processes by deconvolution with best fit conditions of the DSC-curve for *unperfumed base B1_u* for each heating rate

The evolution of the activation energy, E_a, with the conversion degree α for the most prominent process (process # 2 around 65°C) is illustrated in Figure 39.
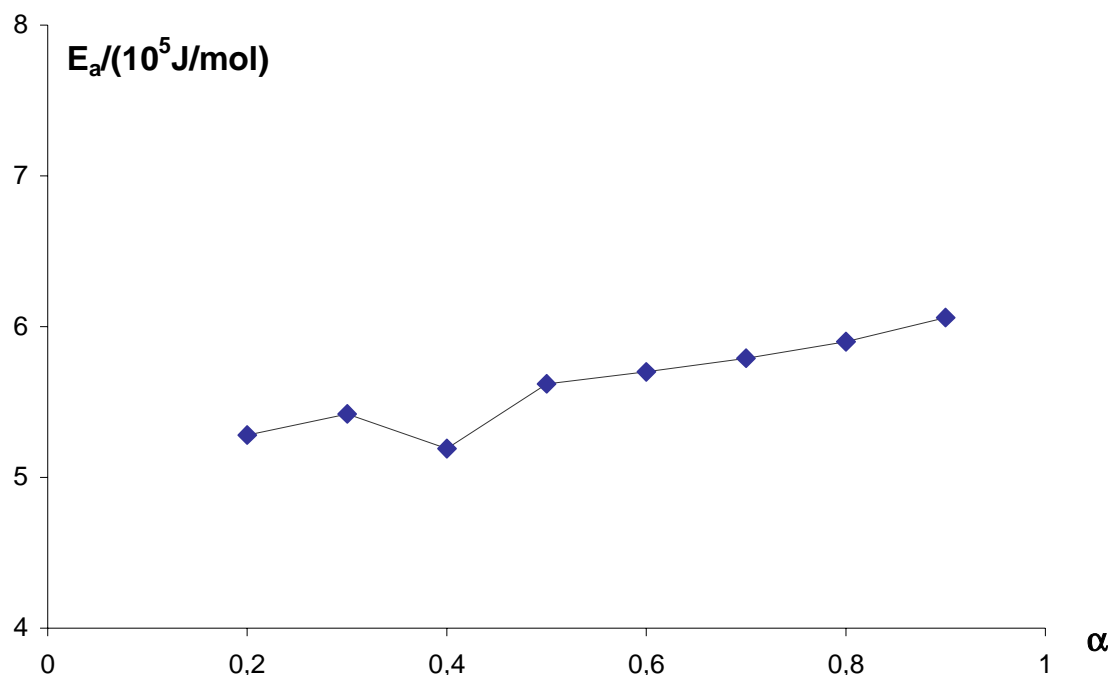
Fig. 39: The dependency of the activation energy, E_a on the degree of conversion α for the separated main process (process # 2) of *unperfumed base B1_u* (deconvolution with best fit conditions)

One observes that as a result of the separation procedure, the value of the activation energy, E_a, is almost constant with α and the kinetic analysis can thus be performed.

The number of Gaussian curves chosen to fit the individual processes is derived sensibly from the curve shape. There is no statistical criterion, that could better approximate the number of parameters of the fit than the very appearance of the thermal signal which describes the underlying physical processes. As for example, for B1_u base, one can notice, beside the main process at approx. 64°C, two shoulders at approx. 60°C and 66°C. At least three Gaussian curves are thus needed to characterise the whole process.

Taking into account that the deconvolution procedure separates the whole process into elementary steps, not only the differential method of Friedman, but also the integral iso-conversional method of Flynn-Wall-Ozawa can be applied. Table 6 gives the values of the kinetic parameters obtained for the unperfumed base B1_u by means of the two most important iso-conversional methods mentioned above, as well as by the Kissinger method, with the assumption of n=1.

Tab. 6: Kinetic parameters for *unperfumed base B1_u*, after deconvolution in three individual processes with best fit conditions; the peak temperature corresponding to the β=10°C/min, $T_p^{\beta=10°C/min}$ is also given

Method	Type of process	$T_p^{\beta=10°C/min}$ °C	$\dfrac{E_a}{10^5\,J/mol}$	$\ln(A/s^{-1})$	$\ln(k_{25°C}/s^{-1})$
Friedman	Process # 1	61.9	2.86 ± 0.30	99.4 ± 1.05	-16.0
	Process # 2	**64.1**	$\mathbf{5.62 \pm 0.21}$	**198 ± 7.52**	**-28.6**
	Process # 3	67.0	5.82 ± 1.23	245 ± 43.7	-32.6
Kissinger	Process # 1	61.9	3.22 ± 0.45	113 ± 24.5	-17.3
	Process # 2	**64.0**	$\mathbf{4.93 \pm 0.58}$	**173 ± 29.2**	**-25.7**
	Process # 3	67.0	11.0 ± 1.51	358 ± 63.0	-74.2
Flyn-Wall-Ozawa	Process # 1	61.9	3.24 ± 0.26		
	Process # 2	**64.0**	$\mathbf{5.04 \pm 0.17}$		
	Process # 3	67.0	8.90 ± 1.68		

The results show a fairly good agreement of the values corresponding to the main process and also to one of the secondary processes, but this cannot be said for the remaining one (process # 3). Accordingly, a further refinement of the analysis is necessary.

4.1.1.2.2.2. *Deconvolution with best fit and restrictions*

A way for optimising the deconvolution is to impose an additional condition for the fitting procedure. A suitable condition is that the area of each Gaussian curve used for the deconvolution should remain constant irrespective of the heating rate. The physical meaning of this condition is, that the enthalpy of an elementary process remains constant at any heating rate β_j. This additional condition can be expressed as:

$$H_{0,\,i}^{\;\beta_j} = \text{constant} \tag{4.2.}$$

This restriction is implemented as follows: the values of total and deconvoluted area obtained at the first heating are taken as reference. For each subsequent heating one considers the ratios of the total area to the reference and applies the value of the ratios to all deconvoluted areas of the process.

Furthermore, the additivity of individual areas to obtain the area of the whole signal is respected. For simplicity, the total area is taken as a reference (unity scaling condition):

$$\sum_{i=1}^{p} H_{0,\,i}^{\;\beta_j} = 1 \tag{4.3.}$$

with i ranging from 1 to p, where p is the total number of processes and j defining each heating rate.

More precisely, for non-isothermal experiments, where variable t is changed to T:

$$\sum_{i=1}^{p} \frac{1}{H_{0,i} \cdot \beta_j} \cdot \int_{T_{initial}}^{T_{final}} \frac{H_{t_i}}{dt} \cdot dT = 1 \qquad \textbf{(4.4.)}$$

Taking these conditions into account, the complex endothermic pattern was separated for each heating rate of the temperature programme. The separation was done by imposing additional conditions. The results together with the evolution obtained for each individual process with the heating rate are illustrated for unperfumed base B1_u in Figure 40. One observes the better distribution of the individual processes within the entire process for each heating rate, so that the signal shape is more realistically fitted.
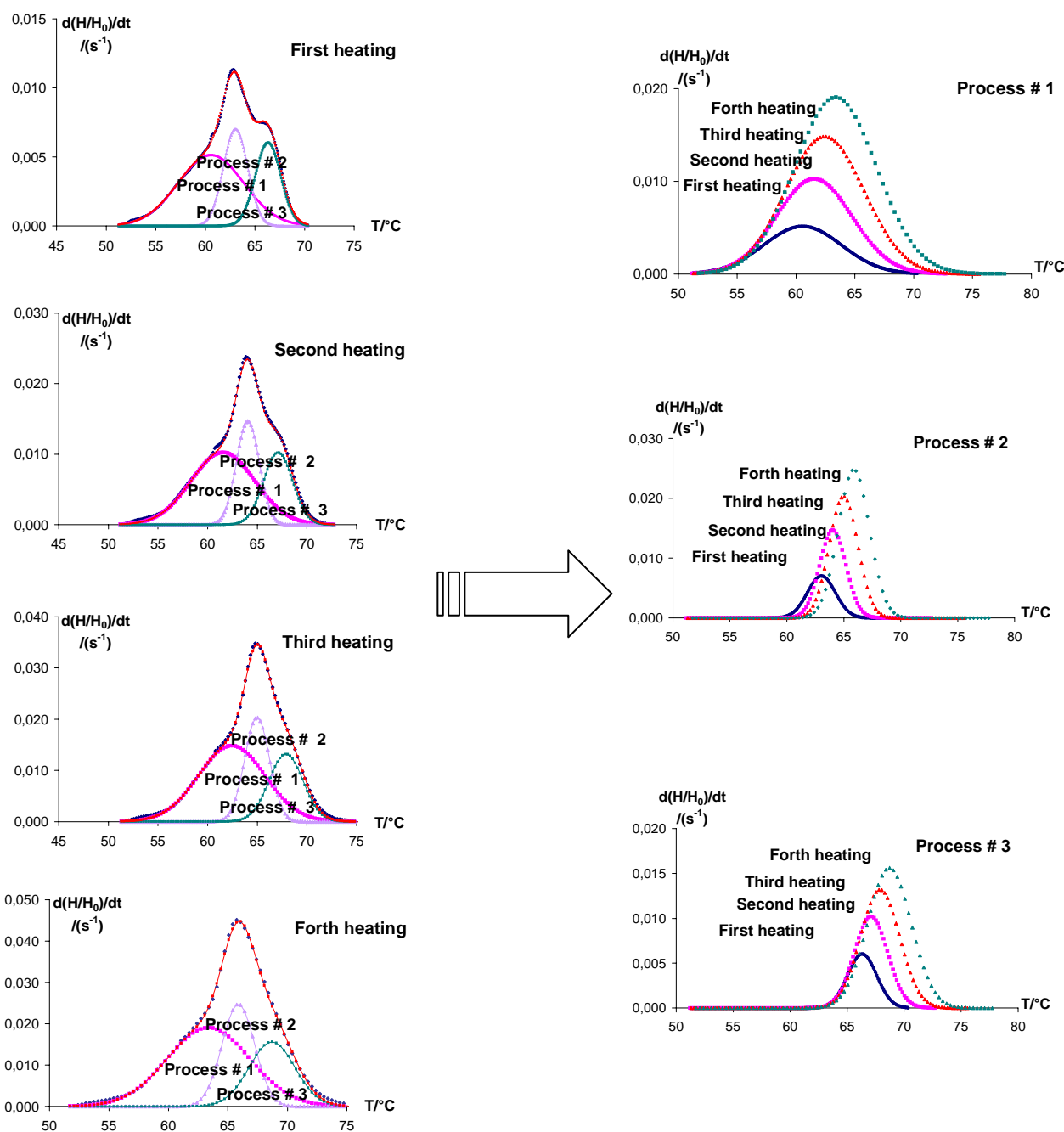
Fig.40: Separation of individual processes by deconvolution of the DSC-curve for *unperfumed base* B1_u with imposing an additional restriction for each heating rate

Figure 41 illustrates the evolution of the activation energy with the degree of conversion for the main process # 2 obtained after imposing the restrictions for the deconvolution procedure.
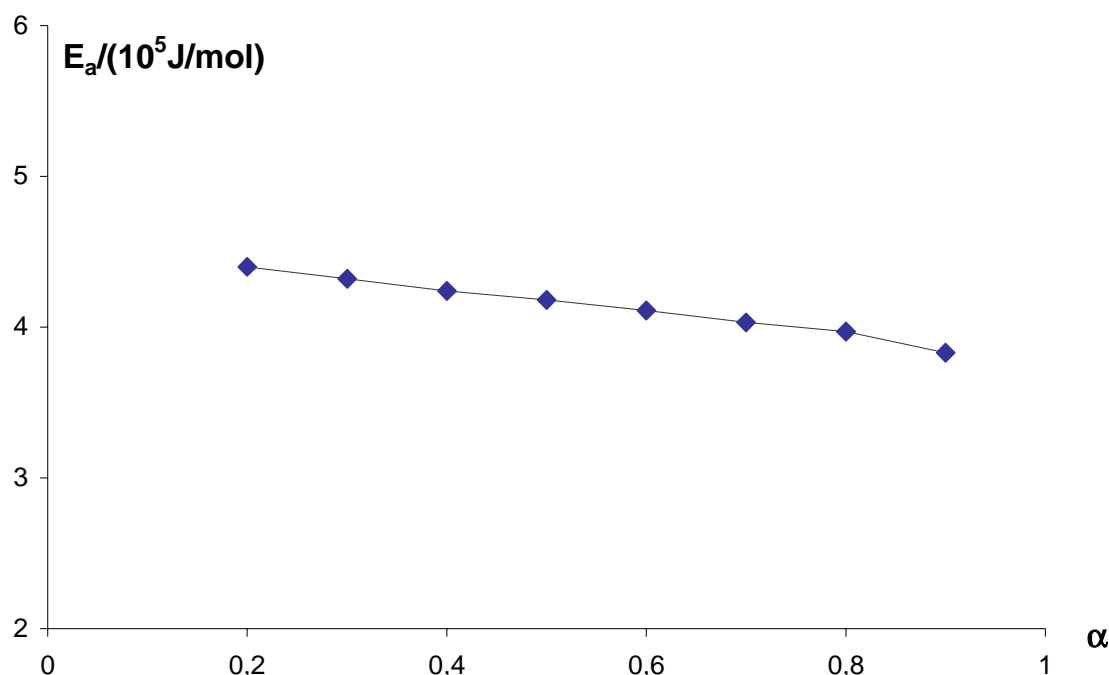
Fig. 41: The dependence of the activation energy E_a on the conversion degree α for the separated process # 2 of *unperfumed base B1_u* (deconvolution with restrictions)

The quasi constancy of the values of activation energy, E_a, at various conversion degrees α is an improved result and justifies the imposed constraints. The kinetic parameters obtained by taking into account these constraints, beside the best fit criterion, are summarised in Table 7 for the three different kinetic methods.

Tab. 7: Kinetic parameters for *unperfumed base B1_u*, after deconvolution in three individual processes with additional conditions; the peak temperature corresponding to the $\beta=10°C/min$, $T_p^{\beta=10°C/min}$ is also given

Method	Type of process	$\dfrac{T_p^{\beta=10°C/min}}{°C}$	$\dfrac{E_a}{10^5\,J/mol}$	$\ln(A/s^{-1})$	$\ln(k_{25°C}/s^{-1})$
Friedman	Process # 1	61.5	4.30 ± 0.13	151 ± 5.26	-22.4
	Process # 2	**64.0**	**4.13 ± 0.13**	**145 ± 4.56**	**-21.5**
	Process # 3	67.0	3.80 ± 0.48	132 ± 16.8	-21.3
Kissinger	Process #1	61.5	4.46 ± 0.56	158 ± 28.8	-22.5
	Process # 2	**64.0**	**4.66 ± 0.43**	**164 ± 23.7**	**-24.2**
	Process # 3	67.0	5.38 ± 1.00	188 ± 44.5	-29.5
Flyn-Wall-Ozawa	Process # 1	61.5	4.53 ± 0.14		
	Process # 2	**64.0**	**4.54 ± 0.12**		
	Process # 3	67.0	5.46 ± 0.70		

The kinetic parameter values obtained with different methods are in this case in closer agreement than before and, also, closer to the values obtained with the general Kissinger method for the whole process. This suggests that when rearrangements are no more taking place in the sample while running the temperature programme, then the Kissinger method applied to the main peak of the whole endothermic process is a good approximation for obtaining accurate parameter values.

It seems that the chosen restrictions are not only improving the fit significantly, but are giving more physical sense to the deconvolution procedure.

Against this background it appears sensible to analyse the samples of the base B1 with fragrances by using the same procedure. The DSC plots of perfumed samples of B1 base are deconvoluted with a minimal number of curves (revealed by both the heating and the cooling pattern) by means of a fit with the restrictions discussed above. All perfumed samples are deconvoluted into three individual processes. The exception is sample B1_kt3 which, because of its more complicated pattern, has to be described by at least four individual processes; this sample also shows clear rearrangements and the individual processes are not giving a constant relative contribution. This is the reason why a restriction fit does not give the best results. Only best fit conditions can be used.

A relatively constant evolution of the activation energy with the conversion degree is obtained for almost all perfumed samples of the B1 base (see Figure 42). The perfumed sample B1_ac1 is an exception, but this is rather due to possible artifacts rather than to the method applied or the conditions imposed.
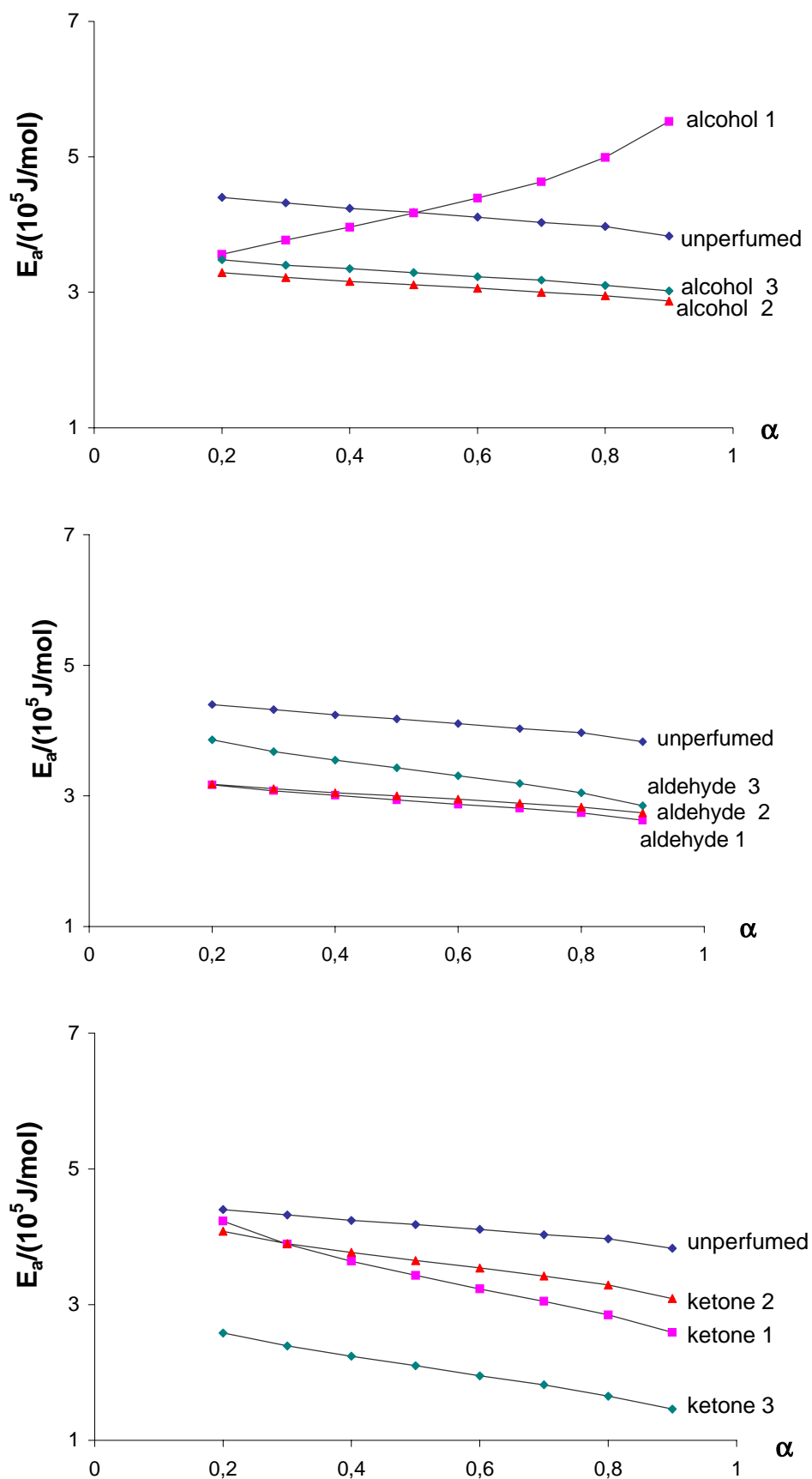
Fig. 42: The dependency of the activation energy on conversion degree (after deconvolution with additional conditions) for the main process corresponding to the three main groups of perfumed samples: *B1 bases_ac1,_ 2, _3, B1 bases_ad1, 2, 3, and B1 bases_kt1, _2, _3.*

The kinetic parameters of all perfumed samples calculated with the three kinetic methods of Friedman, Flynn-Wall-Ozawa and Kissinger, after restricted deconvolution, are comparatively summarised in Tables 8-10 together with the results obtained for the main peaks of the same samples from analysis of the whole effect with the Kissinger method.

Tab. 8: Kinetic parameters for the group *B1_ac1, B1_ac2, B1_ac3* for different methods and type of analysis; the peak temperature corresponding to β=10°C/min, $T_p^{\beta=10°C/min}$ is also given; in bold characters are the main proceses observed in undeconvoluted signal

Sample	Type of analysis	Method	Type of process	$T_p^{\beta=10°C/min}$ °C	E_a 10^5 J/mol	$\ln(A/s^{-1})$	$\ln(k_{25°C}/s^{-1})$
B1_ac1	**whole process**	Kissinger		**63.9**	**4.76 ± 0.79**	**167 ± 37.4**	**-24.7**
	fit (best fit conditions)	Friedman	Process # 1	57.0	2.70 ± 0.73	94.2 ± 26.1	-14.8
			Process # 2	*63.2*	*4.37 ± 0.45*	*153 ± 16.0*	*-23.1*
		F-W-O	Process # 1	57.0	1.74 ± 0.47		
			Process # 2	*63.2*	*3.43 ± 0.36*		
		Kissinger	Process # 1	57.0	1.45 ± 0.23	48.9 ± 15.9	-9.62
			Process 2	*63.2*	*3.13 ± 0.60*	*109 ± 30.0*	*-17.4*
B1_ac2	**whole process**	Kissinger		**64.5**	**3.66 ± 0.41**	**128 ± 23.1**	**-19.2**
	fit (additional conditions)	Friedman	Process # 1	52.4	1.88 ± 0.16	64.9 ± 5.49	-10.9
			Process # 2	61.0	2.77 ± 0.01	96.1 ± 0.35	-15.7
			Process # 3	*65.0*	*3.08 ± 0.10*	*107 ± 3.37*	*-17.4*
		F-W-O	Process # 1	52.4	1.73 ± 0.17		
			Process # 2	61.0	2.79 ± 0.01		
			Process # 3	*65.0*	*3.44 ± 0.10*		
		Kissinger	Process # 1	52.4	1.61 ± 0.27	55.9 ± 17.6	-9.05
			Process # 2	61.0	2.78 ± 0.40	97.0 ± 22.8	-15.3
			Process # 3	*65.0*	*3.52 ± 0.41*	*123 ± 23.1*	*-19.6*
B1_ac3	**whole process**	Kissinger		**64.5**	**4.06 ± 0.73**	**142 ± 34.7**	**-22.1**
	fit (additional conditions)	Friedman	Process # 1	53.2	2.17 ± 0.22	75.5 ± 7.62	-12.1
			Process # 2	61.2	3.05 ± 0.01	107 ± 0.42	-16.6
			Process # 3	*64.9*	*3.26 ± 0.10*	*113 ± 5.32*	*-18.2*
		F-W-O	Process # 1	53.2	1.95 ± 0.22		
			Process # 2	61.2	3.06 ± 0.02		
			Process # 3	*64.9*	*3.68 ± 0.12*		
		Kissinger	Process # 1	53.2	1.78 ± 0.2	62.3 ± 14.7	-9.57
			Process # 2	61.2	3.12 ± 0.31	109 ± 19.3	-16.7
			Process # 3	*64.9*	*3.78 ± 0.45*	*132 ± 24.6*	*-20.2*

Tab. 9: Kinetic parameters for the group *B1_ad1, B1_ad2, B1_ad3* for different methods and type of analysis; the peak temperature corresponding to β=10°C/min, $T_p^{\beta=10°C/min}$ is also given; in bold characters are the main proceses observed in undeconvoluted signal

Sample	Type of analysis	Method	Type of process	$T_p^{\beta=10°C/min}$ / °C	E_a / 10^5 J/mol	$\ln(A/s^{-1})$	$\ln(k_{25°C}/s^{-1})$
B1_ad1	**whole process**	Kissinger		**65.4**	**4.47 ± 0.75**	**156 ± 36.4**	**-24.0**
	fit (additional conditions)	Friedman	Process # 1	56.2	2.44 ± 0.24	84.8 ± 8.24	-13.7
			Process # 2	62.9	3.11 ± 0.03	108 ± 1.14	-17.4
			Process # 3	*66.2*	*2.90 ± 0.12*	*100 ± 4.29*	*-16.7*
		F-W-O	Process # 1	56.2	2.10 ± 0.19		
			Process # 2	62.9	3.06 ± 0.03		
			Process # 3	*66.2*	*3.46 ± 0.14*		
		Kissinger	Process # 1	56.2	1.97 ± 0.12	68.7 ± 11.2	-10.9
			Process # 2	62.9	2.90 ± 0.22	101 ± 15.3	-16.3
			Process # 3	*66.2*	*3.53 ± 0.29*	*123 ± 18.1*	*-20.0*
B1_ad2	**whole process**	Kissinger		**64.5**	**3.89 ± 0.59**	**136 ± 29.2**	**-21.2**
	fit (additional conditions)	Friedman	Process # 1	54.0	2.83 ± 0.55	99.6 ± 19.5	-14.6
			Process # 2	60.9	3.23 ± 0.21	113 ± 7.49	-17.7
			Process # 3	*65.4*	*2.97 ± 0.10*	*103 ± 3.49*	*-17.1*
		F-W-O	Process # 1	54.0	2.24 ± 0.47		
			Process # 2	60.9	2.87 ± 0.21		
			Process 3	*65.4*	*2.93 ± 0.09*		
		Kissinger	Process # 1	54.0	1.97 ± 0.13	69.0 ± 15.0	-10.5
			Process # 2	60.9	2.71 ± 0.32	94.5 ± 20.0	-14.9
			Process# 3	*65.4*	*3.25 ± 0.94*	*113 ± 41.7*	*-18.4*
B1_ad3	**whole process**	Kissinger		**63.2**	**4.89 ± 0.96**	**172 ± 43.6**	**-25.0**
	fit (additional conditions)	Friedman	Process # 1	53.2	2.70 ± 0.18	95.0 ± 6.31	-14.0
			Process # 2	60.4	3.98 ± 0.11	140 ± 4.20	-20.6
			Process # 3	*64.7*	*3.37 ± 0.23*	*117 ± 8.14*	*-19.0*
		F-W-O	Process # 1	53.2	2.76 ± 0.26		
			Process # 2	60.4	4.27 ± 0.08		
			Process # 3	*64.7*	*4.07 ± 0.26*		
		Kissinger	Process # 1	53.2	2.63 ± 0.12	93.8 ± 50.4	-12.4
			Process # 2	60.4	4.61 ± 0.12	164 ± 61.6	-22.2
			Process # 3	*64.7*	*3.89 ± 0.79*	*136 ± 37.2*	*-21.3*

Tab. 10: Kinetic parameters for the group *B1_kt1, B1_kt2, B1_kt3* for different methods and type of analysis; the peak temperature corresponding to β=10°C/min, $T_p^{\beta=10°C/min}$ is also given; in bold characters are the main proceses observed in undeconvoluted signal

Sample	Type of analysis	Method	Type of process	$T_p^{\beta=10°C/min}$ °C	E_a 10^5 J/mol	$\ln(A/s^{-1})$	$\ln(k_{25°C}/s^{-1})$
B1_kt1	**whole process**	Kissinger		**65.0**	**7.29 ± 0.63**	**246 ± 31.2**	**-48.2**
	fit (additional conditions)	Friedman	Process # 1	53.5	3.61 ± 0.28	129 ± 10.1	-16.3
			Process # 2	61.7	4.11 ± 0.14	144 ± 5.26	-21.6
			Process # 3	*66.9*	*3.36 ± 0.38*	*116 ± 0.38*	*-19.5*
		F-W-O	Process # 1	53.5	3.76 ± 0.39		
			Process # 2	61.7	4.44 ± 0.08		
			Process # 3	*66.9*	*4.33 ± 0.46*		
		Kissinger	Process # 1	53.5	2.38 ± 0.52	84.7 ± 9.06	-11.3
			Process # 2	61.7	4.37 ± 0.78	155 ± 37.3	-21.9
			Process # 3	*66.9*	*4.44 ± 0.47*	*155 ± 25.7*	*-24.7*
B1_kt2	**whole process**	Kissinger		**63.0**	**4.07 ± 0.51**	**143 ± 26.9**	**-21.3**
	fit (additional conditions)	Friedman	Processs# 1	54.9	3.06 ± 0.12	108 ± 3.60	-15.4
			Processs # 2	60.7	4.65 ± 0.03	164 ± 0.66	-23.8
			Process # 3	*64.9*	*3.59 ± 0.23*	*125 ± 8*	*-20.0*
		F-W-O	Processs# 1	54.9	3.01 ± 0.12		
			Processs # 2	60.7	4.69 ± 0.03		
			Process # 3	*64.9*	*4.18 ± 0.25*		
		Kissinger	Process # 1	54.9	2.85 ± 0.42	101 ± 24.1	-13.6
			Process # 2	60.7	4.48 ± 1.03	159 ± 46.2	-22.1
			Process # 3	*64.9*	*4.10 ± 0.73*	*143 ± 34.7*	*-22.3*
B1_kt3	**whole process**	Kissinger		**64.4**	**4.25 ± 0.18**	**149 ± 14.1**	**-22.7**
	fit (best fit conditions)	Friedman	Process # 1	56.2	4.20 ± 0.65	150 ± 24.6	-20.0
			Process # 2	61.7	2.86 ± 0.30	99.5 ± 10.8	-16.0
			Process # 3	*64.6*	*2.02 ± 0.26*	*69.8 ± 9.07*	*-11.8*
			Process # 4	66.8	1.56 ± 0.02	53.2 ± 0.96	-9.76
		F-W-O	Process # 1	56.2	5.72 ± 0.29		
			Process # 2	61.7	3.66 ± 0.32		
			Process # 3	*64.6*	*2.59 ± 0.20*		
			Process # 4	66.8	1.53 ± 0.02		
		Kissinger	Process # 1	56.2	5.16 ± 0.85	186 ± 40.1	-22.2
			Process # 2	61.7	3.34 ± 0.25	117 ± 16.6	-17.2
			Process # 3	*64.6*	*2.61 ± 0.89*	*89.7 ± 40.9*	*-15.7*
			Process # 4	66.8	1.47 ± 0.77	48.1 ± 36.2	-11.2

As we can notice, the results obtained with different methods are in fairly good agreement. Furthermore, the values obtained, after deconvolution, for the main peak compared to those obtained from the whole process, are also congruent. For those cases where the main process, because of the pattern complexity or rearrangements, is hard to distinguish, as for the sample B1_kt1, it is difficult to compare them.

We can also conclude that as long as the signal is not of great complexity, no rearrangements can be observed, and the main processes are easily noticeable, the Kissinger method applied to the observed peaks can provide a reliable and quick estimation of the kinetic parameters.

4.1.1.2.3.   Kinetic analysis of unperfumed base 1 (B1_u) stored at low temperatures

One may now supplement the qualitative observations already made for unperfumed base B1_u, concerning the shape of the heating and cooling curves before and after storage at low temperatures, with information about kinetic parameters of the processes. Although for the samples stored at 4°C, the de-ageing cycle leads to a single main process and deconvolution seems to be not necessary, a deconvolution procedure with the condition of best fit was performed for both control situations. These are at the beginning and after 1.5 years storing, where rearrangements within the sample occur during the de-ageing cycle. In this way, the process of interest at 4°C could be followed in comparison to the controls. In Table 11 the results of the kinetic analysis obtained by applying the Kissinger method are listed. All investigated virgin samples (the control sample and the samples stored at 4°C) were subjected to two de-ageing cycles before analysis.

After storing 1.5 years at 4°C the process at approx. 64°C reveals an increase of rate constant value, i.e. a decrease of stability. The storage at low temperature restores at the beginning (one week at 4°C) the initial value of the rate constant, accompanied by a change in the pattern appearance. With prolonged storage at 4°C (2 weeks), $k_{25°C}$ increases, showing a slight tendency toward destabilisation (the curve pattern from rejuvenation cycle is, however, not changing compared to the first week at 4°C). After 1 month of storage, $k_{25°C}$ reaches the value of the 1.5 years old control sample. This is also accompanied by clear modifications of the curve pattern after the rejuvenation cycle.

Tab. 11: Kinetic parameters for a 1.5 years old *unperfumed base B1_u* stored at low temperature (4°C) for different storage time (7 days, 14 days and 1 month respectively) compared to the 1.5 years old control sample at 25° and to the same base as received; the enthalpy value H_0, for the whole sample, the peak temperature corresponding to β=10°C/min, $T_p^{\beta=10°C/min}$, and the type of the analysed process for the given temperature are also given

Storage time	Storage temperature	Type of process	$\dfrac{H_0}{J/g}$	$\dfrac{T_p^{\beta=10°C/min}}{°C}$	$\dfrac{E_a}{10^5\,J/mol}$	$\ln(A/s^{-1})$	$\ln(k_{25°C}/s^{-1})$
As received	25°C	main	9.18 ± 0.10	64.03	4.66 ± 0.43	164 ± 23.7	-24.2
1.5 years	25°C	main & secondary	10.3 ± 0.62	63.40	2.67 ± 0.16	92.2 ± 14.1	-15.8
+7 days	4°C	main	6.24 ± 0.54	61.70	4.45 ± 0.37	157 ± 21.6	-22.4
+14 days	4°C	main	5.80 ± 0.46	62.03	3.89 ± 0.38	137 ± 22.0	-20.2
+1month	4°C	main	6.24 ± 0.09	62.53	3.33 ± 0.46	116 ± 24.8	-18.2

4.1.1.3.   Influence of the de-ageing

4.1.1.3.1.   Unperfumed samples

A problem which has to be investigated is whether the number of de-ageing cycles affects the results of the kinetic analysis.

As it has already been mentioned, we have chosen two cycles of de-ageing prior the kinetic analysis. The question is whether the number of performed cycles influences the results of the kinetic analysis.

In the first instance we will concentrate on the unperfumed bases and B1_u was taken as a model substance.

This phenomenon was studied for three different storage times for which the thermal properties of the sample do not vary too much. These moments are at the beginning, after 1 month and after 6 months. The curve shapes of the first and second heating-cooling run in form of the conversion rates for these three storage times are shown in Figure 43. The results are related to those obtained for longer storage periods, namely for 1.5 and 2.5 years.

Storage time	First thermal run	Second thermal run
As received		
1 month		
6 months		
1.5 years		
2.5 years		
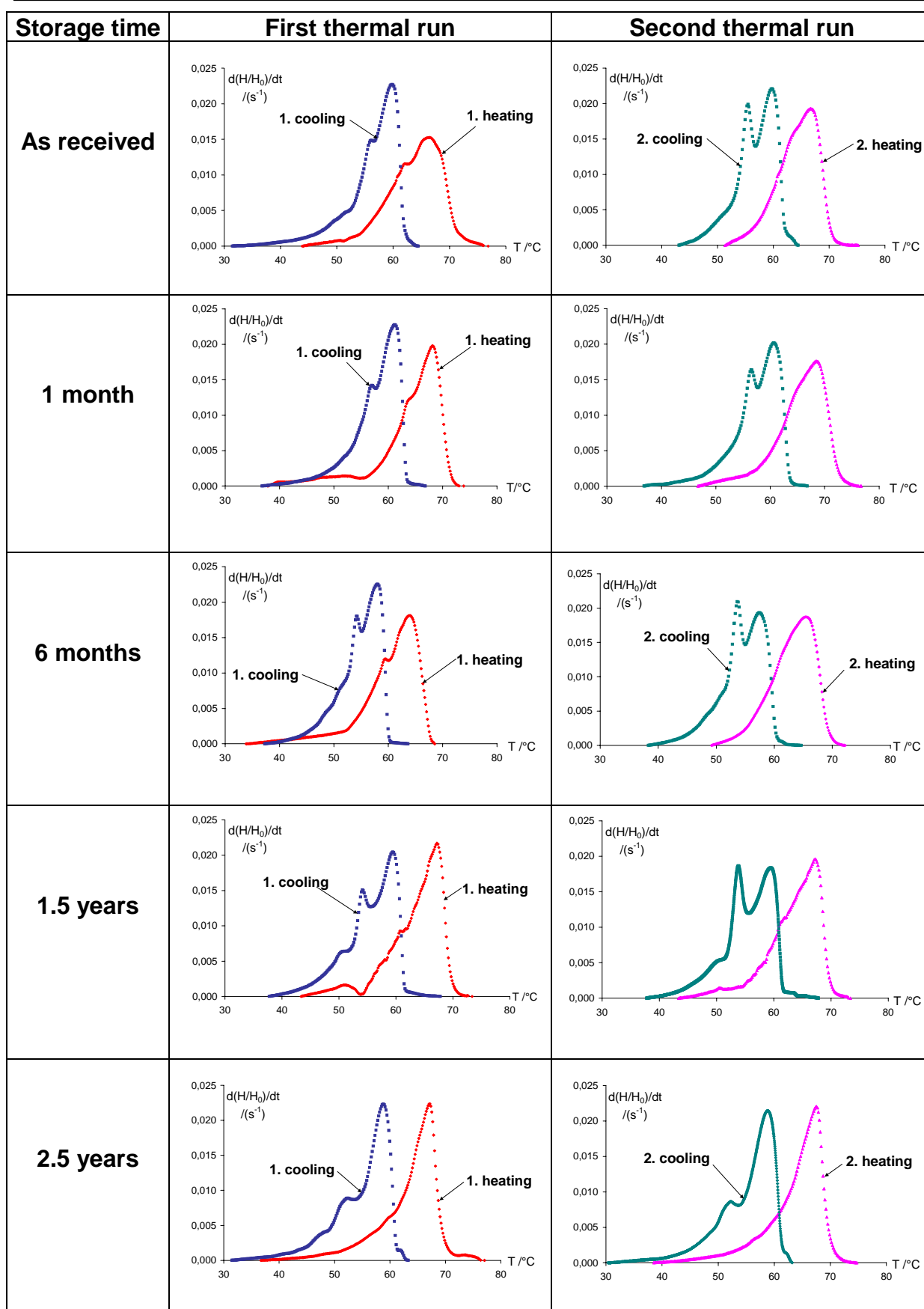
Fig. 43: *Unperfumed base B1_u* at five different moments in time. Conversion rates from DSC plots ($\beta=10$°C/min for heating and cooling

For unperfumed base B1_u, deconvolution is a necessary procedure for calculation because of the rearrangements that are observed while performing the cycles. After 2.5

years of storage, the sample shows a simple main peak pattern and deconvolution can be avoided. This effect of rearrangement raises difficulties in applying additional conditions for the deconvolution procedure all the more as the contribution of individual processes does not remain the same during each heating session of the de-ageing cycles. For this reason, the conversion rate patterns of the unperfumed sample B1_u were deconvoluted with the condition of best linear fitting, if less than two de-ageing cycles were performed. The method of Kissinger was applied after that for the calculation of kinetic parameters of each process.

Because of the rearrangements that take place while performing the de-ageing cycles, the contributions of different processes change. As a result, the comparison of the kinetic parameters, calculated for the deconvoluted processes, should be done at the same temperature.

As shown in Figure 44, the unperfumed base B1_u analysed as received is interchanging the importance of the main peak from approx. 67°C to approx. 64°C while heating, after the performance of a second thermal cycle. After two thermal cycles the sample reaches a stable configuration (rearrangements are not taking place any more) with the main peak at approx. 64°C. This phenomenon is observed until 1.5 years of storage.

Fig. 44: *Unperfumed base B1_u* during four heating-cooling thermal runs ($\beta=10°C/min$). The interchange of importance of the main peaks from approx. 67°C (full arrow) to approx. 64°C (dashed arrow) is indicated.

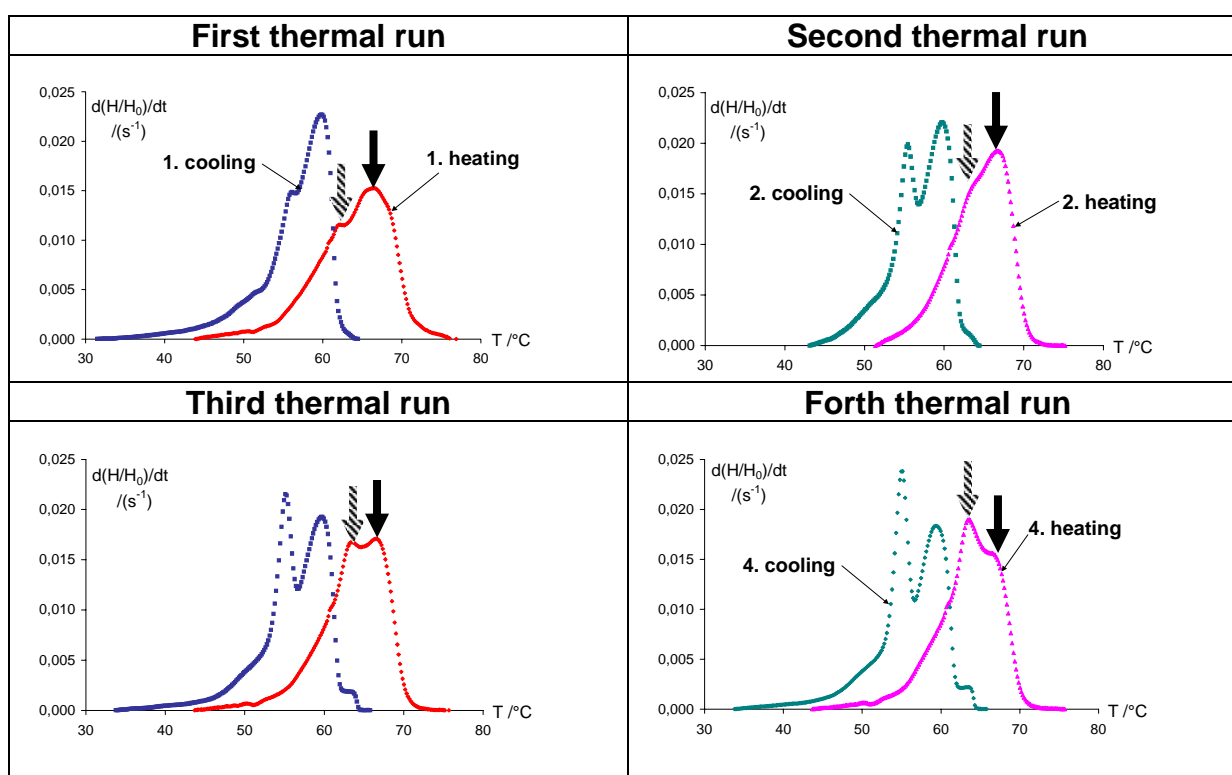The results of the kinetic analysis for the process with the main peak at aprox. 64°C (dashed arrow in Figure 44) , are summarised in Table 12.

The 2.5 years old sample, as illustrated in Figure 43, displays a stable configuration from the first thermal cycle. The heating and cooling runs superpose. The main peak during heating remains unchanged at approx. 67°C, without undergoing any transition to 64°C. Therefore, in the analysis of the peak at 64°C, the storage time will be considered up to 1.5 years.

Tab. 12: Kinetic parameters of *unperfumed base B1_u* for the main thermal process resulting after two de-ageing cycles as depending on the number of thermal cycles and time, obtained with Kissinger method; temperature cycles were performed with the same sample; the enthalpy, H_0, for the whole sample, the peak temperature corresponding to $\beta=10°C/min$, $T_p^{\beta=10°C/min}$, and the type of the analysed process for the given temperature are also given

Storage time	Type of process	$\dfrac{H_0}{J/g}$	Number of de-ageing cycles	$\dfrac{T_p^{\beta=10°C/min}}{°C}$	$\dfrac{E_a}{10^5\,J/mol}$	$\ln(A/s^{-1})$	$\ln(k_{25°C}/s^{-1})$
As received	main	9.18 ± 0.10	2	64.0	4.66 ± 0.43	164 ± 23.7	-24.2
1month	main & secondary	10.6 ± 0.12	1	64.6	5.19 ± 2.24	182 ± 89.8	-27.3
6months		9.27 ± 0.45	0	63.5	2.08 ± 0.33	70.9 ± 20.3	-19.2
1.5 years	main & secondary	10.3 ± 0.62	2	63.4	2.67 ± 0.16	92.9 ± 14.1	-15.5
1.5 years		10.4 ± 0.22	1	63.5	3.59 ± 1.07	126 ± 48.9	-19.3
1.5 years		10.3 ± 0.58	0	65.1	3.14	109	-17.7

It is noticeable, that the performance of a thermal cycle leads to a lowering of the rate constant values, which indicates the formation of a more stable structure. Two thermal cycles lead to an increase of the rate constant, $k_{25°C}$, showing a slight destabilisation, however, without reaching the initial value of $k_{25°C}$. In any case, once de-aged, the unperfumed sample B1_u remains fairly resistant to modifications with respect to a new thermal cycle.

The same tendency is observed after storage for 1.5 years. One thermal cycle seems to induce a slight stabilisation effect; two successive cycles lead to a slight destabilisation; this slight destabilisation can be regarded as a recovery effect. The 1.5 years old sample is initially fairly resistant to modifications with respect to a new thermal cycle; moreover, for the 1.5 years old sample, important differences with respect to the number of thermal

cycles cannot be noticed anymore. The sample has after 1.5 years of storage at room temperature a new, more compact, defined configuration, characterised by a quite high resistance against thermal stress .

In any case, one can observe that the storage of B1_u for 1.5 years at room temperature leads to an increase of the rate constant comparative to the state as received, irrespective of the number of thermal cycles performed. That means that storage time can have a contribution to the decrease of the B1_u sample stability.

This destabilisation effect in time is consequently associated with a new, more compact and defined structure, resistent to thermal modifications.

The kinetic parameters for the process at approx. 67°C (full arrow in Figure 44) which was initially the most important (before performing de-ageing) and which becomes with time again (after 2.5 years of storage) the stable main process irrespective of the thermal procedure, are listed in Table 13. The performance of one de-ageing cycle shows that the 2.5 years old sample has a very stable structure, as we can notice from the superposition of all heating and cooling curves in Fig 43.

Base B1_u is analysed for three characteristic storage times of time after one de-ageing cycle. From the kinetic point of view, the sample shows a destabilisation after 1.5 years of storage at room temperature, i.e. the rate constant decreases as compared to the 1 month old sample (when the sample has still the same thermal behaviour as when received). But it recovers to the same value of the rate constant after 2.5 years of storage. The DSC pattern and the stable microscopic appearance of base B1_u after 2.5 years support the hypothesis of a very stable unperfumed softener base.

Tab. 13: Kinetic parameters of *unperfumed base B1_u* for the main initial thermal process for one de-ageing cycle and for different storage times; temperature cycles were performed with the same sample; whole enthalpy of the process, H_0, the peak temperature corresponding to $\beta=10°C/min$, $T_p^{\beta=10°C/min}$, and the type of the analysed process for the given temperature are also given

Storage time	Type of process	$\dfrac{H_0}{J/g}$	Number of de-ageing cycles	$\dfrac{T_p^{\beta=10°C/min}}{°C}$	$\dfrac{E_a}{10^5 \, J/mol}$	$\ln(A/s^{-1})$	$\ln(k_{25°C}/s^{-1})$
1month	main & secondary	10.6 ± 0.12	1	68.4	4.40 ± 1.49	152 ± 62.1	-25.6
1.5 years	main & secondary	10.4 ± 0.22	1	67.0	5.53 ± 1.42	193 ± 61.1	-30.1
2.5 years	main	9.31 ± 0.34	1	67.9	4.36 ± 0.43	151 ± 23.6	-24.7

The unperfumed sample B2_u can be taken as another example for the analysis of the influence of the de-ageing cycle on kinetic parameters. For sample B1_u, storage times are chosen, namely "as received", 1 month and 6 months storage. Figure 45 summarises the DSC-curves. As it can be noticed, the second heating-cooling is similar for all three investigated unperfumed sample (corresponding to "as received", 1 month and 6 months storage), therefore parameters can be compared. Furthermore, for a large period of storage (after 2.5 years), when the changes of curve shape are obvious, the values of the kinetic parameters after one thermal cycle - which is, as it has been mentioned, a sufficient condition for curve superposition - could be also compared with those already obtained.
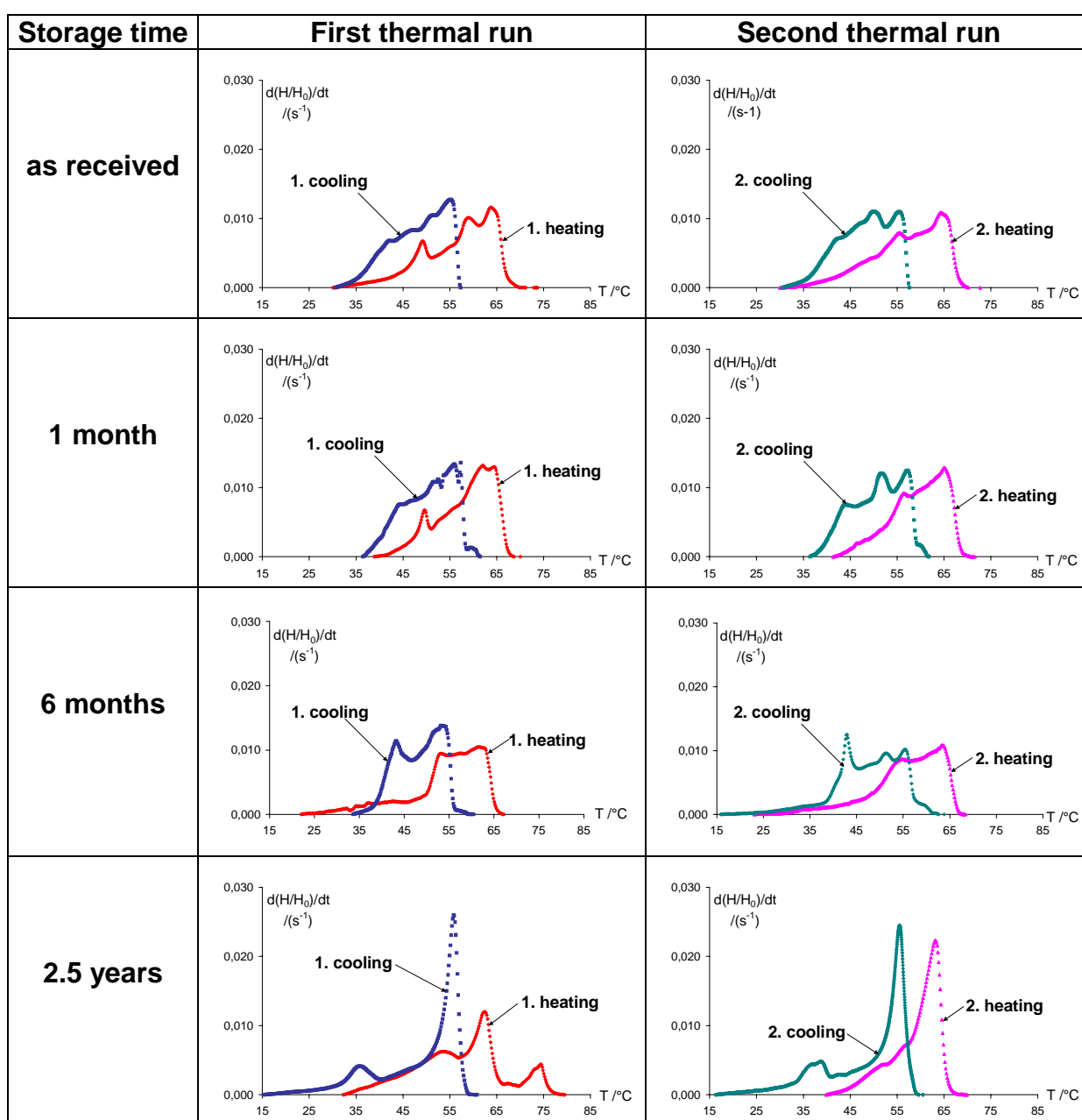
Fig. 45: *Unperfumed base B2_u* for four storage times. Conversion rates from DSC curves recorded with 10°C/min for heating and cooling

Compared to unperfumed base B1_u, unperfumed base B2_u exhibits a simple single main peak structure after 2.5 years and deconvolution can be avoided. However, for the initial sample, after 1 month and after 6 months storage a complex DSC-pattern is obvious while thermal cycles are performed, so that deconvolution is required. Moreover, the same observation as for B1_u base is made: due to structural rearrangements, only best fit conditions for the deconvolution procedure can be applied.

While performing de-ageing procedures, the process at approx. 56°C turns from the main into the secondary one upon heating, while for the process at approx. 64°C the reverse is registered, as illustrated in Figure 46.
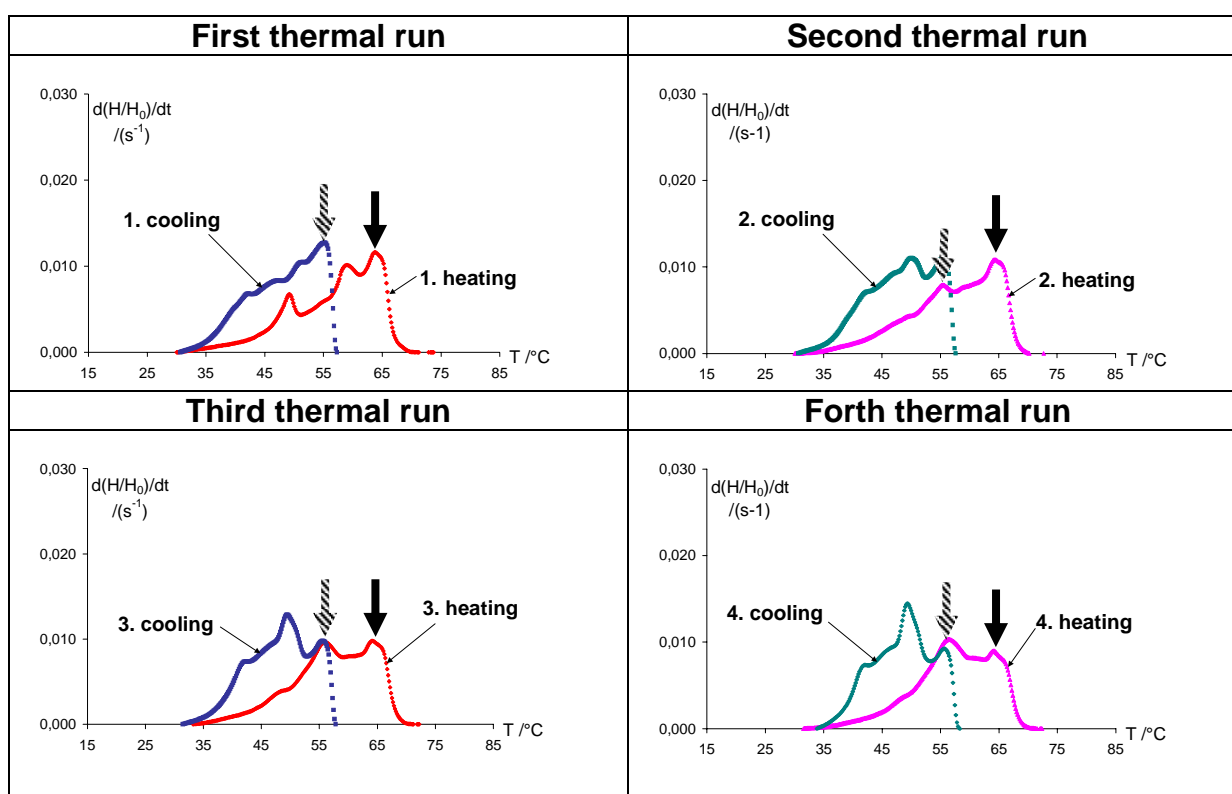
Fig. 46: *Unperfumed base B2_u* during four heating-cooling thermal runs (β=10°C/min). The interchange of importance of the main peaks at approx. 64°C (full arrow) to approx. 56°C (dashed arrow) is indicated.

The results for the kinetic analysis of the two processes which are interchanging their importance, namely the process at approx. 64°C (full arrow in Figure 56) and the process at approx. 56°C (dashed arrow in Figure 46), are summarised in Table 14.

The evolution with storage time of the rate constant values, $k_{25°C}$, is similar for both peaks. This can be interpreted as follows: the first thermal cycle is accompanied by a lowering of rate constants for both thermal effects. This may be the consequence of the formation of a more stable structure. The formation of this structure is due to a new association of the surfactants molecules in micellar and liposomal constructs after separation of the

components upon heating and is triggered by cooling. An additional thermal cycle almost recovers the initial value of $k_{25°C}$ and this indicates a quite flexible emulsion structure which still preserves its thermal properties under stress conditions.

A similar thermal behaviour was observed for the unperfumed base B1_u for the main peak at 64°C, depending to the number of thermal cycles.

After 2.5 years of storage and one thermal cycle, the unperfumed sample B2_u has already the value of the rate constant, which it had initially after two thermal cycles. This means, time causes a destabilisation of the sample. On the other hand, comparing the values of the rate constant for the once rejuvenated sample, this confirms that a destabilisation takes place with time.

As the 2.5 years old sample is already hardened and exhibits only one of the initial peaks - the peak at aprox. 64°C - we can speculate that this peak could be seen in correspondence to the viscosity properties. This is supported by the fact that while running the temperature cycles, this peak gains importance at the expense of the initial main peak at approx. 56°C.

Tab. 14: Kinetic parameters of *unperfumed base B2_u* for the two most important thermal process as depending on the number of thermal cycles and storage time, obtained with the Kissinger method; temperature cycles were performed with the same sample; the enthalpy, H_0, for the whole process, the peak temperature corresponding to the $\beta=10°C/min$, $T_p^{\beta=10°C/min}$, and the type of the analysed process for the given temperature are given

Storage time	Number of rejuvenating cycles	$\dfrac{H_0}{J/g}$	Type of process	$\dfrac{T_p^{\beta=10°C/min}}{°C}$	$\dfrac{E_a}{10^5\,J/mol}$	$\ln(A/s^{-1})$	$\ln(k_{25°C}/s^{-1})$
As received	2	9.36 ± 0.15	main	57.1	2.71 ± 0.36	95.6 ± 24.7	-13.8
			secondary	64.5	4.32 ± 0.51	151 ± 30.4	-23.1
1month	1	8.76 ± 0.52	main	65.2	7.82 ± 0.51	276 ± 35.3	-39.6
			secondary	56.8	5.18 ± 0.84	186 ± 39.6	-22.6
6months	0	9.80 ± 0.26	main&	63.4	3.40 ± 0.77	119 ± 36.5	-18.5
			secondary	55.3	2.93 ± 0.19	105 ± 14.3	-13.7
2.5years	1	11.3 ± 0.20	main	63.5	4.29 ± 0.54	151 ± 27.8	-22.5

An important observation is that both unperfumed bases, B1_u and B2_u have similar behaviour with respect to the number of de-ageing cycles performed: a first thermal cycle

causes a slight destabilisation, but an additional one almost leads to recoverage of the initial state. This is one more reason to analyse samples which were subjected to a double de-ageing procedure.

B1_u and B2_u bases have, however, different time stabilities. After 2.5 years B1_u remains stable while B2_u suffers the phenomenon of hardening. This difference in thermal behaviour is supported by the different variations of the rate constant with time: while B1_u has a similar value of the rate constant after 2.5 yeras, B2_show an increased value of the rate constant, which means a destabilisation.

4.1.1.3.2.   Cooling curves

Also of interest is the information which can be derived from the cooling curves of a thermal cycle. For this reason again, unperfumed sample B1_u was taken as a model and subjected to two different kinds of temperature programmes: one with four times the same and another one with four different heating rates (5, 10, 15 and 20°C), while the same cooling procedure was maintained in both cases, namely four different cooling rates of 5, 10, 15 and 20°C. The samples were de-aged for one time. The kinetic parameters inferred by applying Kissinger's method to the main processes at approx. 54°C of the cooling curves are given in Table 15. It has to be mentioned that this process gains importance as a result of the thermal cycle procedure as well as a consequence of time of storage at the expense of the initial main process at approx. 59°C.

Tab. 15: Kinetic parameters of 1.5 years old *unperfumed base B1_u* calculated for one of the main processes from the cooling curves of runs with different samples or with the same sample in a cycle with same or different heating rates; the value of the enthalpy, H_0, for the whole process and the peak temperature corresponding to $\beta=10°C/min$, $T_p^{\beta=10°C/min}$, are also given for comparison

Type of analysis	Type of programme		$T_p^{\beta=10°C/min}$ °C	Type of process	$\dfrac{H_0}{J/g}$	$\dfrac{E_a}{10^5\,J/mol}$	$\ln(A/s^{-1})$	$\ln(k_{25°C}/s^{-1})$
	Heating run	Cooling run						
Separate runs	Constant heating rate	Constant cooling rate	53.8	secondary	8.55 ± 0.71	5.03 ± 0.97	210 ± 43.7	6.52
Cycle	Constant heating rate	Several cooling rates	53.5	main	9.68 ± 0.38	5.60 ± 0.69	233 ± 35.3	6.49
Cycle	Several heating rates	Several cooling rates	54.0	main	9.47 ± 0.26	5.25 ± 1.20	218 ± 54.1	5.67
			54.3	main	8.26 ± 0.61	5.13 ± 1.24	213 ± 56.2	6.10
			54.1	main	8.67 ± 0.59	4.66 ± 0.68	196 ± 35.0	7.45
			54.0	main	9.27 ± 0.21	4.87 ± 0.81	203 ± 40.5	6.86
			Mean	main	8.92 ± 0.58	4.98 ± 0.25	207 ± 9.68	6.52 ± 0.77

Irrespective of the heating cycle procedure, either with the same or a different rate, and irrespective of performing a cycle with the same sample or separate runs with new samples, the kinetic parameters obtained from the cooling signals of the temperature cycle give similar values of the rate constant $k_{25°C}$ for the main process. This similarity gives evidence about the stability of the process and is corroborated by the superposability of the cooling curves recorded under various conditions. It has to be underlined that the effects, recorded during heating, do not superpose. This seems to support the assumption of reorientation of structures during heating.

Comparing the kinetic parameters of a once de-aged unperfumed sample B1_u, obtained from the heating part of a temperature cycle, with those obtained from the cooling stage, one observes that the latter are much higher. This suggests that the processes which take place in the sample during cooling are faster than those which occur during heating and therefore are decisive for sample stability.

The results of the kinetic analysis for the secondary process which occurs during cooling at approx. 59°C in a cyclic temperature programme, are summarised in Table 16.

Tab. 16: Kinetic parameters of 1.5 years old *B1_u unperfumed base* calculated for the main initial processes from the cooling curves of runs with different samples or with the same sample in a cycle with the same or different heating rates; the value of the enthalpy, H_0, for the whole process and the peak temperature corresponding to the β=10°C/min, $T_p^{\beta=10°C/min}$, are also given

Type of analysis	Type of programme		$T_p^{\beta=10°C/min}$ °C	Type of process	$\dfrac{H_0}{J/g}$	$\dfrac{E_a}{10^5\,J/mol}$	$\ln(A/s^{-1})$	$\ln(k_{25°C}/s^{-1})$
	Heating run	Cooling run						
separate runs	constant heating rate	constant cooling rate	59.5	main	8.55 ± 0.71	5.11 ± 0.73	210 ± 34.5	3.42
cycle	constant heating rate	several cooling rates	58.3	secondary	9.68 ± 0.38	2.88 ± 0.11	128 ± 11.8	12.0
cycle	several heating rates	several cooling rates	59.3	secondary	9.47 ± 0.26	3.07 ± 0.79	135 ± 38.7	11.4
			58.8	secondary	8.26 ± 0.61	3.10 ± 0.67	137 ± 34.2	11.4
			59.5	secondary	8.67 ± 0.59	3.00 ± 0.72	133 ± 36.3	11.4
			59.5	secondary	9.27 ± 0.21	3.50 ± 0.88	151 ± 42.3	9.49
			Mean	secondary	8.92 ± 0.58	3.17 ± 0.22	139 ± 8.01	10.9 ± 0.93

The values obtained for $k_{25°C}$ are close, irrespective of the heating procedure. If separate runs with different rates are conducted and each time with a new sample, the rate constant has lower values. This phenomenon has already been observed for this base during the analysis of the heating runs with the same or different samples. It can be explained by considering that a sample suffers a longer accelerated procedure of thermal stress when an entire cycle is performed than when subjecting it to a single run. This phenomenon is observed for the peak around 59°C which is the peak that looses its importance with storage time and under the accelerated conditions of thermal stress offered by the de-ageing procedure.

4.1.1.3.3.   Perfumed samples

After investigating the influence of the number of rejuvenation cycles on representative samples of unperfumed bases, a further step is to test how the repetitive procedure of the thermal cycle affects the thermal properties of perfumed samples. B1 base perfumed samples are investigated first.

After 1 month of storage there is no significant difference of the curve shapes not only in case of unperfumed base B1_u, as it has been already shown, but also for the perfumed samples of the base. This is illustrated for one of each type of fragrances in Figure 47.

Sample	t=0	t=1month
B1_ac3		
B1_ad3		
B1_kt1		
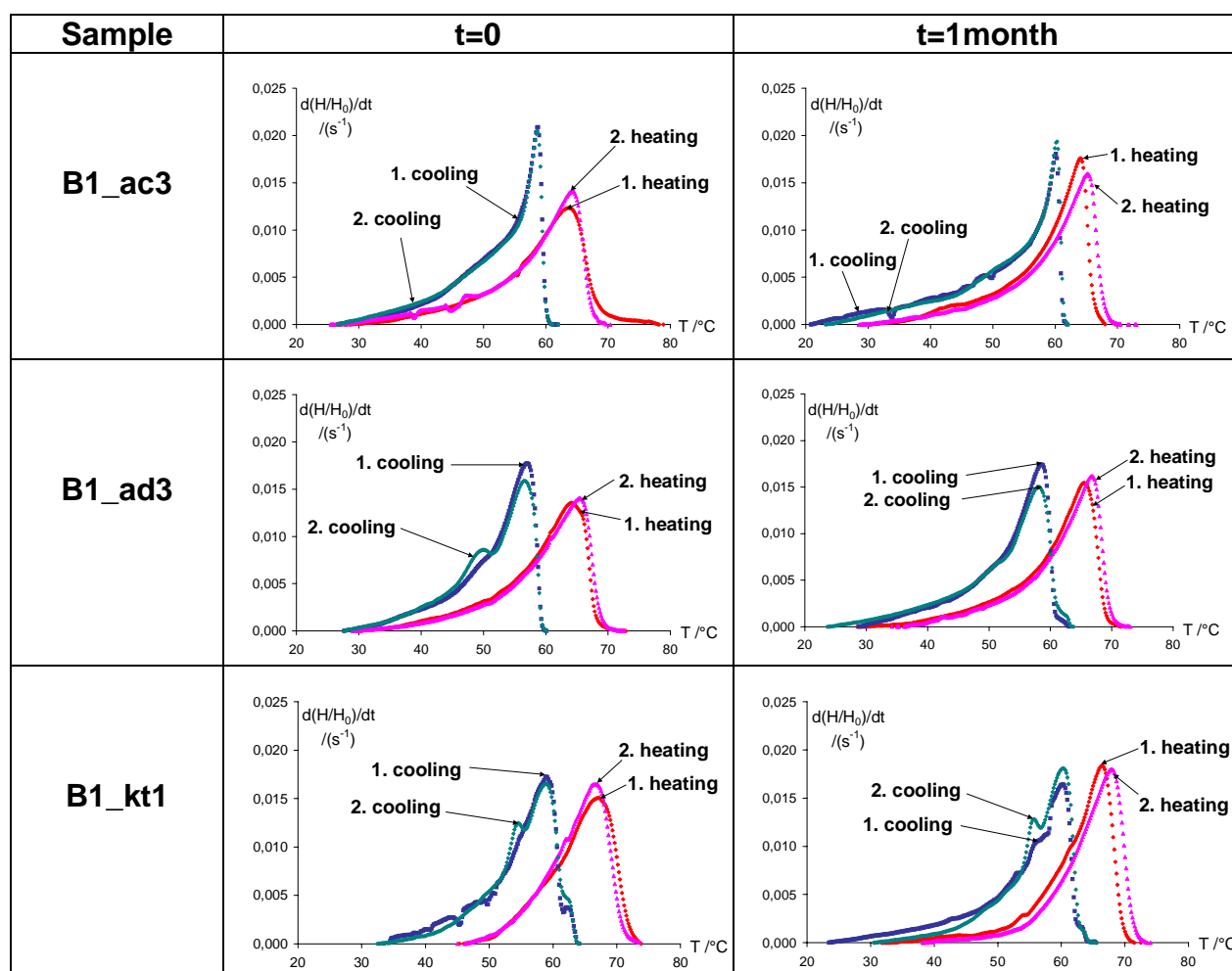
Fig. 47: Reaction rates from the thermal cycle (two cycles with 10°C/min) of *unperfumed base B1_u* with one of each type of fragrance after 1 month of storage at room temperature compared to those of the start material.

This observation enables to compare the kinetic parameters of perfumed samples de-aged once (1month old) and twice. In Table 17 the kinetic parameters calculated for the processes which corresponds to the main peak of the whole endothermic effect and which were obtained after a previous deconvolution with restrictions for the fit, are listed together with the kinetic parameters calculated from the analysis of the whole effect.

Tab. 17: Kinetic parameters for *B1 base with different fragrances* after one single rejuvenation cycle, calculated with the Kissinger method; individual processes obtained after deconvolution which correspond to the peak temperature of the main process from the whole signal are compared for the kinetic parameters; the whole enthalpy of the process, H_0, and the peak temperature corresponding to $\beta=10°C/min$, $T_p^{\beta=10°C/min}$, are given.

Fragrance	$\dfrac{H_0}{J/g}$	Type of analysis	$\dfrac{T_p^{\beta=10°C/min}}{°C}$	$\dfrac{E_a}{10^5\,J/mol}$	$\ln(A/s^{-1})$	$\ln(k_{25°C}/s^{-1})$
B1_ac1	9.77 ± 0.21	**whole process**	65.0	4.79 ± 0.64	174 ± 31.2	-26.5
		restricted deconvolution	65.7	4.82 ± 0.53	169 ± 27.2	- 25.8
B1_ac2	11.36 ± 0.20	**whole process**	65.9	5.82 ± 1.03	204 ± 45.9	-30.7
		restricted deconvolution	66.2	5.13 ± 0.40	180 ± 22.6	-27.4
B1_ac3	8.79 ± 0.18	**whole process**	65.5	5.63 ± 1.37	198 ± 59.5	-29.6
		restricted deconvolution	66.0	4.59 ± 0.63	160 ± 32.3	-25.0
B1_ad1	13.11 ± 0.25	**whole process**	66.4	5.92 ± 0.59	208 ± 29.5	-31.4
		restricted deconvolution	66.4	5.16 ± 0.74	180 ± 35.5	-27.9
B1_ad2	11.15 ± 0.17	**whole process**	65.4	8.76 ± 1.69	309 ± 69.8	-44.2
		restricted deconvolution	66.0	8.06 ± 0.93	284 ± 42.1	-41.5
B1_ad3	10.38 ± 0.32	**whole process**	66.5	6.55 ± 0.54	230 ± 27.8	-34.7
		restricted deconvolution	66.9	5.25 ± 0.48	183 ± 25.4	-28.7
B1_kt1	12.65 ± 0.18	**whole process**	68.0	4.68 ± 0.37	162 ± 21.5	-26.6
		restricted deconvolution	68.9	4.58 ± 0.58	159 ± 29.0	-26.4
B1_kt2	9.46 ± 0.61	**whole process**	68.0	4.68 ± 0.37	162 ± 21.5	-26.6
		restricted deconvolution	68.9	4.50 ± 0.50	155 ± 26.1	-26.2
B1_kt3	8.91 ± 0.18	**whole process**	65.0	7.09 ± 0.36	250 ± 140	-36.4
		restricted deconvolution	64.9	3.90 ± 1.40	136 ± 59.2	-21.6

The values of the rate constant $k_{25°C}$ show generally good agreement between the analysis of individual extracted processes corresponding to the main peak of the whole effect and the analysis of the main peak, without deconvolution. This fact suggests that for less complex patterns continuously rearranging while heated, deconvolution can be avoided, which is where the main peak is recognisable and not "embedded" in an overlapped multiple peaks signal structure.

In order to gain an overview about how the addition of fragrances is reflected in changes of the kinetic parameters values, taking also into account the role of de-ageing, the $k_{25°C}$ values of perfumed and unperfumed samples of base B1, rejuvenated once and twice, are summarised in Figure 48.
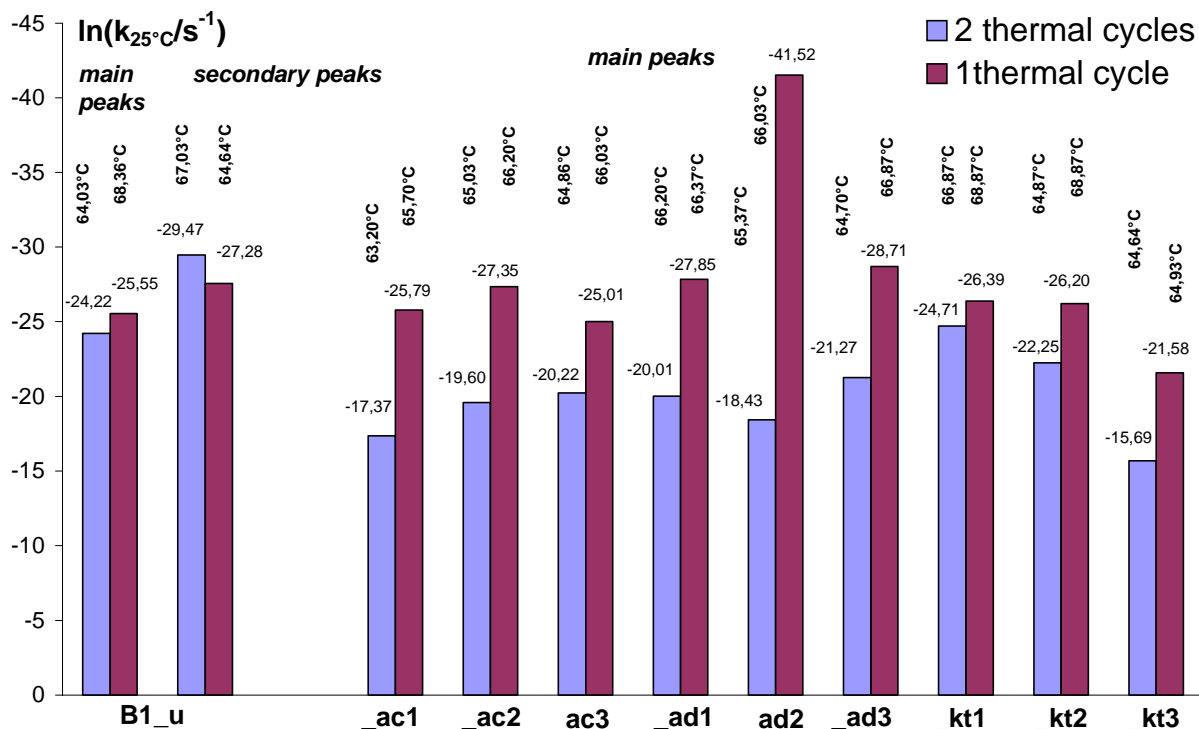

Fig. 48:   Values of the rate constant (Kissinger method for the whole process) for unperfumed and perfumed *B1 bases*: the samples de-aged once (1 month old, 25°C) are compared with the same samples de-aged twice and measured as received

With the only exception of the once rejuvenated sample B1_ad2, perfumed samples display no significant differences in $k_{25°C}$ values compared to their unperfumed base. One has to notice that an additional rejuvenation cycle increases the $k_{25°C}$ values of perfumed samples. One may conclude that the perfumed samples are less stable when twice de-aged. On the other hand, for the unperfumed sample B1_u, the additional de-ageing cycle does not change significantly the $k_{25°C}$ values of both the main and the secondary process. It may be concluded that fragrance addition to the unperfumed base B1_u leads to instability, translated in higher values of the rate constant only after an additional de-ageing cycle. Unlike these, the unperfumed sample B1_u shows a quite stable thermal behaviour, which is confirmed also by its macroscopical appearance after 2.5 years.

An additional confirmation for this stable thermal behaviour of unperfumed sample B1_u is offered by isothermal experiments: measurements over 24 hours at constant temperatures

corresponding to the main processes observed under non-isothermal conditions do not show relevant changes of the conversion rate pattern.

In the case of B2 base, the addition of fragrance does not lead to any significant difference of the curve shapes after one month of storage at 25°C. The same applies to the unperfumed base B2_u. This fact is illustrated in Figure 49 for two of the perfumed samples: B2_ac2 and B2_ad1.
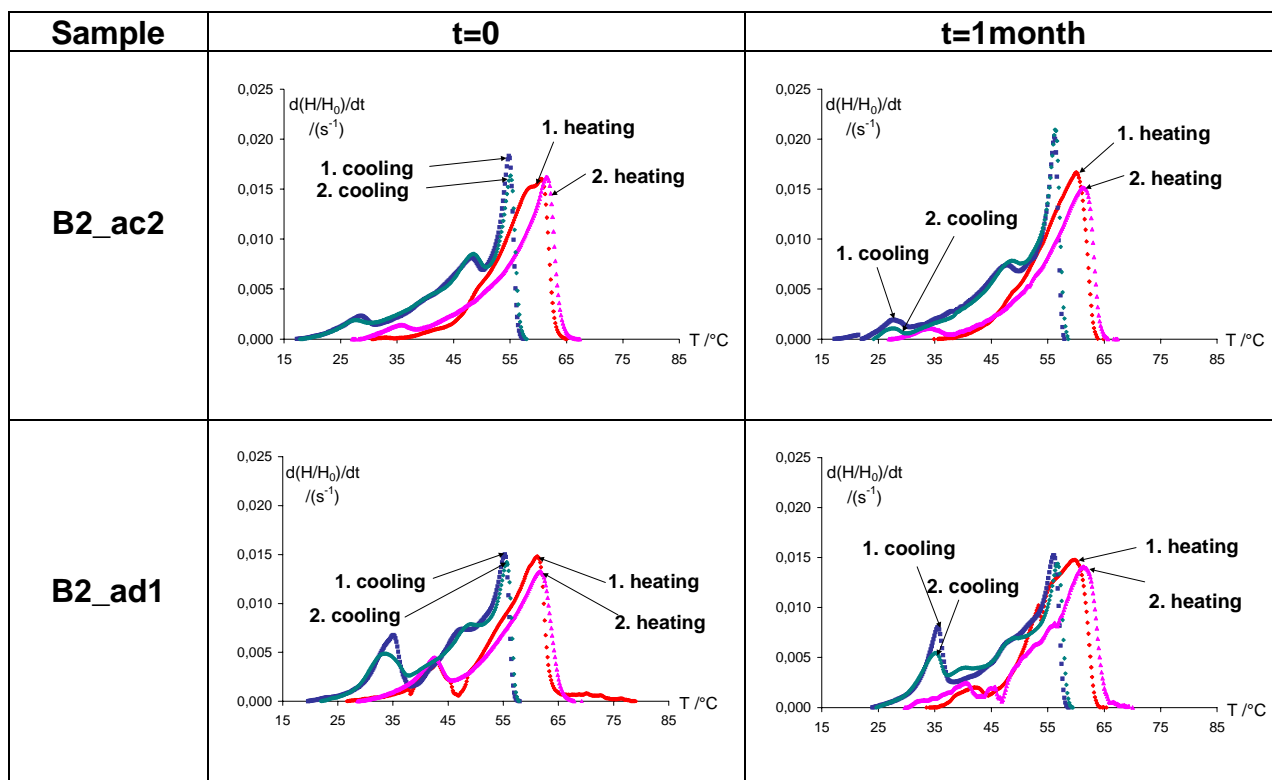
Fig. 49: Conversion rates from the thermal cycle (two cycles with 10°C/min) of *B2 base with two types of fragrances* after 1 month of storage at room temperature compared to those of the starting material

The conversion rate plots for the unperfumed sample B2_u subjected to one (1month) or two (initial) de-ageing cycles were deconvoluted because of the complexity of their shape. Four of the perfumed samples, subjected to the same procedures of one or two de-ageing cycles, were analysed without making a preliminary deconvolution. The results of applying the Kissinger method are summarised in Table 18.

One can observe that addition of fragrances leads to an increase of the rate constant values.

Tab. 18: Kinetic parameters of the main thermal processes in *B2 perfumed and unperfumed bases* after one de-ageing cycle (1month old samples), calculated with the Kissinger method; the enthalpy of the process, H_0, and the peak temperature corresponding to $\beta=10°C/min$, $T_p^{\beta=10°C/min}$, are given.

Sample	$\dfrac{H_0}{J/g}$	$\dfrac{T_p^{\beta=10°C/min}}{°C}$	Type of process	$\dfrac{E_a}{10^5\,J/mol}$	$\ln(A/s^{-1})$	$\ln(k_{25°C}/s^{-1})$
B2_u	8.76 ± 0.52	65.2	main	7.82 ± 0.51	276 ± 35.3	- 39.6
		56.8	secondary	5.18 ± 0.84	186 ± 39.6	-22.6
B2_ac1	10.7 ± 1.71	60.2	main	5.31 ± 1.27	189 ± 55.3	- 25.3
B2_ac2	8.18 ± 0.56	62.0	main	5.04 ± 0.14	179 ± 12.3	- 24.9
B2_ac3	7.52 ± 0.51	61.4	main	4.14 ± 0.35	139 ± 20.9	- 20.6
B2_ad1	7.65 ± 1.90	62.7	main	3.98 ± 0.56	20.0 ± 28.8	- 20.7

The comparative diagram of $k_{25°C}$ values corresponding to the main peak of the perfumed samples at aprox. 60°C is represented in Figure 44. While for the perfumed samples this peak temperature shows no significant shift as a consequence of the de-ageing cycles, for the unperfumed sample, an additional de-ageing transforms the peak from the main into a secondary one. A possible explanation may be that addition of perfume diminishes the freedom of motion and hence the rearrangement possibilities due to increased temperature, because of the insertion of perfume molecules into the vesicles/lamellae structures, already existent in the unperfumed base.

As we can notice from Figure 50, the addition of perfume increases the kinetic constant values. It thus destabilises the unperfumed base B2_u, irrespective of the number of de-ageing cycles.

The perfumed samples B2_ac3 and B2_ad1 do not show a significant modification of the rate constant values after one additional de-ageing cycle. In case of the perfumed samples B2_ac1 and B2_ac2, as well as in the case of the unperfumed sample B2_u, an increase of $k_{25°C}$ and, as a consequence, a slight destabilisation, can be observed as a function of the number of de-ageing cycles.
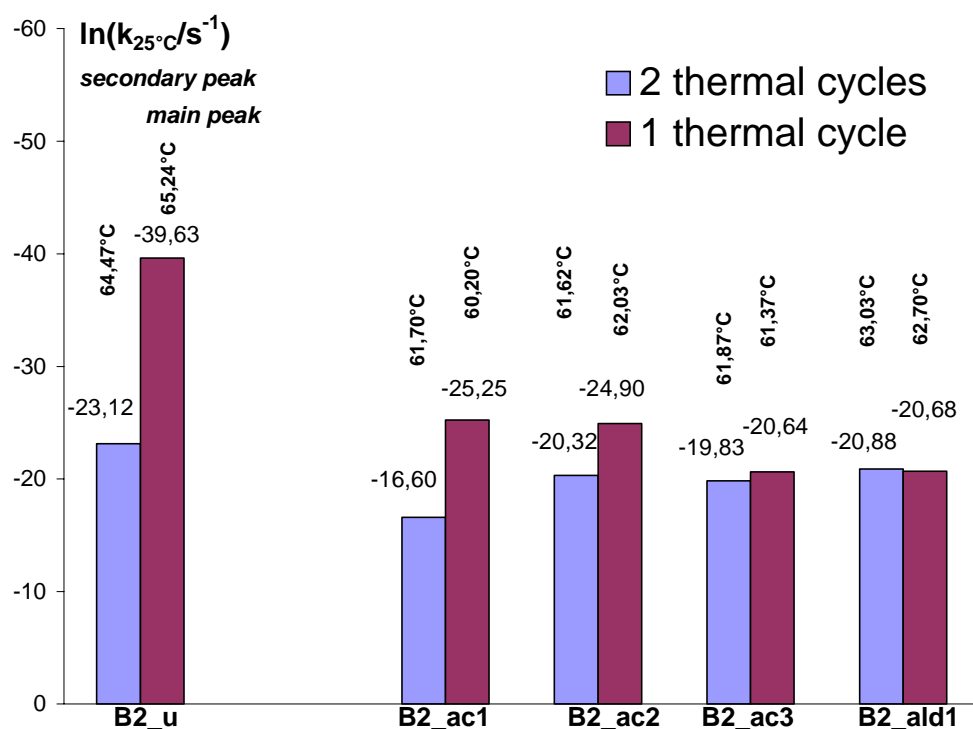
Fig. 50: Values of the rate constant (Kissinger method for the whole process for perfumed samples and for the deconvoluted main process for unperfumed samples) for unperfumed and perfumed *B2 bases*: the 1 month old 25°C samples (one time rejuvenated) are compared with the same samples rejuvenated two times and measured as received.

It can be concluded that for base B2, fragrance addition has a destabilisation effect. Besides, more than one de-ageing cycle increases the instability and this can be observed for both unperfumed and perfumed samples. Compared to perfumed B1 bases, base B2 with fragrances is less stable.

4.1.1.4. Influence of storage at high temperature on unperfumed bases 1 (B1_u) and 2 (B2_u)

As previously mentioned, softeners in daily life may be exposed to extreme temperatures which may alter their properties. The investigation of the role of low and high temperatures may put into evidence therefore not only a very important technological aspect, but also an economical one: the environmental implication during transport and storage before selling of the product. We have already seen the influence of low temperatures on unperfumed base B1_u. We shall investigate now the thermal behaviour of the unperfumed samples when they are subjected to high temperatures. For this reason

samples of unperfumed bases B1_u and B2_u were stored in closed crucibles for 7 days at 40°C before analysis.

Figure 51 shows the modifications of the DSC pattern pattern of unperfumed sample B1_u during the first and second heating-cooling runs of the temperature programme and after storing at 40°C for 7 days, compared to the reference samples. One can observe that secondary processes and shoulders vanish with a simplification of the characteristic pattern of the base for both heating and cooling.

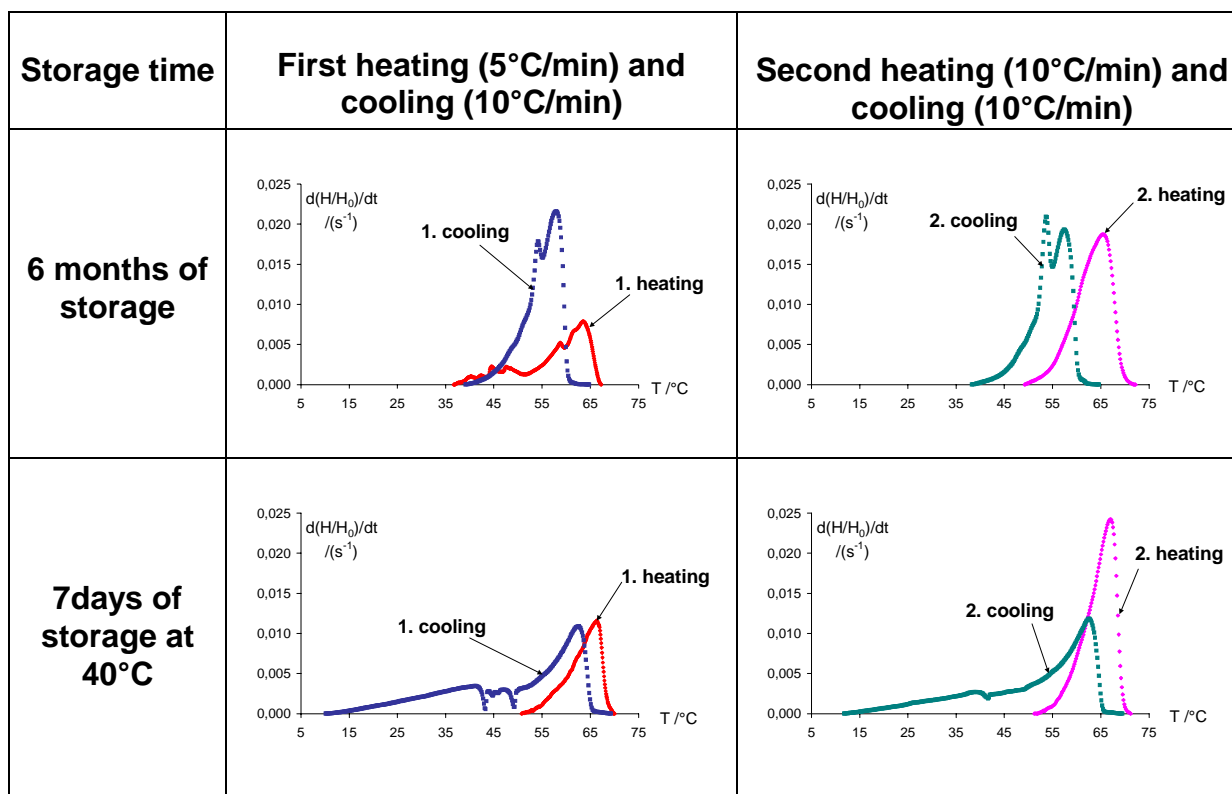| Storage time	First heating (5°C/min) and cooling (10°C/min)	Second heating (10°C/min) and cooling (10°C/min)
6 months of storage		
7days of storage at 40°C		

Fig. 51: Conversion rates of *unperfumed sample B1_u* stored at 40°C compared with the reference (6 months old sample) during the first and second thermal runs

Although heating and cooling curves are not superposed, one can observe that storage at high temperatures leads to a single process-shape not only for heating, but also for cooling. This means that the reformation of emulsion structures during cooling, as it is observed when bases are stored at room temperatures, is impeded. Consequently, the emulsion may become in the case of high temperature storage more consolidated, with a limited possibility of structure reformation.

The way the values of the kinetic parameters are affected by the storage at 40°C for 7 days is pointed out in Table 19.

Tab. 19: Kinetic parameters for *unperfumed baseB1_u* (Kissinger method) after storage for 7 days at 40°C compared to the reference at 25°C; the enthalpy value, H_0, for the whole process and the peak temperature corresponding to $\beta=10$°C/min, $T_p^{\beta=10°C/min}$, are given.

Storage time	Storage temperature (°C)	$\dfrac{H_0}{J/g}$	Type of process	$\dfrac{T_p^{\beta=10°C/min}}{°C}$	$\dfrac{E_a}{10^5\,J/mol}$	$\ln(A/s^{-1})$	$\ln(k_{25°C}/s^{-1})$
Reference	25	9.27 ± 0.45	main & secondary	66.5	2.81 ± 0.01	96.5 ± 12.1	-16.9
7 days	40	8.83 ± 0.85	main	66.9	5.11 ± 0.66	178 ± 31.8	-28.5

The value of the rate constant decreases upon storage at high temperature, a fact that indicates stabilisation. A possible explanation may be the formation of a more compact structure, where additional possibilities of movement are eliminated. This supposition is sustained by the simpler shape of the DSC signal. It is possible that the single peak, which is observable after 7 days at 40°C, may be linked to viscosity properties. This supposition is supported by the more dense macroscopical appearance of the sample. The DSC pattern with a single peak structure at approx. 67°C is also the one the sample displays after 2.5 years of storage at 25°C.

The unperfumed sample B2_u shows a similar behaviour after storage (7 days, 40°C). It displays a simplified pattern for both heating and cooling, as shown in Figure 52, which is maintained throughout the temperature programme.

The kinetic parameters are summarised in Table 20. The values show that the rate constant decreases after 7 days at 40°C, compared to the reference from 25°C, as in the case of unperfumed sample B1_u. Also one may suggest that the single peak, which remains after storage at high temperature, as in case of base B1_u is related to viscosity properties. This peak is also observable for the 2.5 years old sample which suffers the phenomenon of hardening.

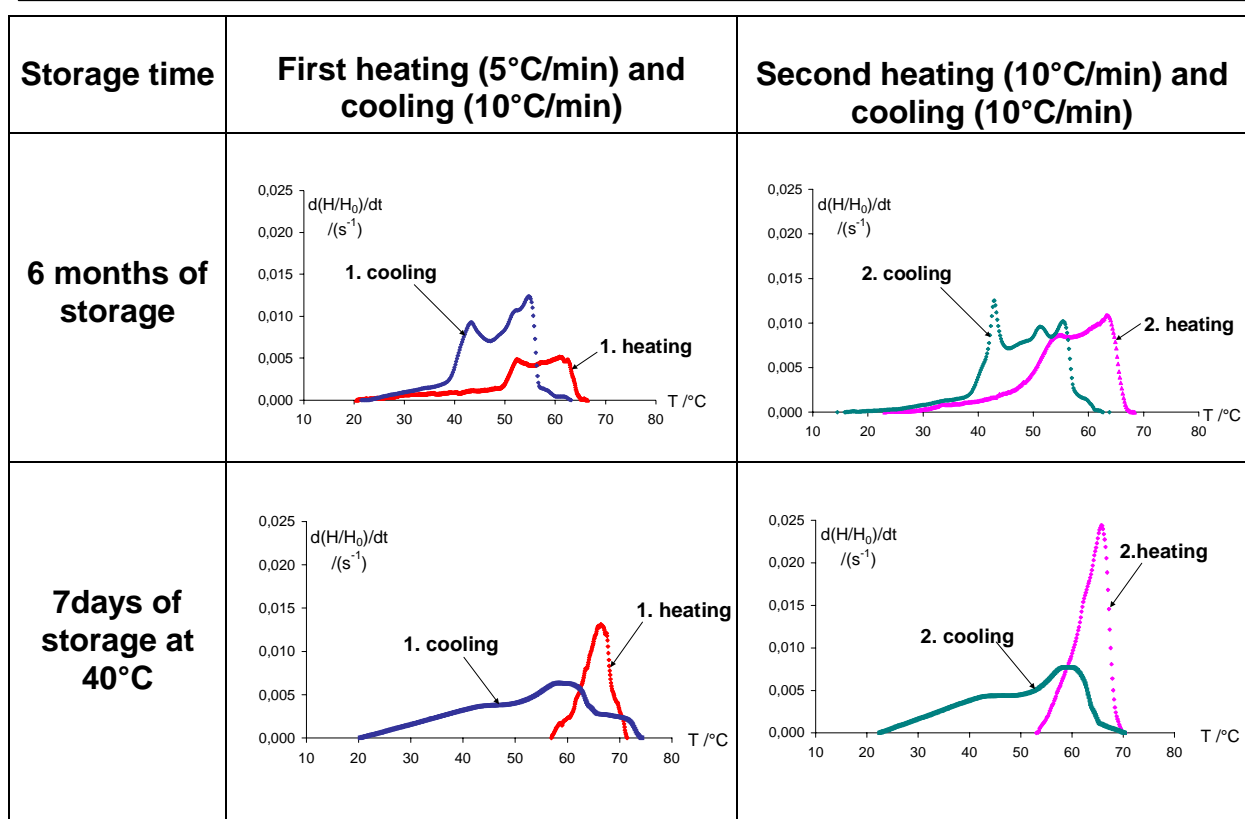| Storage time	First heating (5°C/min) and cooling (10°C/min)	Second heating (10°C/min) and cooling (10°C/min)
6 months of storage		
7days of storage at 40°C		

Fig. 52: Reactions rates of *unperfumed sample B2_u* stored at 40°C compared with the reference (6 months old sample) in the first and second thermal runs

Tab. 20: Kinetic parameters for *unperfumed base B2_u* (Kissinger method) after storage for 7 days at 40°C compared to the reference at 25°C; the enthalpy value, H_0, for the whole process and the peak temperature corresponding to $\beta=10°C/min$, $T_p^{\beta=10°C/min}$, are also mentioned.

Storage time	Storage temperature (°C)	$\dfrac{H_0}{J/g}$	Type of process	$\dfrac{T_p^{\beta=10°C\,min}}{°C}$	$\dfrac{E_a}{10^5\,J/mol}$	$\ln(A/s^{-1})$	$\ln(k_{25°C}/s^{-1})$
Reference	0	9.80 ± 0.26	main & secondary	63.4	3.40 ± 0.77	119 ± 36.5	-18.5
				5.32	2.93 ± 0.19	105 ± 14.3	-13.7
7 days	40	4.27 ± 0.28	main	65.7	4.35 ± 1.91	152 ± 78.9	-23.9

An important aspect to be pointed out is that two unperfumed bases with different compositions and different thermal characteristics, as evidenced by the DSC signal appearance, have finally, after exposure to high thermal stress a similar macroscopic appearance and thermal behaviour. This is a reason, why high temperature may have similar effects for a broad variety of fabric softeners.

4.1.1.5. *Conclusions*

For fabric softener bases, a de-ageing procedure is required before any type of analysis in order to erase the previous thermal history of the sample. In this way, the processes with a long relaxation time are eliminated and the processes which are characterised by a short relaxation time and which are thus more important for sample stability remain those to be analysed.

Fabric softener bases are complex systems and therefore complex, overlapping signals obtained from the DSC experiments have to be separated by means of a linear deconvolution procedure before investigation. Methods which make no assumption about the form of the kinetic function and have therefore a more universal validity – such as iso-conversional methods (e.g. Friedman's and Flynn-Wall-Ozawa's method) - are firstly used. Subsequently, the results obtained in this way are compared with those obtained from assuming a reaction order model (e.g. Kissinger's method). The comparison shows the results to be in good agreement. Moreover, for the samples which display no rearrangement phenomena while performing the temperature programmes, the main processes can be easily and quickly analysed by the method of Kissinger, without performing deconvolution.

The values of the kinetic parameters obtained by applying the methods of non-isothermal kinetics to the thermal transitions taking place in the emulsion systems are in a range of values above that encountered ordinarily in the field of chemical reaction kinetics. The reasons for the high values obtained for the activation energies and pre-exponential factors may be related to the special aggregation form of the bases as emulsions. It should be noted that the methods of non-isothermal kinetics were in fact developed for solid state systems. These systems lead under thermal stress to the formation of gas phases. The application of non-isothermal kinetics methods to systems in other aggregation forms should be regarded with some reservation concerning the interpretation of the kinetic parameters. These kinetic parameters may have another meaning in such more complex systems, where the solvent plays an important role and where additional interactions such as between molecules and solvent cages have to be taken into account. As a consequence, the concepts of activation energy and pre-exponential factor for emulsion systems should not be regarded independently, but need to be considered as being linked together in the form of the rate constant. The rate constant as parameter is in this way a measure of system's stability and used furtheron for comparison of thermal properties between systems.

As a consequence of the kinetic analysis, the three bases B1, B2 and B3 can be classified with respect to their stability. The most stable one proves to be unperfumed base B1_u. Unperfumed base B3_u is the most unstable one. Low and high temperatures lead to a simplification of the DSC patterns of the unperfumed bases. Storage of one of the unperfumed bases (the most stable one) – B1_u - at low temperature (4°C) for one week has a stabilisation effect on the sample; for longer storage times, however, the base progressively destabilises. A similar effect of stabilisation can also be noticed when stored at high temperature (40°C) for short storage time (one week) for two of the unperfumed bases – B1_u and B2_u . The stabilisation effect is more pronounced for base B1_u.

Because of the macroscopically more dense appearance and of the single peak DSC patterns obtained after storage at high and low temperatures, as well as because of the similar variation of kinetic parameters as a consequence of storage in both cases, the observed effect of stabilisation with extreme temperatures is speculated to be associated with viscosity properties.

4.2. DSC investigation of commercial cosmetic creams and lotions

4.2.1. Qualitative observations

Cosmetic emulsions such as lotions and creams are rarely simple two-phase oil-and-water systems. Such preparations often contain several interacting excipients and may be composed of additional phases apart from oil and water, such as lamellar liquid crystalline or gel networks[47, 74]. These phases enhance emulsion stability. Emulsion stability is further increased when the multilayers are extensively swollen with water; in this way, liquid crystalline or gel networks of a vastly swollen bilayer form[75]. The liquid crystalline networks are mostly optically anisotropic and can be directly observed in an optical microscope with polarised light.

The structural appearance of three different cosmetic skin creams: an oil-in-water, a water-in-oil and a water-in-oil–in-water emulsion are illustrated in Figure 53 in transmitted and polarised light. One observes optically anisotropic structures when examining them under cross-polarisers.
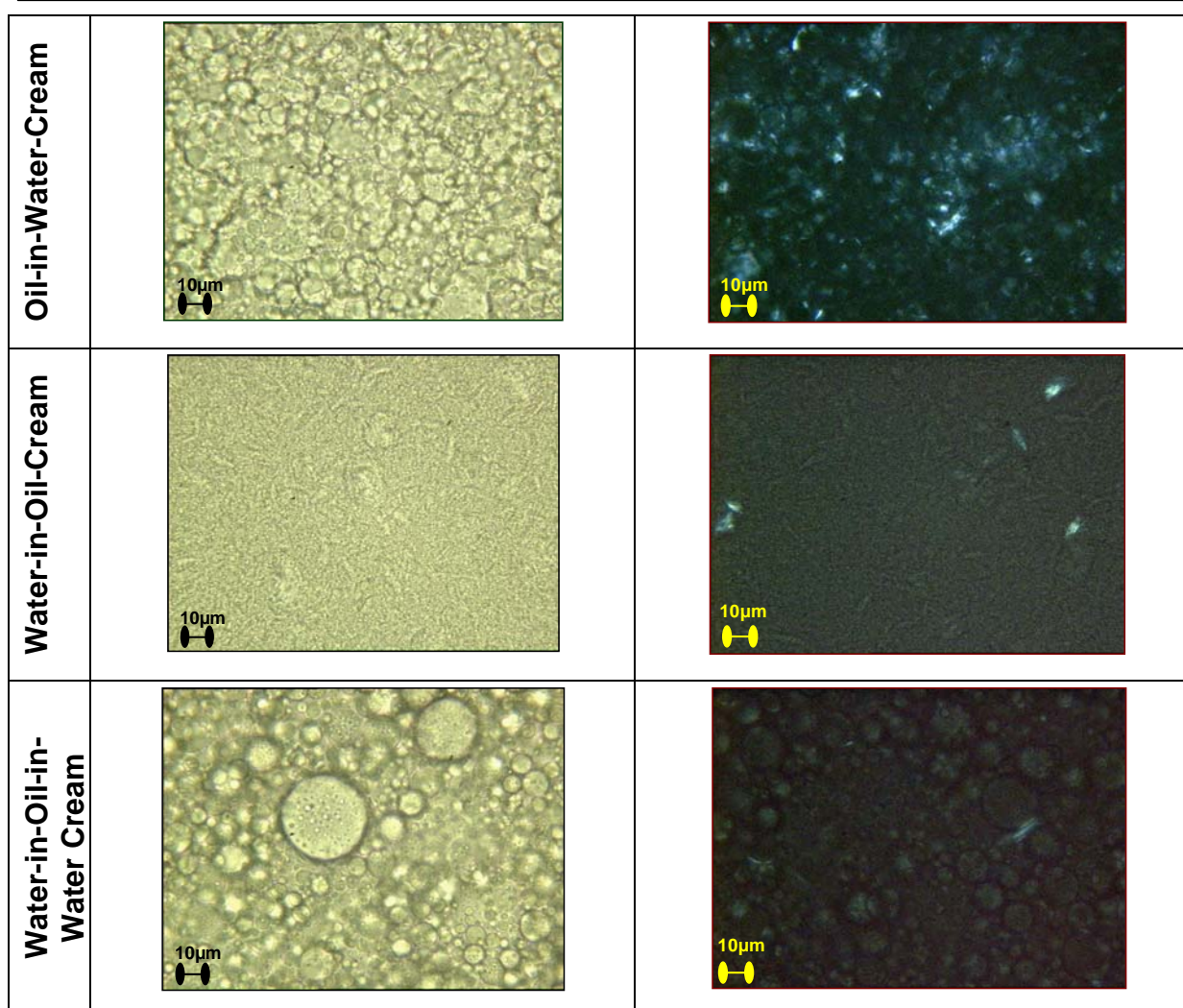
Fig. 53:   Optical micrographs in bright light and polarised light of three different types of skin creams: *oil-in-water*, *water-in-oil* and *water-in-oil-in-water emulsions*

The reaction rates obtained from the DSC pattern of the first thermal run, and the evolution of the pattern while a second temperature programme are performed, is shown in Figure 54 for all of the three types of emulsions.
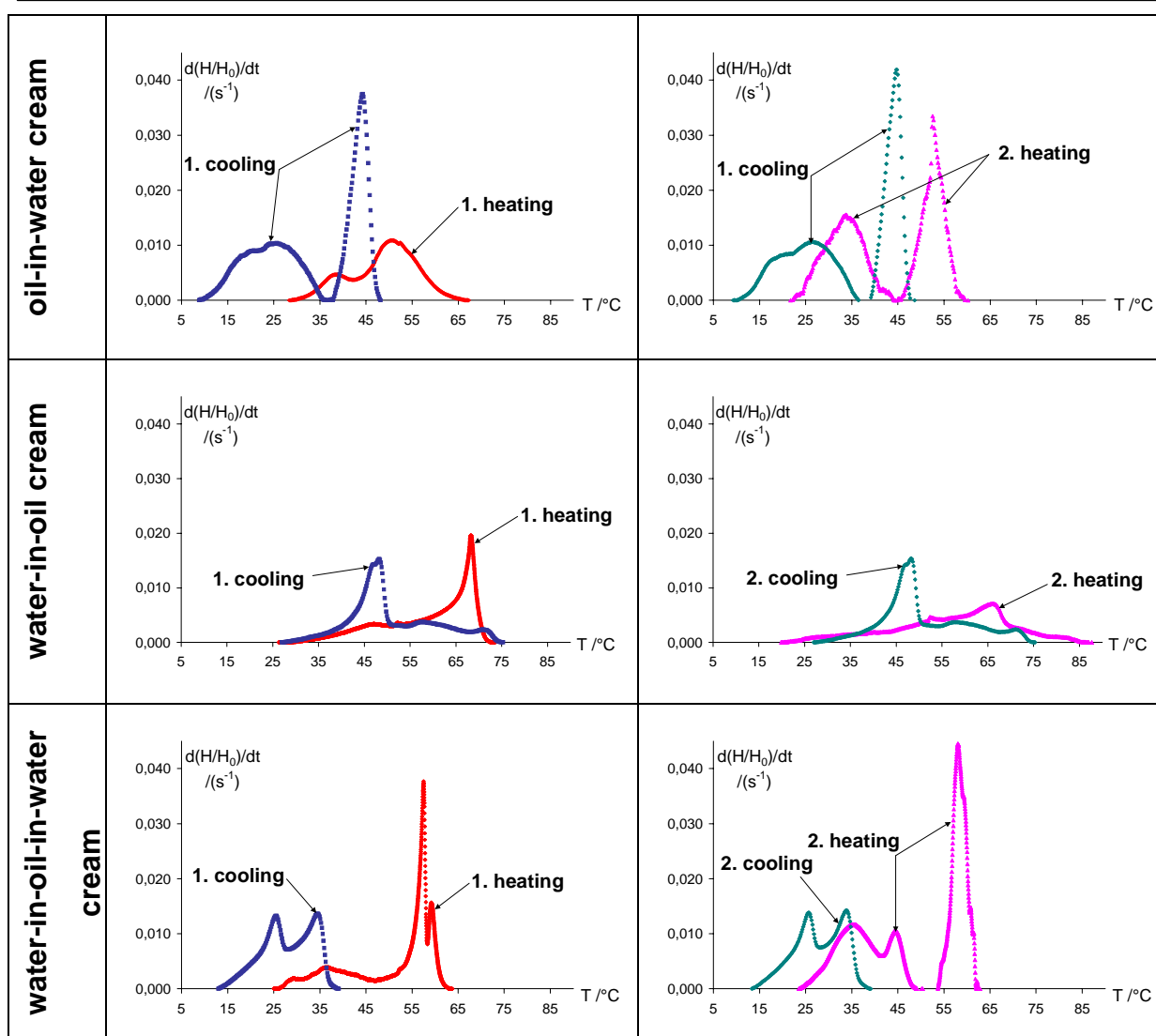
Fig. 54: Conversion rates of the first and second thermal runs with 10°C/min for three different types of cosmetic creams: *oil-in-water*, *water-in-oil* and *water-in-oil-in-water emulsions*, respectively

The main peaks correspond presumably to the transition of a lamellar gel to a liquid crystalline state.

A thermal characteristic of all samples is that they display identical cooling signals in a cyclic procedure; second heating as well as cooling signals show after 1 month good reproducibility (time dependence not shown). This allows supposing that a stable structure is formed after performing the first heating-cooling programme.

Lotions and creams are complex multicomponent formulations; we cannot expect from such complex systems to exhibit the same thermal reversibility as simple emulsion systems such as fabric softeners. This is why they have to be kinetically analysed after a temperature programme with a new sample for each scanning rate.

In the following section, three different cosmetic commercial products in emulsion form (an oil-in-water (o/w) lotion, an water-in-oil (w/o) cream and an water-in-oil–in-water (w/o/w) cream) with defined compositions will be studied in some detail.

4.2.2. A commercial cosmetic o/w emulsion

The microscopic aspect of a commercial cosmetic lotion of the oil-in-water (o/w) emulsion type in ordinary and polarised light is illustrated in Figure 55 before and after a DSC heating-cooling programme with 10°C/min. The oil droplets dispersion in water is associated with multilamellar vesicles and a lamellar gel phase, which appear anisotropic under cross-polarisers. The subjection to a heating-cooling thermal run is followed by rearrangements of the initial emulsion components in a new oil-in-water emulsion with birefringent lamellar structures.

The presence of anisotropic structures does not surprise. The emulsion contains among others, glycerol stearat and lecithin, components which the literature reports to form a lamellar liquid crystalline gel phase with increasing instability[181,182,183].

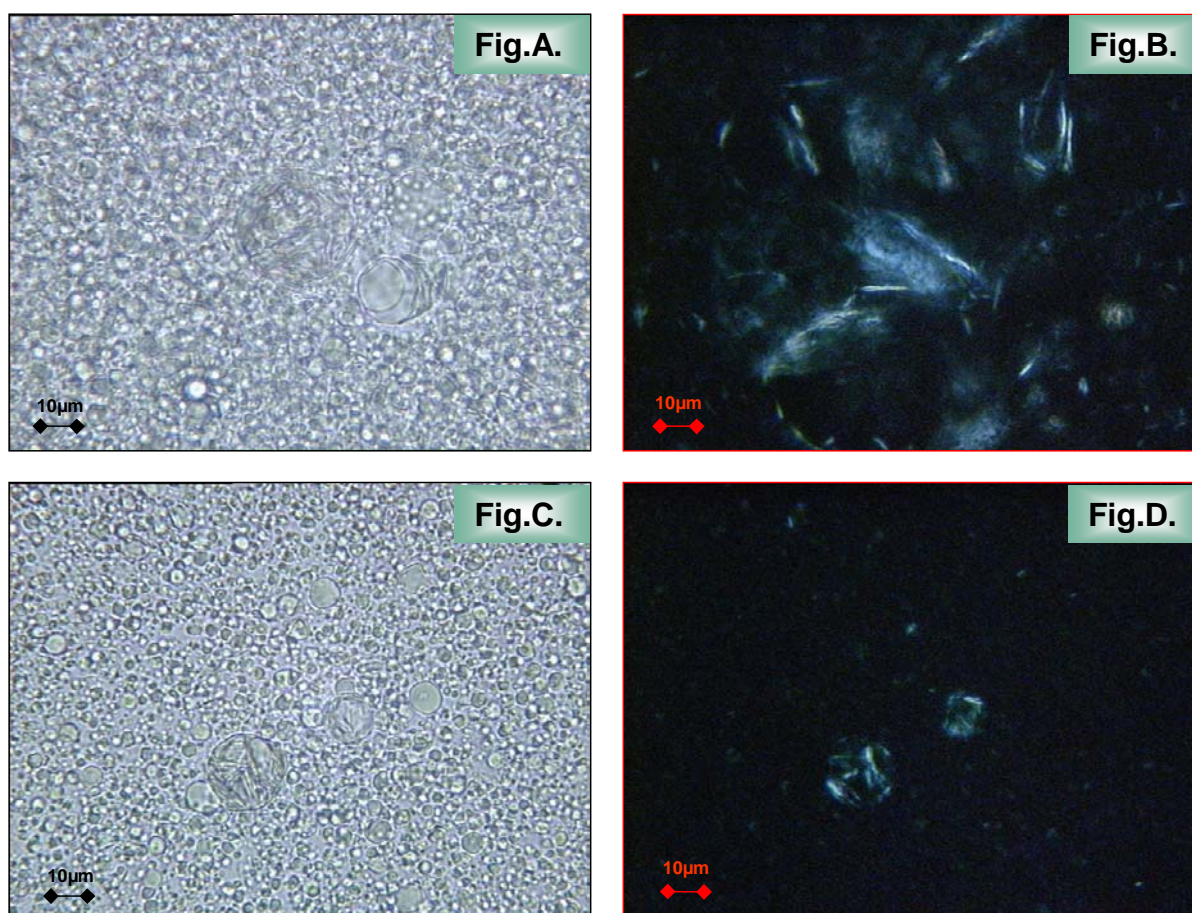Fig. 55: Optical micrographs in bright and polarised light of a *commercial cosmetic o/w emulsion* before (Fig. A and Fig. B) and after (Fig. C and Fig. D) a DSC heating-cooling thermal run with 10°C/min (magnification 400 ×)

The formation of a new structure after the thermal cycling is noticeable also from the DSC experiments. Figure 56 displays the reaction rates of the first heating-cooling thermal run

together with the reaction rates after the second thermal run for four storage times. After an initial double peak, four months later, the emulsion displays one single peak. One of the two former peaks has become a shoulder. This shoulder later vanishes and the single peak remains, showing also reproducibility. The ageing of the emulsion is accompanied with the formation of a new, stable structure. This fact is supported by reproducibility of the reaction rate profile for the first heating and larger storage times, by the reproducibility of the main contribution of the second heating, as well as by the superposition of the first and second cooling. Additionally, a certain similarity is observed between second heating and the cooling profiles.
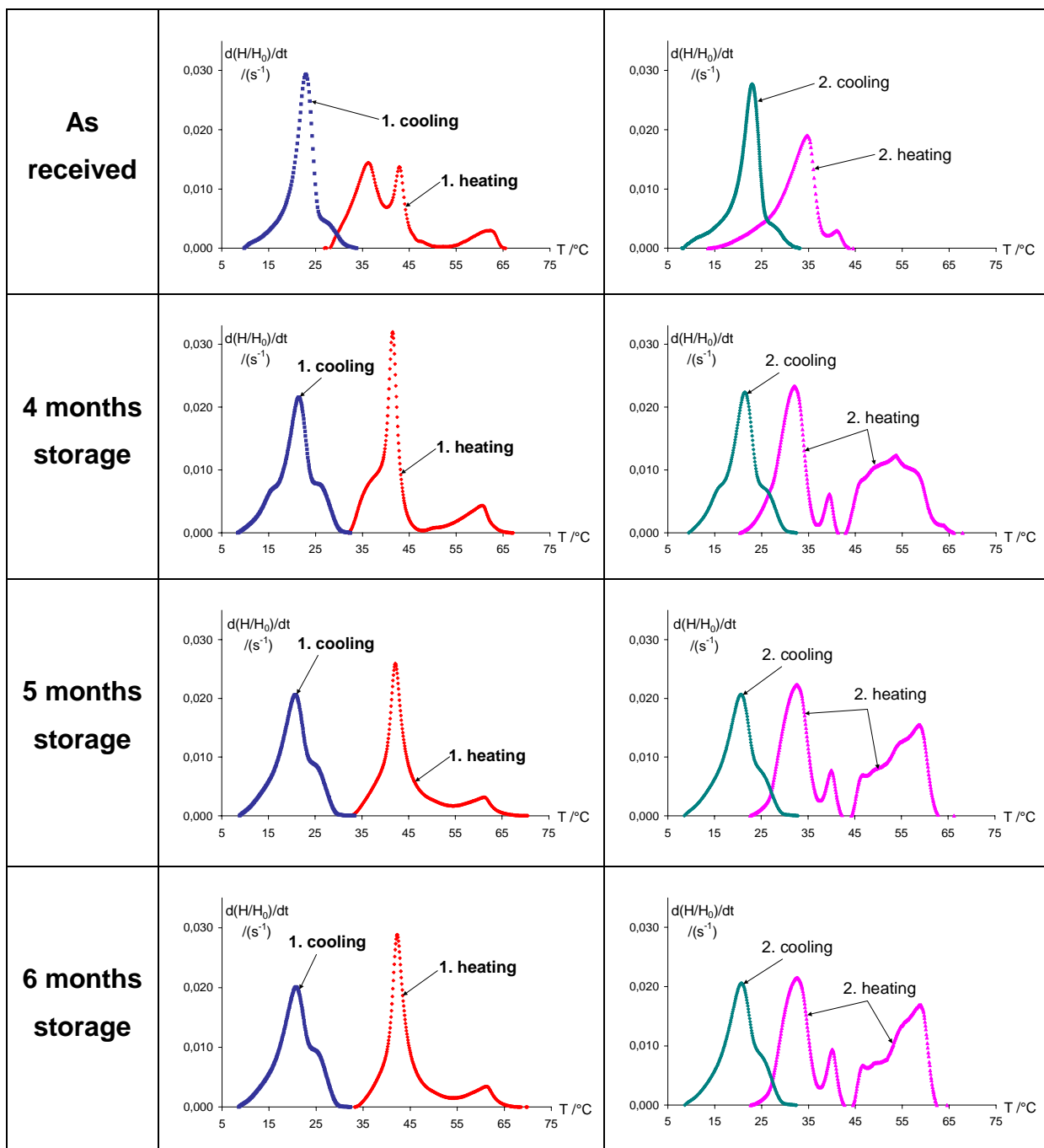
Fig. 56: Conversion rates of the first and second thermal runs with 10°C/min of a *commercial cosmetic o/w emulsion* for four storage times

Thermo-microscopic investigations of the sample on the heating-cooling stage with a scanning rate of 5°C/min as illustrated in Figure 57 show that at approx. 35°C, which corresponds to the main DSC peak, one observes rearrangements of droplets from big associated structures to new agglomerates. Because these effects are confined to small areas, they could be regarded as relaxation phenomena that do not affect the emulsion system to a large extent. This is a reason for not associating the 35°C DSC peak, which vanishes with time, with destabilisation phenomena.

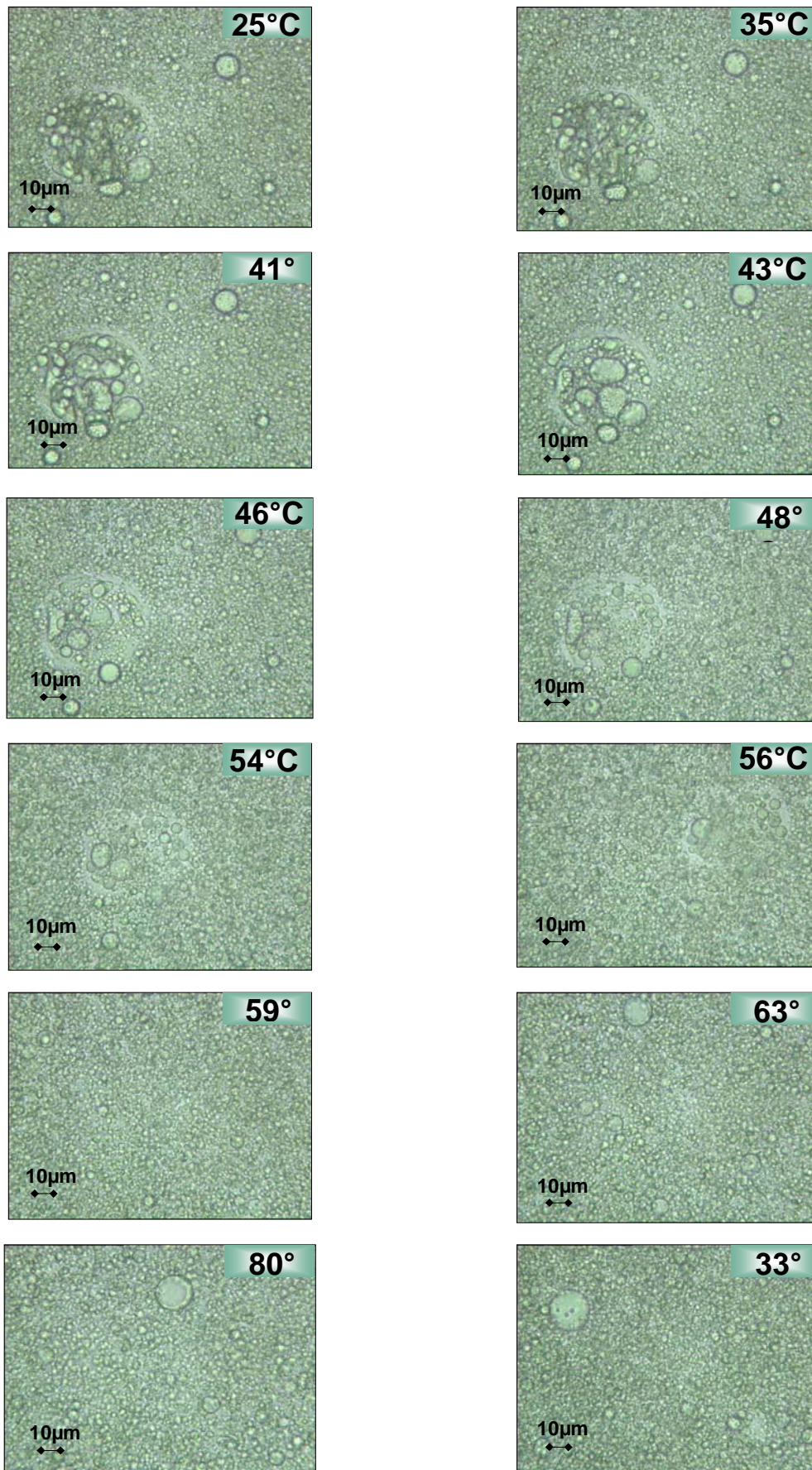Fig. 57: Optical micrographs of a *commercial cosmetic o/w emulsion* during a heating-cooling programm with 5°C/min between 25°C and 80°C (magnification 320×)

A dramatic change in structure starts around 43°C: the big structures disappear, and a fluidisation of the mass with a loss of the initial structure is observed. At 59°C, a temperature which corresponds to the second peak of the DSC curve, the initial big structures disappear completely. The cooling confers to the lotion a new, stable structure.

The kinetic parameters of the main peaks, calculated with Kissinger's method after performing a DSC programme with seven heating rates (1; 2.5; 5; 7.5; 10; 15 and 20°C/min) for the initial moment and with three heating rates after four months (5; 7.5 and 10°C/min) are given in Table 21. For each scanning rate, a new sample was used.

Tab. 21: Kinetic parameters of the main thermal processes for a *commercial cosmetic o/w emulsion* calculated from a temperature programme with seven different heating rates (for the initial moment) and three different heating rates (4 months storage) with Kissinger's method; a new sample was taken for every scan; the peak temperature corresponding to $\beta=10°C/min$, $T_p^{\beta=10°C/min}$, and the type of the analysed process for the given temperature are also mentioned

Status	Heating	$T_p^{\beta=10°C/min}$ °C	Type of process	$\dfrac{E_a}{10^5 \, J/mol}$	$\ln(A/s^{-1})$	$\ln(k_{25°C}/s^{-1})$
As received	first	35.2	main I	7.40 ± 0.68	287 ± 33.6	-11.6
		42.0	main II	7.31 ± 0.41	277 ± 22.3	-17.8
		61.3	secondary	4.95 ± 0.16	176 ± 13.0	-24.1
	second	34.4	main	7.22 ± 0.68	280 ± 33.6	-11.7
		40.5	secondary	5.24 ± 0.33	199 ± 19.6	-12.8
4 months storage	first	41.4	main	9.25 ± 0.85	352 ± 41.9	-20.9
		60.5	secondary	5.26 ± 0.01	188 ± 5.03	-24.7
	second	31.8	secondary	-	-	-
		39.4	main	8.80 ± 2.88	337 ± 122	-18.0

The values of the rate constant, $k_{25°C}$, corresponding to the main peak at 42°C decrease slightly with time, suggesting that a more stable structure is formed. When calculated from the second heating run, that is under an increased temperature stress, for both moments in time, the values increase, suggesting destabilisation. However, after one month, this increase of the rate constant value is not so dramatic, supporting the idea of the formation of a more stable structure with storage. No difference can be observed between

calculations from the first and second heating for the peaks around 35°C and 60°C, respectively. The peak at 35°C is the main peak of the stable structure formed under accelerated thermal stress for any storage time. The peak at 60° is the second peak formed with time and under accelerated thermal stress.

4.2.3. A commercial cosmetic w/o emulsion

The appearance of a commercial cosmetic cream of water-in-oil emulsion type in bright and polarised light is illustrated comparatively before and after the performance of a DSC heating-cooling run in Figure 58. One observes that the initial structure of the emulsion which is characterised by extended anisotropic associations changes after the crystallisation of the melt with reformation of new birefringent small size structures.
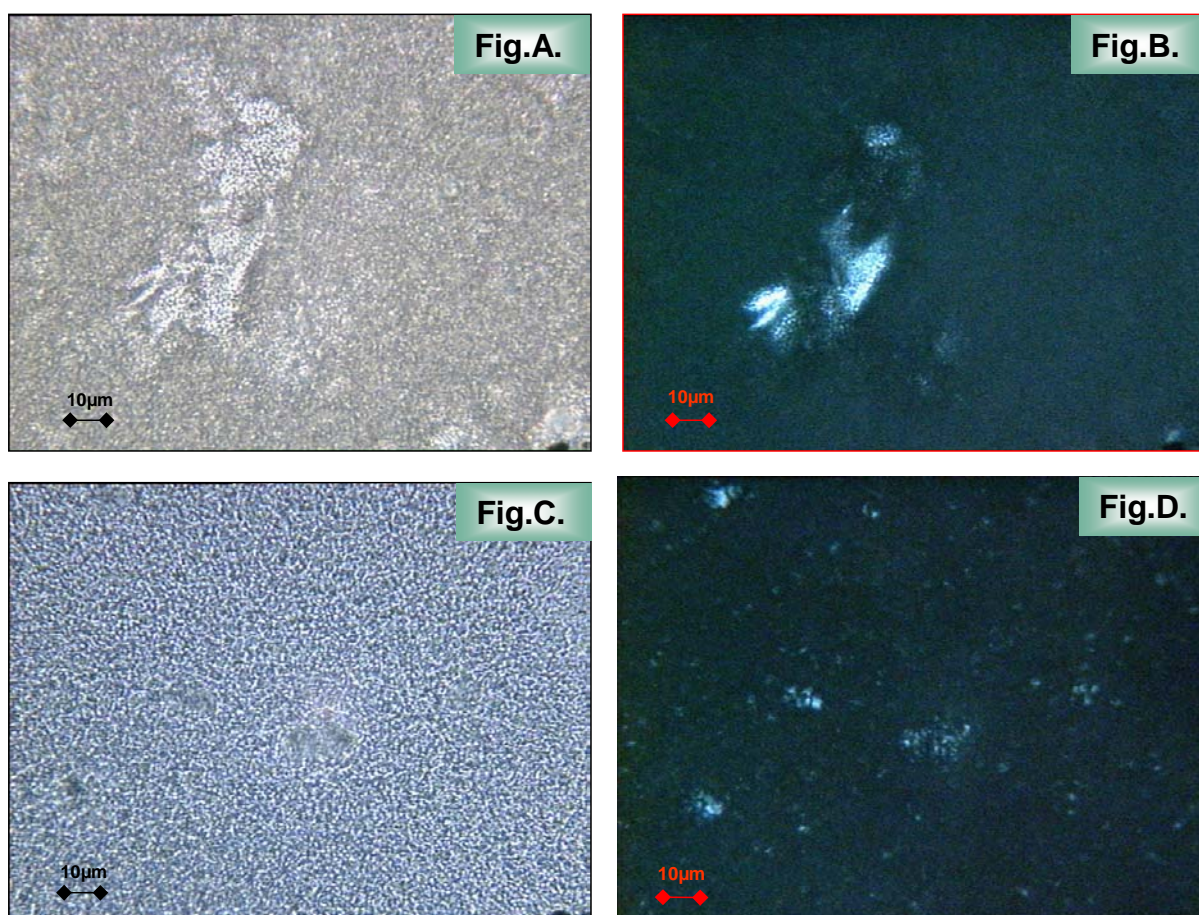

Fig. 58: Optical micrographs in bright light and polarised light of a *commercial cosmetic w/o emulsion* before (Fig. A and B) and after (Fig. C and D) a DSC heating-cooling programm with 7.5°C/min (magnification 400 ×)

The thermal evolution of the emulsion is illustrated in Figure 59 for four storage times after the first and second heating-cooling runs.
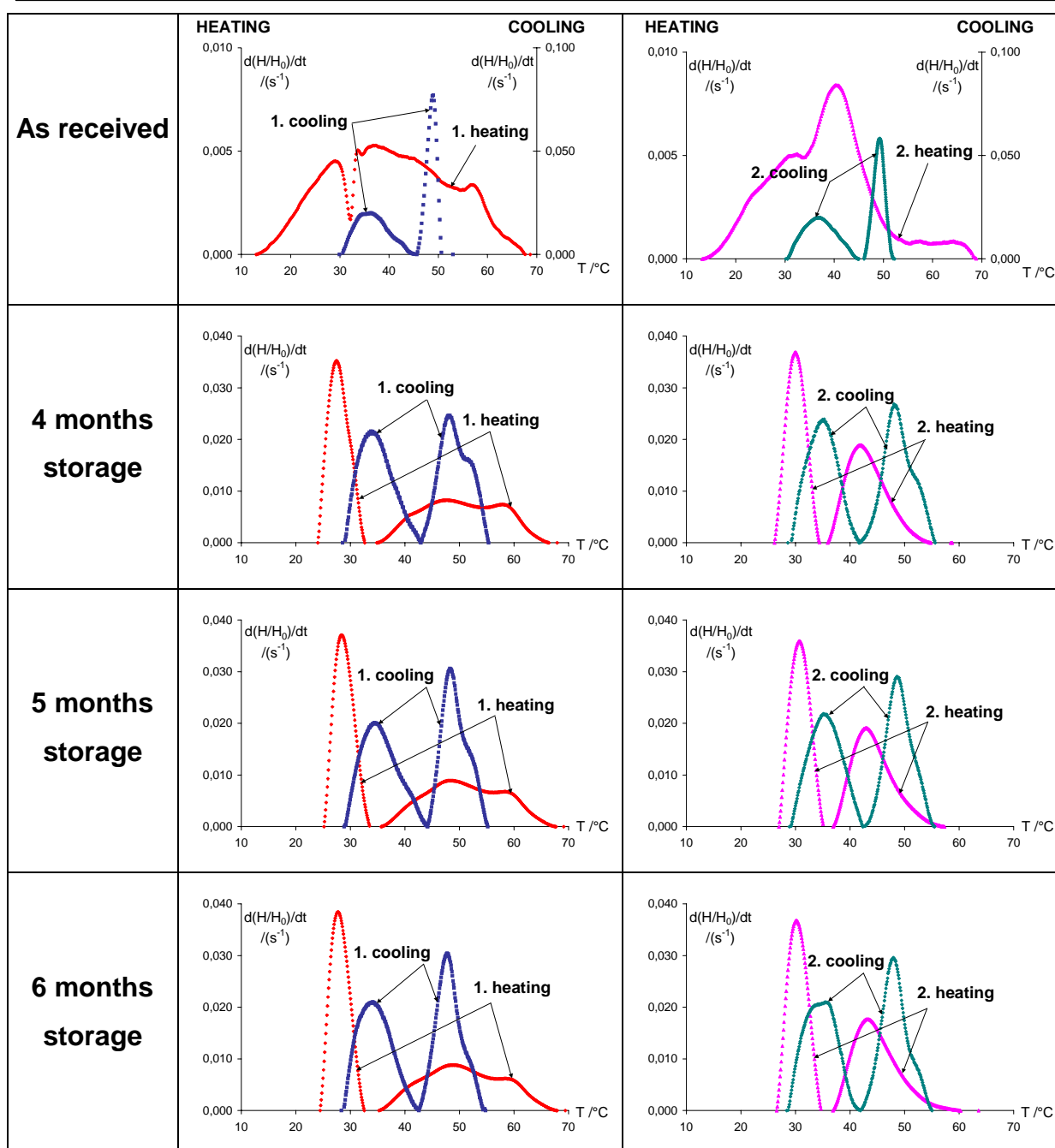
Fig. 59: Conversion rates of the first and second thermal runs with 10°C/min of a *commercial cosmetic w/o emulsion* for four different storage times

One can observe that the emulsion displays a very stable behaviour in time. Although apparently different at the initial moment, the first heating run exhibits a reaction rate profile whose reproducibility becomes evident for all other storage times. Although apparently the pattern of the emulsion "as received" seems to differ from those of the emulsion stored for various periods of time, after the first heating run one achieves similar patterns. This supposition is sustained also by the reproducibility for the second heating and of the cooling runs in time, as well as by the superposability of the first and second cooling runs for every storage time. Additionally, one can also observe that, as for the o/w emulsion, for the w/o emulsion the second heating curve shows similarity to the cooling

profiles. This suggests that, for the w/o emulsion, there is a stable structure formation with time or under the accelerated thermal stress of a temperature programme.

The results for the kinetic parameters corresponding to the main peaks of the reaction rate plots calculated for the initial moment and for six months storage by means of Kissinger's method are summarised in Table 22. A temperature programme with four heating rates (10; 15; 20 and 20°C/min) for the initial moment and with three heating rates after six months (2.5; 5 and 10°C/min) was performed with a new sample for each scanning rate.

Tab. 22: Kinetic parameters of the main thermal processes in a *commercial cosmetic w/o emulsion* calculated from a temperature programme with four different heating rates rates (for the initial moment) and three different heating rates (for 4 months later) with Kissinger's method, taking a new sample for every scan; the peak temperature corresponding to $\beta=10°C/min$, $T_p^{\beta=10°C/min}$, and the type of the analysed process for the given temperature are also mentioned

Status	Heating	$\dfrac{T_p^{\beta=10°C/min}}{°C}$	Type of process	$\dfrac{E_a}{10^5\,J/mol}$	$\ln(A/s^{-1})$	$\ln(k_{25°C}/s^{-1})$
As received	first	36.4	main	1.89 ± 0.66	70.2 ± 34.2	-6.09
		57.4	secondary	4.94 ± 1.38	178 ± 59.8	-21.8
	second	39.7	main	1.82 ± 0.58	66.8 ± 31.0	-6.63
6 months storage	first	48.4	main	1.95 ± 0.10	69.9 ± 9.77	-8.82
		58.5	secondary	2.08 ± 0.06	72.5 ± 7.96	-11.5
		39.0	shoulder	1.83 ± 0.26	67.4 ± 16.80	-6.43
	second	43.0	main	3.70 ± 0.92	138 ± 45.3	-10.9

The rate constant, $k_{25°C}$, corresponding to the initial main peak around 37°C shows the same value irrespective of the evolution of the peak with storage time (it becomes a shoulder after six months) or of accelerated thermal stress conditions (calculation from the second heating run).

With time, the conversion rate pattern displays the main peak around 48°C. This peak is also the main peak of the stable structure formed under accelerated thermal stress for any storage time. As for the o/w emulsion, where the main peak has the tendency to preserve its rate constant values, the peak at 48°C shows under accelerated thermal conditions stable values of the rate constant, $k_{25°C}$ (calculation from the second heating run for the 6

months old sample). The second peak, around 58°C, shows a slight destabilisation in time, its rate constant, $k_{25°C}$, has increased after 6 months of storage. This peak vanishes under accelerated thermal stress.

4.2.4. A commercial cosmetic w/o/w emulsion

Optical micrographs of a commercial cosmetic cream of w/o/w emulsion type show in bright and polarised light a polydisperse distribution of water-in-oil-in-water droplets. Anisotropic lamellar structures surrounding the protective bilayers of the water-containing oil droplets are visible under cross-polarisers as illustrated in Figure 60.
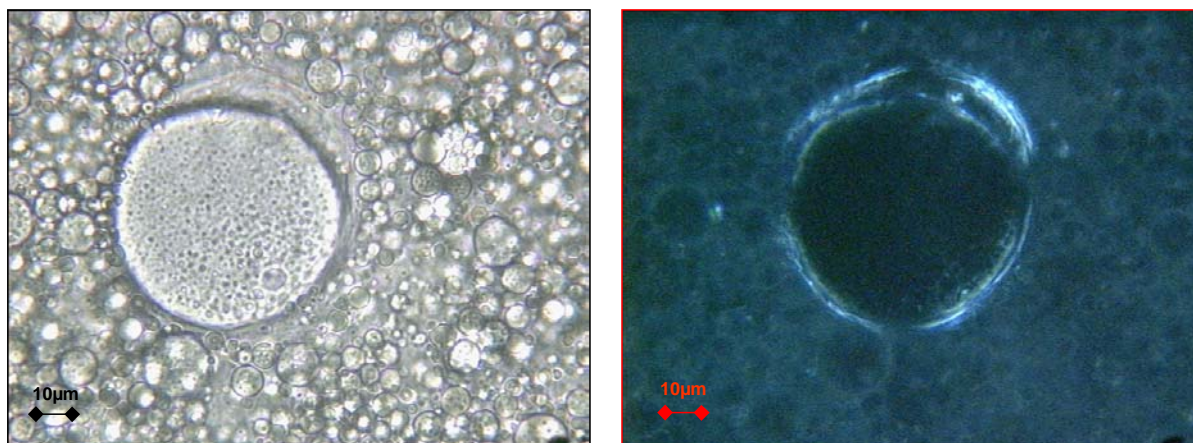

Fig. 60: Optical micrographs in bright light and polarised light of a *commercial cosmetic w/o/w emulsion* (magnification 400 ×)

The thermal evolution of the water-in-oil-in-water emulsion can be followed when examined on the heating-cooling stage with a constant scanning rate of 5°C/min.

Thermo-microscopy examination of the sample as given in Figure 61 shows that at approx. 58° the flow threshold is reached; this temperature is associated with the transformation from a double emulsion into a simple one of the oil-in-water type. This corresponds to the main peak of the reaction rate plots when heating with the same heating rate. Around 35°C, a mobilisation of internal water droplets entrapped within oil globules is induced, together with modifications of the oil droplets boundary into a continuous phase. This is the temperature of the prepeak from the reaction rate plot. Upon cooling, a new stable structure is formed, but this implies the irreversible process of the destruction of the initial water-in-oil-in-water with the formation of a simple oil-in-water emulsion.
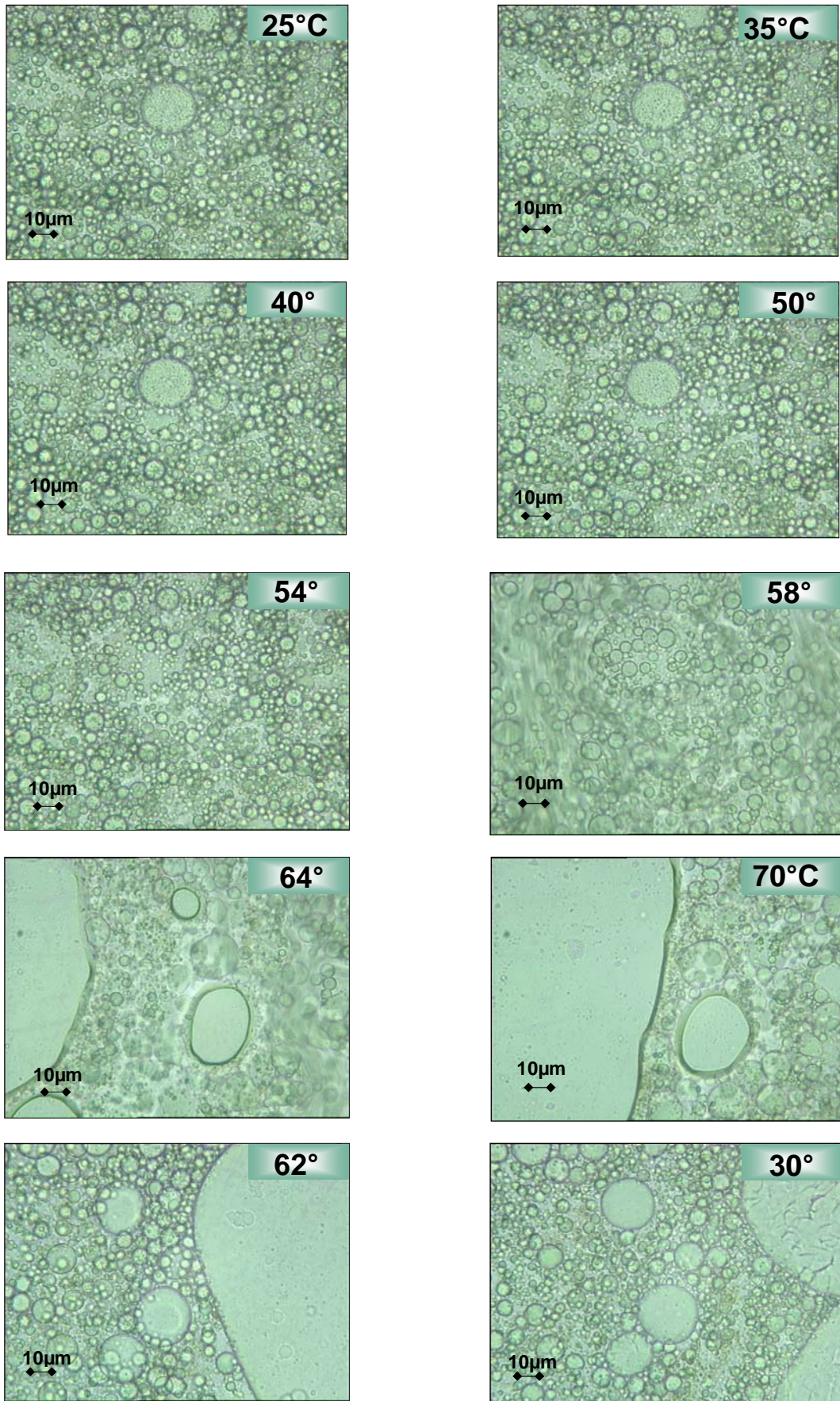
Fig. 61: Optical micrographs of a *commercial cosmetic w/o/w emulsion* during a heating-cooling programm with 5°C/min between 25°C and 80°C (magnification 320 ×)

The evolution in time of the reaction rate patterns can be followed for the first and second heating-cooling runs with 10°C/min in Figure 62. As for the o/w and w/o emulsions, not only the second heating and the first and second cooling are reproducible in time, but also their profile is similar, suggesting that a stable structure, different from the initial one, is formed. The first heating is fairly reproducible in time. The only difference seems to consist in the prepeak appearance: upon storage it seems that two populations are formed in the emulsion mass; after two months this phenomenon seems to outline accurately.

Fig. 62:   Conversion rates of the first and second thermal runs with 10°C/min of a *commercial cosmetic w/o/w emulsion* for three different storage times

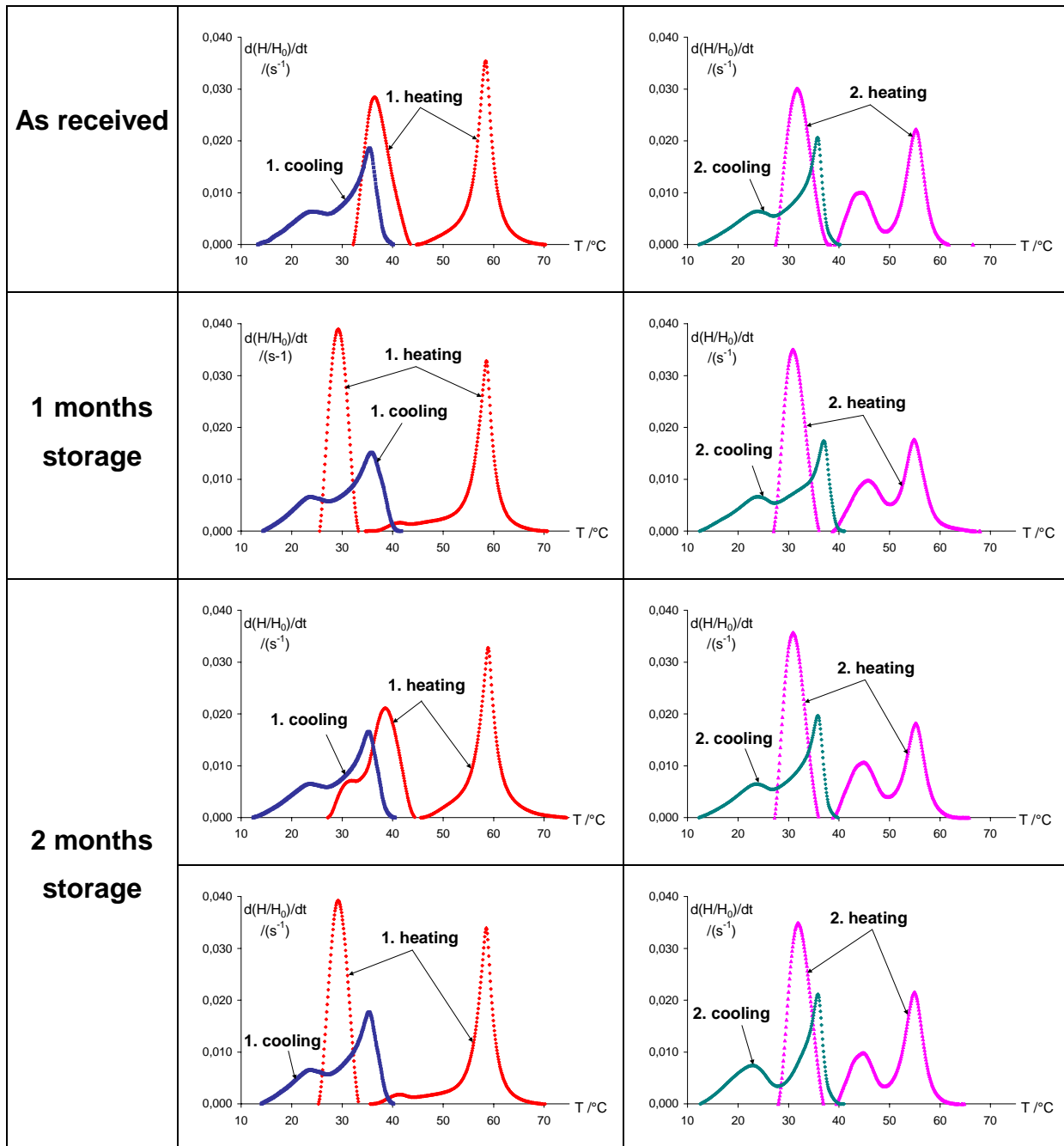The kinetic parameters corresponding to the main peaks of the reaction rate plot calculated for the initial moment by means of Kissinger' method for four heating rates (5; 7.5; 10 and 20°C/min) are given in Table 23. A new sample was used for each scanning rate.

The rate constant, $k_{25°C}$, calculated under conditions of accelerated thermal stress (second heating) has a slightly increased value as compared with the value calculated from the first heating. This suggests the formation of a more stable structure after a heating-cooling cycle. The rate constant value of the prepeak is higher than that of the main peak. This means it corresponds to a less stable structure, that vanishes during the second heating run.

Tab. 23: Kinetic parameters of the main thermal processes in a *commercial cosmetic w/o/w emulsion* calculated from a temperature programme of four different heating rates and new sample for every scan. Kissinger's method was used; the peak temperature corresponding to $\beta=10°C/min$, $T_p^{\beta=10°C/min}$, and the type of the analysed process for the given temperature are also mentioned

Status	Heating	$T_p^{\beta=10°C/min}$ °C	Type of process	$\dfrac{E_a}{10^5\,J/mol}$	$\ln(A/s^{-1})$	$\ln(k_{25°C}/s^{-1})$
1 month after first measurement	first	36.40	prepeak	1.59 ± 0.08	58.3 ± 10.8	-5.86
		58.50	main	3.60 ± 0.17	128 ± 13.4	-17.6
	second	55.20	main	4.75 ± 0.67	172 ± 34.6	-19.9

We can speculate that for all three commercial creams the main peak corresponds to the transition from a lamellar gel to a lamellar liquid crystalline phase. The exact attribution of DSC peaks to structure changes can succeed only when bringing in other experimental evidences [45,49].

The kinetic parameters – the rate constants – of the main peaks suggest the cosmetic w/o/w emulsion is more stable than the two other products, that is the o/w and the w/o emulsions. Also, the DSC evidence shows that heating-cooling cycles of these emulsions destabilise mainly the w/o emulsion. This serves as an indicator for the storage and transport conditions of these commercial cosmetic emulsions.

5.   __APPENDIX__[184,185]

5.1. Statistics

The confidence interval for a sample mean of y data values is defined as:

$$y_\theta = \bar{y} \pm t_\theta \cdot \frac{s}{\sqrt{N}},$$

where $\bar{y}$ is the sample mean, s the standard deviation and t_θ is a tabled value for most common θ values and number of observations. θ is the level of significance of a statistical test and commonly employed at 0.05 limit, less at 0.01 and 0.1 limits.

The sample mean is:

$$\bar{y} = \sum_{i=1}^{N} \frac{y_i}{N},$$ **(5.1.)**

where y_i represent the individual observations and N is the number of observations.

The standard deviation is:

$$s = \sqrt{\frac{\sum_{i=1}^{N}(y_i - \bar{y})^2}{N-1}}$$ **(5.2.)**

In this work is applied a value of θ=0.05. For the significance level of 95%, $t_{\theta=0.05}$=1,96.

For *y* data values, the coefficient of determination r^2 and the F-value have the expression:

$$r^2 = 1 - \frac{sse \cdot (N-1)}{ssm \cdot (DOF-1)}$$ **(5.3.)**

$$F = \frac{\dfrac{ssm - sse}{m-1}}{\dfrac{sse}{DOF}}$$ **(5.4.)**

with $ssm = \sum_{i=1}^{N}(y_i - \bar{y})^2$ the sum of square about mean **(5.5.)**

$sse = \sum_{i=1}^{N}(y_\Diamond - y_i)^2$ the sum of square due to error(squared residuals) **(5.6.)**

and DOF=N-m the degree of freedom, **(5.7.)**

where N is the total number of points, m the total number of parameters fitted, $\bar{y}$ the mean of the y data values and $y_\Diamond$ the estimated y value.

5.2. Composition of commercial cosmetic emulsions

The investigated cosmetic creams were kindly provided by Beiersdorf AG (Hamburg, Germany) and had the following ingredients:

*Nivea Body Lotion (o/w emulsion)

aqua, caprylic/capric triglyceride, myristyl myristate, alcohol denat., dimethicone, glycerol stearate citrate, cetearyl alcohol, octyldodecanol, tocopheryl acetate, sodium carbomer, serine, lecithin, glycine, alanine, potassium phosphate, disodium phosphate, phenoxyethanol, methylparaben, ethylparaben, propylparaben, butylparaben, isobutylparaben, perfume

*Nivea Classic (w/o emulsion)

aqua, paraffinum liquidum, cera microcristallina, glycerin, lanolin alcohol (eucerit®), paraffin, magnesia sulfate, decyl oleate, octyldodecanol, aluminium stearates, panthenol, citric acid, magnesium stearate, perfume

*Nivea Cream Optimale 3 (w/o/w emulsion)

aqua, ricinus communis, caprylic/capric triglyceride, cyclomethicone, glyceryl stearate, glycerin, cetyl alcohol, C12-15 alkyl benzoate, ethylhexyl methoxycinnamate, sodium chloride, PEG-40 stearate, tocopheryl acetate, octyldodecanol, biotin, panthenol, magnesium ascorbyl phosphate, sodium hyaluronate, citric acid, lactic acid, glutamic acid, PCA, mannitol, arginine, serine, sucrose, citrulline, glycogen, histidine, alanine, threonine, lysine, titanium dioxide, alumina, silica, sodium polyacrylate, phenoxyethanol, methylparaben, ethylparaben, propylparaben, butylparaben, isobutylparaben, methyldibromo glutaronitrile, BHT, perfume

6.   __CONCLUSIONS__

The aim of this work was to characterise the thermal stability of emulsion systems by means of kinetics of non-isothermal reactions applied to data obtained from DSC experiments. Optical microscopy examination in bright and polarised light before and after a temperature programme, as well as thermo-microscopy investigations on a heating-cooling stage of the microscopic evolution under non-isothermal conditions gave additional information about temperature-induced structural changes in emulsions.

Fabric softeners, as simple emulsion systems, and commercial cosmetic emulsions, as complex multicomponent systems, were investigated. Two groups of fabric softeners were first analysed as model emulsions. The first group was represented by a case study of three unperfumed bases (B1_u, B2_u and B3_u) to whom three different fragrances of three different types were added, i.e. alcohol (B1_ac1, B1_ac2 and B1_ac3), aldehyde (B1_ad1, B1_ad2 and B1_ad3) and ketone (B1_kt1, B1_kt2 and B1_kt3). Addition of fragrances to fabric softeners, temperature and storage time lead to two major physical instability phenomena: a separation and a hardening of the emulsion.

In order to eliminate thermal processes which play no role in the long-term behaviour of fabric softener samples, such as relaxation phenomena due to storage, a thermal cycling (de-ageing) procedure was applied before analysis. The established quasi reversibility of DSC profiles after the heating-cooling cycles suggested the performance of cyclic temperature programmes with different heating and equal cooling rates. Due to the complexity of DSC patterns, a model-free approach was first used for the kinetic analysis of endothermic transitions in fabric softeners emulsions. The differential isoconversional method of Friedman was applied. This method makes no assumption about the form of the kinetic function $f(\alpha)$ and permits the calculation of the activation energy in the most general way. Because of the dramatic variation of the activation energy E_a with the conversion degree, iso-conversional methods could not be applied for the whole thermal process and a peak separation was required. In order to extract the individual contributions to the whole process, a linear deconvolution procedure was implemented. The endothermic effect was separated in a ponderable sum of individual Gauss curves, because the Gauss function approximates best the evolution of the reaction rate. Beside the condition of best fit additional conditions were imposed for a better agreement with experimental curves .

Kinetic parameters can be obtained by applying various kinetic methods to the individual separated processes – an integral iso-conversional method (Flynn-Wall-Ozawa) and a model-based method (Kissinger) which assumes the kinetic function of the general form $f(\alpha) = (1 - \alpha)^n$. The results were compared to those already calculated by means of the iso-conversional differential method of Friedman. Comparison was also made with the kinetic parameters obtained by using the model-based methods of Kissinger to the entire endothermic effect. The chosen first order kinetics (n=1) fitted fairly well thermal evolution of perfumed and unperfumed samples. It was also found that for simple DSC profiles, the deconvolution can be avoided.

For the first group of fabric softeners (B1, B2 and B3 bases), the influence of fragrance addition to unperfumed bases was examined not only in terms of kinetic parameters but also as DSC patterns and microscopic appearance. The influence of the number of thermal cycles on DSC patterns and kinetic parameters of unperfumed and perfumed samples was also analysed.

For two unperfumed bases, B1_u and B2_u, a similar behaviour was observed depending on the number of thermal cycles: a slight destabilisation after the first thermal cycle and a recovery after an aditional one.

DSC profiles of bases with fragrance show a simplified pattern, probably due to the formation of a more compact structure after fragrance molecules incorporation. Optical micrographs showed a texture of vesicles and multilamellar structures in all samples. However, no large difference between perfumed and unperfumed samples could be observed. For B2 bases kinetic parameter calculation indicated, that fragrance addition led to instability effects, irrespective of the number of de-ageing cycles. For B1 bases, fragrance addition led to instability effects after two thermal cycles. For B3 a similar discrimination between perfumed and unperfumed sample was not possible. However, base B3 with different fragrance substances showed the largest values of the rate constant, $k_{25°C}$, indicating the highest tendency towards instability. This is also confirmed by the observation that with storage time they suffered a separation effect. As a general trend, an effect of stabilisation with the de-ageing procedure could be noticed for the unperfumed samples B1_u and B2_u. Among all unperfumed bases the lowest values of the rate constant were obtained for unperfumed base B1_u.

The results of the DSC evaluation are supported by the practical experience: after 2.5 years of storage at room temperature, unperfumed base B1_u remained stable, whereas B2_u has undergone hardening and B3_u separation.

When analysing the processes taking place upon cooling for unperfumed sample B1_u, the calculated rate constant values $k_{25°C}$ were larger than those found upon heating and therefore they are probably decisive for sample stability.

The evolution with time of selected, unperfumed bases and the effect of storage at low (4°C) and high temperatures (40°C) on defined unperfumed bases were separately analysed. One week storage of unperfumed base B1_u at 4°C is accompanied by a modification of the initial sample structure with the formation a new, more stable structure. A progressive slight destabilisation (increase of the rate constant) was observed after that, starting with 2 weeks storage at 4°C. After 1 month storage, one can notice also clear modifications of the DSC profile. The storage of two unperfumed bases (B1_u and B2_u) for one week at 40°C was associated with smaller values of the rate constant, $k_{25°C}$, indicating the formation of a more stable, compact structure. The fact was supported by the appearance of simplified DSC curves. It was speculated that this could be related with viscosity properties.

Commercial cosmetic lotions and creams in the form of oil-in-water, water-in-oil and water-in-oil-in-water emulsions were finally investigated. With time and under accelerated thermal stress (DSC temperature programms), they transform into a new, more stable structure, according to the kinetic calculations. This affirmation is also supported by microscopic examinations under dynamic, non-isothermal conditions (thermo-microscopy). We can conclude that DSC profiles form a promising tool for investigating structural changes in technical and commercial emulsions by providing experimental data for kinetic analysis. The kinetic parameters obtained from the non-isothermal analysis of DSC data, both for fabric softeners and for commercial lotions and creams can provide information about instability phenomena as such, but not on the form of instability (hardening, or phase separation etc). The results obtained from DSC and kinetic analysis should be supplemented with other experimental evidence (for instance optical microscopy) for a deeper understanding of the phenomena.

7. <u>REFERENCES</u>

[1] Reng, A., Parfümerie und Kosmetik, 80:5, 8-9 (1999)

[2] Cannell, J.S., Int.J.Cosmet. Sci., 7, 291-303 (1985)

[3] Tadros, T., Advances in Colloid & Int. Sci., 108-109, 227-258 (2004)

[4] Förster, A.H.; Herrington, T.M, Int.J. Cosmet. Sci, 20, 317-326 (1998)

[5] Terrisse, I.; Seiller, M.; Rabaron, A.; Grossiord, J.L., Int.J. Cosmet. Sci, 15, 53-62 (1993)

[6] Brummer, R.; Griebenow, M.; Hetzel, F, F.; Schlesiger, V.; Uhlmann, R, 14.DGK-Symposium Proceedings, Hamburg (2001)

[7] Salmon, J.-B.; Becu, L.; Manneville, S., Colin, A., Eur.Phys.J.E, 10, 209-221 (2003)

[8] Zilles, J.U., SÖFW-J., 129:10, 42-44 (2003)

[9] Pena, L.E.; Lee, B.L.; Stearns, J.F., J.Soc.Cosmet.Chem., 44, 337-345 (1993)

[10] Pena, L.E., Lee, B.L., Stearns, J.F., J.Soc.Cosmet.Chem., 45, 77-84 (1994)

[11] Kopecky; M.; Phan, K.-H.; Wortmann, F.-J., Höcker, H.; Körner, A., DWI Reports, 109 (Aachener Textiltagung, 1991), 661-669 (1992)

[12] Junginger, H.; Heering, W.; Führer, C.; Geffers, I., Colloid & Polym.Sci., 259, 561-567 (1981)

[13] Gunning, A.P.; Mackie, A.R., Wilde, P.J.; Morris, V.J., Langmuir, 20, 116-122 (2004)

[14] de Luca, M., Int.J. Cosmet. Sci, 22, 157-161 (2000)

[15] Kühl, T.; Dahms, G., Cossma, 2, 42-43 (2000)

[16] Lopez, C.; Lesieur, P.; Keller, G.; Ollivon, M., J.Colloid Int. Sci., 229, 62-71 (2000)

[17] Lopez, C.; Lesieur, P.; Keller, G.; Ollivon, M., J.Colloid Int. Sci., 240, 150-161 (2001)

[18] Lopez, C.; Lesieur, P.; Keller, G.; Ollivon, M., J.Colloid Int. Sci., 254, 64-78 (2002)

[19] Reynolds, P.A.; Henderson, M.J.; White, J.W., Colloids and Surfaces A: Physicochem.Eng.Aspects, 232, 55-65 (2004)

[20] Rambhau, D.; Phadke, D.S.; Dorle, A.K., J.Soc.Cosmet.Chem., 28, 183-196 (1977)

[21] Dalal, J.N.; Dalal, N.S.; Lim, J.K., J.Soc.Cosmet.Chem., 38, 1-9 (1987)

[22] Dukhin, A.S.; Goetz, P.J.; Wines, T.H.; Somasundaran, P., Colloids&Surfaces A:Physicochem.Eng.Aspects (2000)

[23] Song, M.G.; Jho, S.H.; Kim, J.-Y.; Kim, J.-D., J.Colloid Int. Sci., 230, 213-215 (2000)

[24] Brummer, R.; Berg, T.; Friedrich, S.; Wittern, K.-P., SÖFW-J., 128:7, 2-9 (2002)

[25] Kühl, T.; Dahms, G., Cossma, 11, 50-51 (2001)

[26] Jiao, J.; Rhods, D.G.; Burgess, D.J., J. Colloid&Int.Sci., 250, 444-450 (2002)

[27] Möhle, H.L., SÖFW-J., 129:6, 58-65 (2003)

[28] Lade, O., SÖFW-J., 129:10, 50-62 (2003)

[29] Honda, K.; Tsugita, A.; Yoneya, T., J.Soc Cosmet.Chem., 32, 255-273 (1981)

[30] Wortmann, F.-J.; Springob, C.; Sendelbach, G., J.Cosmet.Sci., 53, 219-228 (2002)

[31] Foerster, Th.; Hütter, I.; Kleen, A.; Kintrup, L.; Schlotmann, K., SÖFW-J., 127:9, 28-38(2001)

[32] Cao, J., Thermochim. Acta, 335, 5-9 (1999)

[33] Ladbrooke, B.D.; Chapman, D., Chem.Phys.Lipids, 3, 304-367 (1969)

[34] Koyama, T.M., Stevens, C.R.; Borda, E.J.; Grobe, K.J.; Cleary, D.A., The Chem. Ed., 5:3, 1-4 (2000)

[35] Mattai, J.; Froebe, C.L.;, Rhein L.D.; Simion A.; Ohlmeyer H.; Su, T.S.; Friberg, S.E., J.Soc.Cosmet.Chem., 44, 89-100 (1993)

[36] Motwani, M.R., Rhein, L., Zatz, J.L., J.Cosmet.Sci., 52, 211-224 (2001)

[37] Motwani, M.R.; Rhein, L.D.; Zatz, J.L., J.Cosmet.Sci, 53, 35-42 (2002)

[38] Flandin, F.; Masmejean, M.; Buffevant, C.; Romeu, M., Int.J.Cosmet.Sci., 6, 115-121 (1984)

[39] Friberg, S.E., J.Soc.Cosmet.Chem., 41, 155-171 (1990)

[40] Brooks, G.; Idson, B., Int.J.Cosmet.Sci., 13, 103-113 (1991)

[41] Arct, J.; Pytkowska, K., Euro Cosmetics, 5, 19-22 (2003)

[42] Moreau, C.; Potier, L., Raynal, S.; Clausse, D., Cal.Anal.Therm., 23: 281-288 (1992)

[43] Moreau, C.; Potier, L., Raynal, S.; Clausse, D., Cal.Anal.Therm., 23: 57-64 (1992)

[44] Eccleston, G.M., J.Soc.Cosmet.Chem., 41, 1-22 (1990)

[45] Ribeiro, H.M.; Morais, J.A.; Eccleston, G.M., Int.J.Cosmet.Sci., 26, 47-59 (2004)

[46] Jungiger.,H.; Führer, C.; Ziegenmeyer, J.; Friberg, S., J.Soc.Cosmet.Chem., 30, 9-23 (1979)

[47] Jungiger.,H., J.Soc.Cosmet.Chem., 35, 45-57 (1984)

[48] Führer, C.; Parmentier,W., Proc.7IFSCC Congress, Hamburg, 447-460 (1972)

[49] Rose, C., *„Stabilitätsbeurteilung von O/W-Cremes auf Basis der Wasserhaltiges Hydrophilen Salbe DAB 1996"*, PhD, TU Braunschweig (1999)

[50] Bucci, R.; Magri, A.D.; Magri, A.L., J.Therm.Anal.Cal, 61, 369-376 (2000)

[51] Vora, A.; Dollimore, D.; Alexander, K., J.Therm.Anal.Cal., 75, 709-717 (2004)

[52] Wabel, C., *„Influence of lecithin on structure and stability of parental fat emulsions"*, PhD, TU Erlangen-Nürenberg (1998)

[53] de Medeiros, A.C.D.; de Cervantes, N.A.B; Gomes, A.P.B., Macedo, R.O., J.Therm.Anal.Cal, 64, 745-750 (2001)

[54] Ciohodaru, L., Revista de Chimie, 54:1, 27-32 (2003)

[55] Breuer, *„Untersuchung zur thermischen Stabilität einer Öl-in-Wasser Emulsion"*, PhD, RWTH Aachen (1993)

[56] Zografi, G., J.Soc.Cosmet.Chem, 33, 345-358 (1982)

[57] Clarke, D.E.; Small, S., Patent No. WO 2000071807, PCT Int.Appl. (2000),

[58] Ewbank, E.; Tummers, D., Patent No. US 2002010104, U.S.Appl.Publ. (2002)

[59] Mohammadi, M.S.; Ormandi, K.A.; Wright, J.E. Briggs, A.M., Patent No. WO 2001046360, PCT Int.Appl., (2001)

[60] Mohammadi, M.S., Patent No. WO 9943777, PCT Int.Appl. (1999)

[61] Buron, H.L.; Jones, C.W.; Martinez-Escolano, P.; Soubiran, L, Patent No. WO 2001004254, PCT Int.Appl. (2001)

[62] Dewez, J.; Thibert, E., Patent No. WO 9708285, PCT Int.Appl. (1997)

[63] Becher, P., *„Emulsions. Theory and practice"*, 3.Edition, Oxford University Press, New York (2001)

[64] Schrader, K., *„Grundlage und Rezepturen der Kosmetika"*, 2. Auflage, Hütthig Verlag (1989)

[65] Jellinek, J.S., *„Kosmetologie. Zweck und Aufbau kosmetischer Präparate"*, 2.Auflage, Dr.Alfred Hüthig Verlag, Heidelberg (1967)

[66] Heymann, E., *„Haut, Haar und Kosmetik. Eine chemische Wechselwirkung"*, Wissenschaftliche Verlagsgesellschaft mbH, Stuttgart (1994)

[67] M.M. Breuer, M.M. (Editor), *„Cosmetic Science"*, vol.2, Academic Press, London (1980)

[68] Heusch, R. *„Emulsionen"* in *„Dentalchemie bis Erdölverarbeitung"*, Ullmans Enzyklopädie der technischen Chemie, 4. Edition, 10, 449-473 (1975)

[69] Umbach, W.(Editor), *„Kosmetik"*, 2.Auflage, Georg Thieme Verlag, Suttgart (1995)

[70] Malaszkiewicz, J., Förg, F., *„Hautkosmetika"*, Ullman's Enzyklopedie, 4.Edition, 12:557-567 (1976)

[71] Everett, D.H.(Publisher), Kopal, L.K., *Manual of symbols and terminology for physicochemical quantities and units./ Definitions, Terminology and symbols in colloid and surgace chemistry:Part I., Appendix II*, Pure and Appl.Chem, 21:1 (2001)

[72] Friberg, S.E., Formulation Forum'99, Orlando, U.S.A. (1999)

[73] Killian, H.-G.; Weiss, A. (Editors), *„Surfactants, Micelles and Liquid Crystals"*, Progress in Colloid & Polymer Science 69, Steinkopff Verlag, Darmstadt (1984)

[74] Friberg, S.E., J.Soc.Cosmet.Chem., 30, 309-319 (1979)

[75] Eccleston, G.M, J.Soc.Cosmet.Chem., 41, 1-22 (1990)

[76] Brinon, L.; Geiger, S.; Alard, V.; Tranchant, J.-F.; Pouget, T.; Couarraze, G., J.Cosmet.Sci., 49, 1-11 (1998)

[77] Bechhold, H., „*Einführung in die Lehre von den Kolloiden*", Theodor Steinkopff Verlag, Dresden Leipzig, 1, (1934)

[78] Schutz, C., SÖFW-J., 129:8, 16-19 (2003)

[79] Wennerström, H.; Söderman, O.; Lindman, B., Colloids and surfaces. A: Physicochem& Eng. Aspects, 123-124, 13-26 (1997)

[80] Tadros, T.; Izquierdo, P.; Esquena, J.; Solans, C., Advances in Colloid&Int. Sci., 108-109, 303-318 (2004)

[81] Mlodozeniec, A.R., J.Soc.Cosmet.Chem, 29, 659-683 (1978)

[82] Jayakrishnan, A.; Kalaiarasi, K.; Shah, D.O., J.Soc.Cosmet.Chem., 34, 335-350 (1983)

[83] Rosano, H.I.; Cavallo, J.L.; Chang, D.L.; Whittam, J.H., J.Soc.Cosmet.Chem., 39, 201-209 (1988)

[84] Tadros, T.F., Int.J.Cosmet.Sci., 14, 93-111 (1992)

[85] Pfüller, U., „*Mizellare Beeinflussung analytischer Reaktionen und Prozesse*, Analytiker Tachenbuch, Springer Verlag, Berlin/Heidelberg. 9, 23-90 (1990),

[86] Glasstone, S.; Lewis, D., „*Elements of Physical Chemistry*", 2. Edition, MacMillan&CoLtd, London (1966)

[87] Adam, G.; Läuger, P.; Stark, G., „*Physikalische Chemie und Biophysik*", 3. Auflage, Springer Verlag, Berlin Heidelberg (1995)

[88] Mlodozeniec, A*.*, J.Soc.Cosmet,Chem., 29, 659-683 (1978)

[89] Engels, T., von Rybisnki, W., J.Mat.Chem., 8, 1313 (1998)

[90] de Luca, M.; Rocha-Filho, P.; Grossiord, J.L., Rabaron, A.; Vaution, C.; Seiller, M., Int.J.Cosmet.Sci., 13, 1-21 (1991)

[91] Zatz, J.L.; Cueman, G.H., J.Soc.Cosmet.Chem., 39, 211-222 (1988)

[92] Baillet, A.; Pirishi, E.; Vaution, C.; Grossiord, .L.; Ferrier-Baylocq, D.; Seiller, M., Int.J.Cosmet.Sci., 16, 1-15 (1994)

[93] Garti, N.; Aserin, A., Advances in Colloid & Int.Sci., 65, 37-69 (1996)

[94] Vasudevan, T.; Naser, M.S*.*, J.Colloid & Int.Sci., 256, 208-215 (2002)

[95] de Luca, M., Int.J. Cosmet. Sci, 22, 157-161 (2000)

[96] Gohla, S.H., SÖFW-J., 128:7, 10-13 (2002)

[97] Wissing, S.A.; Saupe, A.; Müller, R.H., Euro Cosmetics, 5, 14-17 (2003)

[98] Th.F.Tadros, IFSCC Magazine, 3:4, 31-38 (2000)

[99] Cheng, D.C.-H., Int.J.Cosmet.Sci, 9, 151-191 (1987)

[100] Atkins, P.W., „*Physical Chemistry*", 5. Edition, Oxford University Press, Oxford (1994)

[101] Popescu, A.I.*, „Biofizica moleculara si supramoleculara"*, All Educational Ed., Bucharest (1997)

[102] Eccleston, G.M.; Florence, A.T., Int.J.Cosmet.Sci., 7, 195-212 (1985)

[103] E.D.Goddard, B.Vincent (Editors), „Polymer Adsorbtion and dispersion stability", Am.Chem.Soc, Washington D.C. (1984)

[104] Goddard, E.D., J.Soc.Cosmet.Chem., 41, 23-49 (1990)

[105] Miguel, M. da G.; Burrows, H.D.; Formosinho, S.J.; Lindman, B., J. Molec. Structure, 563-564, 89-98 (2001)

[106] Gasbarrone, P.; La Mesa, C., Colloid Polym. Sci, 279, 1192-1199 (2001)

[107] Rodriguez, C.; Hemayet Uddin, Md; Watanabe, K.; Furukawa, H.; Harashima, A.; Kunieda, H., J.Phys.Chem. B, 106, 22-29 (2002)

[108] Zhou, Z.; Li, M.; Yan, H., Colloids& Surfaces A: Physicochem&Eng. Aspects, 175, 263-266 (2000)

[109] Grell, E.; Lewitzki, E.; Schneider, R.; Ilgenfritz, G.; Grillo, I.; von Raumer, M., J.Therm.Anal.Cal., 68, 469-478 (2002)

[110] Caffrey, M.; Bywater, M.T., J.Soc.Cosmet.Chem., 39, 159-167 (1988)

[111] Vamvakaki, M.; Patrickios, C.S., J.Phys.Chem.B, 105, 4979-4986 (2001)

[112] J.Bibette, F.Leal-Calderon „Emulsions science. Basic principles.An overview", Springer Verlag (2002)

[113] Henning, T., SÖFW-J., 130, 7, 69-77 (2003)

[114] Arditty, S.; Whitby, C.P.; Binks, B.P.; Schmitt, V.; Leal-Calderon, F., Eur.Phys.J.E, 11, 273-281 (2003)

[115] Daniels, R., Euro Cosmetics, 1, 34-39

[116] Lang, F.; Berenbold, H., SÖFW-J., 117, 690-694 (1991)

[117] Wahle, B., Falkowski, J., Rev.Prolog.Color, 32:118-124 (2002)

[118] Jakob, G.&all, „Waschmittel", Ullmans' Enzyklopedie, 4.Edition, 24:63-160 (1983)

[119] Kosswig, K., „Tensid", Ullmans' Enzyklopedie, 4.Edition, 22:455-515 (1982)

[120] Habereder, P.and Bereck, A., Rev.Prolog.Color, 32:125-137 (2002)

[121] Hauthal, H.G., SÖFW-J., 10:12-26 (2003)

[122] Bauer, K., Garbe, D., „Riech-und Aroma Stoffe", Ullmans' Enzyklopedie, 4.Edition, 20:199-187 (1981)

[123] Aebi, H.&Co (Editors), „Kosmetika, Riechstoffe und Lebensmittelzusatzstoffe", Georg Thieme Verlag, Stuttgart (1978)

[124] Friberg, S.E.; Zhang, Z., J.Cosmet.Sci., 50, 203-219 (1999)

[125] Carlotti, E.; Gallarate, M.; Morel, S.; Ugazio, E., J.Cosmet.Sci., 50, 281-295 (1999)

[126] Gallarate, M.; Carlotti, M.E.; Cagliani, I:; Negri, D., J.Cosmet.Sci., 51, 209-226 (2000)

[127] Thoma, K.; Pfaff, G., J.Soc.Cosmet.Chem., 27, 221-234 (1976)

[128] Blakeway, J.M.; Bourdon, P.; Seu, M., Int.J.Cosmet.Sci, 1, 1-15 (1979)

[129] Abe, M.; Mitzguchi, K.; Kondo, Y.; Ogino, K.; Uchiyama, H.; Scamehorn, J.F.; Tucker, E.E.; Sherril, D.C., J.Colloid Interface Sci., 160, 16-23 (1993)

[130] Zhang, Z.; Denler, T.; Friberg, S.E., Int.J.Cosmet.Sci, 22, 105-119 (2000)

[131] Zhang, Z.; Friberg, S.E., Aikens, S.E., Int.J.Cosmet.Sci, 22, 181-199 (2000)

[132] Al-Bawab, A., J.Cosmet.Sci., 54, 429-441 (2003)

[133] Al-Bawab, A., Friberg, S.E., J.Cosmet.Sci., 53, 151-164 (2002)

[134] Friberg, S.E.,Yin, Q.; Aikens, S.E., Int.J.Cosmet.Sci, 20, 355-367 (1998)

[135] Friberg, S.E., Int.J.Cosmet.Sci, 19, 75-86 (1997)

[136]Turi, A. (Editor), „*Thermal Characterization of Polymeric Materials*", vol.1, 2. Ed. (1997)

[137] Ferguson, H.F.; Frurip, D.J., Pastor, A.J.; Peerey, L.M.; Whiting, L.F., Thermochim. Acta, 363, 1-21 (2000)

[138] Mathot, V.B.F., Thermochim. Acta, 355:1-33 (2000)

[139] Ozawa, T., Thermochim. Acta, 355, 35-42 (2000)

[140] Becker, F*., „Thermisch-kalorische Meßverfahren",* Ullman's Enzyklopedie, 4.Edition, 5:779-796 (1980)

[141] Wendlandt, W., „*Thermal methods of analysis*", John Wiley&Sons, 2.Edition (1974)

[142] Heide, W., „*Dynamische thermische Analysemethoden*", VEB Deutscher Verlag für Grundstoffindustrie, Leipzig (1979)

[143] Haines, P.J., (Editor), „*Principles of thermal analysis and Calorimetry*", Royal Soc. of Chem., Cornwall (2002)

[144]Charsley, E.L.; Varrington (Editors), S.B., „*Thermal Analysis-Techniques & Applications*", Royal Society of Chemistry (1992)

[145]Hemminger, W.F.; Cammenga, H.K., „*Methoden der thermischen Analyse*", Springer Verlag, Berlin Heidelberg (1989)

[146]Ehrenstein, G.W.; Riedel, G.; Trawiel,P., „*Praxis der thermischen Analyse von Kunststoffen*", Carl Hauter Verlag, München (1998)

[147] Blažek, A., „*Thermal analysis",* van Nostrand Reinhold Company, London (1973)

[148] M.J.Pilling, „*Reactions kinetics*", Oxford University Press (1975)

[149] J.Esperson, "*Chemical Kinetics and reaction mechanisms",* 2.Edition, Mc.Graw-Hill, Inc (1995)

[150] K.A.Connors, *"Chemical Kinetics. The study of reaction rates in solution"*, VCH Publishers, Inc. (1990)

[151] E. Segal, D.Fatu, *„Introducere in cinetica neizoterma"*,"Academiei" Ed., Bucuresti (1983)

[152] C. Iditoiu, *„Chimie fizica si coloidala"*, Ed. Aurel Vlaicu, Arad, 1 (1999)

[153] C. Popescu, E. Segal, Int. J. Chem. Kinet., 30, 313-327 (1998)

[154] J.Berger, *Affinität und Reaktion.Über die Enstehung der Reaktionskinetik in der Chemie des 19.Jahrhunderts"*, VWR Verlag, Berlin (2000)

[155] Brown, M.E.; Maciejewski, M.; Vyazovkin, S.; Nomen, R.; Sempere, J.; Burnham, A.; Opfermann, J.; Strey, R.; Anderson, H.L.; Kemmler, A.; Keuleers, R.; Janssens, J.; Desseyn, H.O.;Li, C.-R.; Tang, T.B.; Roduit, B.; Malek, J.; Mitsuhashi, T., Thermochim. Acta, 355, 125-143 (2000)

[156] S. Vyazovkin, Int. J. Chem. Kinet., 28, 95-101 (1996)

[157] Privalov, P.L., Advances in Prot. Chem., 35, 1-104 (1982)

[158] Odlyha, M.; Cohen, N.S.; Foster, G.M., Thermochim. Acta, 365, 35-44 (2000)

[159] Buchhardt, F.; *„Zur Dekonvolution im Zeitbereich"*, Bundesanstalt für Materialforschung und-prüfung (BAM), Berlin (1992)

[160] Silvia, M.T.; Robinson, E.A., *„Deconvolution of geophysical time series in the exploration for oil and natural gas"*, Elsevier Scientific Company, Amsterdam (1979)

[161] P. Rennert, H. Schmiedel (Editors), *„Physik"*, BI Wissenschaftsverlag, Mannheim Leipzig (1995)

[162] Barankov, G.; Chostak, R.; Demidovitch, B.; Efimenko, V.; Frolov, S.; Kogan, S.; Lountz, G.; Parchneva, E.; Sytcheva, E.; Yanpolski, A., „Recueil d'exercices et de problemes d'analyse mathematique", Mir Editions, U.R.S.S. (1972)

[163] Ozawa, T.*,* J.Therm.Anal.Cal., 64, 109-126 (2001)

[164] Ozawa, T., J.Therm.Anal.Cal., 60, 887-894 (2000)

[165] Gorbachev, V.M., J.Therm.Anal., 8:27-30 (1975)

[166] Madhusudanan, P.M.; Mohammed Yusuff, K.K., J.Therm.Anal., 8:31-43 (1975)

[167] Mianowski, A.; Radko, T., Thermochim. Acta, 204, 281-293 (1992)

[168] Urbanovici, E.; Popescu, C.; Segal, E., J .Therm.Anal.Cal., 60, 581-594 (2000)

[169] Li, C.-R.; Tang, T.B., Thermochim. Acta, 325, 43-46 (1998)

[170] Opfermann, J., J.Therm.Anal.Cal., 60, 641-658 (2000)

[171] Zhang, H.; Mitchell, B.S., J.Mater.Res., 15:4, 1000-1007 (2000)

[172] Kissinger, H.E., Anal. Chem., 29:11, 1702-1706 (1957)

[173] S. Vyazovkin and C.A.Wight, Annu.Rev.Chem, 48, 125-149 (1997)

[174] Sunol, J.J., J.Therm.Anal.Cal., 25-33 (2003)

[175] Friedman, H.L., J. Polym.Sci:Part C, 6, 183-195 (1965)

[176] Flynn, J.H.; Wall, L., J.of Research of the International Bureau of Standards-A. Physics and Chemistry, 70A:6, 487-523 (1966)

[177] Boukhnikachvili, T.; Vacus, J., PCT Int.Appl. (1998)

[178] Zuidam, N.J.; Gouw H.K.; Barenholz, Y.; Crommelin, D.J., Biochim. Biophys. Acta, 1240(1), 101-110 (1995)

[179] Fraser, S.B., PCT Int.Appl. (2000)

[180] Qiu, X.; Pidgeon, C., Biochemistry, 33(4), 960-972 (1994)

[181] Engels, T.; Förster, T.; von Rybinsky, W., Colloids & Surfaces A: Physicochem. & Eng. Aspects, 99, 141-149 (1995)

[182] O'Laughlin, R.; Sachs, C.; Brittain, H.; Cohen, E.; Timmins, P.; Varia, S., J.Soc.Cosmet.Chem., 40, 215-229 (1989)

[183] Phillips, M.C:; Ladbrooke, B.D:; Chapman, D., Biochim.Biophys.Acta, 196, 35-44 (1970)

[184] Sachs, L., *„Angewandte Statistik. Anwendung statistischer Methoden",* Springer Verlag (1999)

[185] Ott, L., *„An introduction to statistical methods and data analysis",* PWS Kent, 3rd Ed. (1988)

LEBENSLAUF

Cristina Alina ILIESCU

Persönliche Daten

Geburtsdatum und –ort: 2. Dezember 1973, Bukarest, Rumänien

Familienstand: ledig

Staatsangehörigkeit: rumänisch

Schulausbildung

1988 - 1992 „Spiru Haret" Gymnasium, Bukarest, Rumänien

Studium

1992 - 1997 Fakultät für Physik, Universität Bukarest, Rumänien

Diplomarbeit: " *Untersuchung an induzierten Verletzungen in Chromatin durch Bestrahlung mit beschleunigten Neutronen* "

1997 - 1998 Vertiefte Studien (Master) in Biophysik, Fakultät für Physik, Universität Bukarest, Rumänien

Diplom für
vertiefte Studien: "*Untersuchung an oxidativen Veränderungen der Plasmalipoproteinen*"

Berufserfahrung

1997 - 1999 Forschungsassistentin am „Nicolae Simionescu" Institut für Zellbiologie und Pathologie, Lipoproteinen und Atherogenese Abteilung, Bukarest, Rumänien

1999 - 2001 DAAD Stipendium für Aus- und Fortbildung an der TU Darmstadt, Institut für Botanik, Fachbereich Biologie

Promotion

Okt. 2001 - März 2005 Promotion am Deutschen Wollforschungsinstitut an der RWTH Aachen

Thema der Doktorarbeit: *„Untersuchungen zur thermischen Stabilität technischer und kosmetischer Emulsionen"*